THE GEOLOGICAL SOCIETY OF AMERICA®

Orogen transplant: Taconic–Caledonian arc magmatism in the central Brooks Range of Alaska

Justin V. Strauss[1,†], Carl W. Hoiland[2], William P. Ward[3], Benjamin G. Johnson[4], Lyle L. Nelson[5], and William C. McClelland[3]

[1]*Department of Earth Sciences, Dartmouth College, HB6105 Fairchild Hall, Hanover, New Hampshire 03755, USA*
[2]*Department of Geological Sciences, Stanford University, 450 Serra Mall, Stanford, California 94305, USA*
[3]*Department of Earth and Environmental Sciences, University of Iowa, 115 Trowbridge Hall, Iowa City, Iowa 52242, USA*
[4]*Department of Geology and Geography, West Virginia University, 98 Beechurst Avenue, Morgantown, West Virginia 26506, USA*
[5]*Department of Earth and Planetary Sciences, Harvard University, 20 Oxford Street, Cambridge, Massachusetts 02138, USA*

ABSTRACT

The Doonerak fenster of the central Brooks Range, Alaska, exposes a unique package of Cambrian–Devonian(?) volcanic and sedimentary basement rocks (Apoon assemblage) within the Mesozoic–Cenozoic Brookian fold-and-thrust belt. Recognition of a major pre-Mississippian unconformity within the fenster led to previous correlations between the Apoon assemblage and age-equivalent strata in the North Slope subterrane of the composite Arctic Alaska–Chukotka microplate. Previous age constraints on the Apoon assemblage are limited to a handful of Cambrian–Devonian paleontological collections and hornblende K-Ar and $^{40}Ar/^{39}Ar$ ages from mafic dikes ranging from ca. 520 to 380 Ma. We conducted U-Pb and Hf isotopic analyses on igneous and sedimentary units in the Apoon assemblage to test links with the North Slope subterrane and assess the tectonic and paleogeographic setting of this early Paleozoic arc complex. Igneous zircon from a leucogabbro in the Apoon assemblage analyzed using a sensitive high-resolution ion microprobe with reverse geometry (SHRIMP-RG) provided a ^{207}Pb-corrected $^{206}Pb/^{238}U$ age of 462 ± 8 Ma (2σ). Detrital zircon analyzed using laser ablation–inductively coupled plasma–mass spectrometry (LA-ICP-MS) from volcaniclastic and tuffaceous strata of the Apoon assemblage yielded a spectrum of unimodal and polymodal age populations, including prominent age groups at ca. 490–420, 540–520 Ma, 1250–960, 1500–1380, 1945–1750, and 2830–2650 Ma. Lu-Hf isotopic data from the ca. 490–420 Ma age population, including the Middle Ordovician leucogabbro, are highly juvenile (ε_{Hf} ~+7–10), implying a distinct lack of crustal assimilation during Ordovician–Silurian arc magmatism. In context, these data suggest that a juvenile arc complex, herein referred to as the Doonerak arc, marks a prominent tectonic boundary between pre-Mississippian crustal fragments of Laurentian and non-Laurentian affinity in the Arctic Alaska–Chukotka microplate. The U-Pb geochronologic and Hf isotopic data also provide a connection to Taconic–Caledonian arc magmatism along the edge of the Iapetus Ocean and linkages between the Apoon assemblage and the Descon Formation and plutonic equivalents of the Alexander terrane (Prince of Wales Island, Alaska).

[†]justin.v.strauss@dartmouth.edu

INTRODUCTION

Despite a surge in research over the past two decades, the circum-Arctic still suffers from a lack of geological and geophysical constraints on regional tectonic and paleogeographic models. For example, simple kinematic models for the Mesozoic opening of the Canada Basin of the Arctic Ocean are still widely debated (Shephard et al., 2013; Gottlieb et al., 2014; Chian et al., 2016; Houseknecht and Connors, 2016, and references therein). Furthermore, Proterozoic and Paleozoic tectonic reconstructions of the Grenville and Appalachian-Caledonian orogens, two of the most significant accretionary events in North America, still lack consensus on continuity into the Arctic region (e.g., Gee et al., 2008; Cawood et al., 2010, 2015; Pease, 2011; Lorenz et al., 2012). Correlation of the well-calibrated Taconic (ca. 500–450 Ma) and Salinic (ca. 440–420 Ma) orogens of the eastern United States and Atlantic Canada (e.g., van Staal and Barr, 2012) with age-equivalent events in the Arctic is uncertain, as remnants of these Ordovician–Silurian accretionary events are only preserved in highly deformed Caledonian nappes in Scandinavia (Gee et al., 2013; Corfu et al., 2014, and references therein) and East Greenland (Kalsbeek et al., 2000, 2001, 2008; Rehnström, 2010).

Many oceanic and continental fragments in the circum-Arctic and North American Cordillera have Siberian, Baltican, and Laurentian affinities and likely originated along the fringes of the Iapetus Ocean (Trettin, 1987; Grove et al., 2008; Amato et al., 2009; Colpron and Nelson, 2009, 2011; Miller et al., 2011; Beranek et al., 2013a; and many others). The Arctic Alaska–Chukotka terrane or microplate (Churkin et al., 1985; Hubbard et al., 1987) encompasses the Brooks Range, North Slope, and Seward Peninsula of northern Alaska, the Chukotka Peninsula and New Siberian and Wrangel Islands of Arctic Russia, and the adjacent continental shelves of the Bering, Beaufort, and Chukchi Seas (Fig. 1; Miller et al., 2006; Amato et al., 2014; Till et al., 2014a; Moore et al., 2015, and references therein). This composite microplate is characterized by multiple Neoproterozoic–Mesozoic crustal fragments with purported affinities to Baltica, Laurentia, Panthalassa, and Siberia (Churkin et al., 1985; Moore et al., 1994; Natal'in et al., 1999; Miller et al., 2006, 2010, 2011; Amato et al., 2009, 2014; Sokolov, 2010; Strauss et al., 2013; Dumoulin et al., 2014). Given its complex pre-Devonian accretionary history and centralized location along the edge of the Canada Basin (Fig. 1), the geology of the Arctic Alaska–Chukotka microplate provides first-order piercing points for Mesozoic tectonic

GSA Bulletin; May/June 2017; v. 129; no. 5/6; p. 649–676; doi: 10.1130/B31593.1; 11 figures; 2 tables; Data Repository item 2016366; published online 10 February 2017.

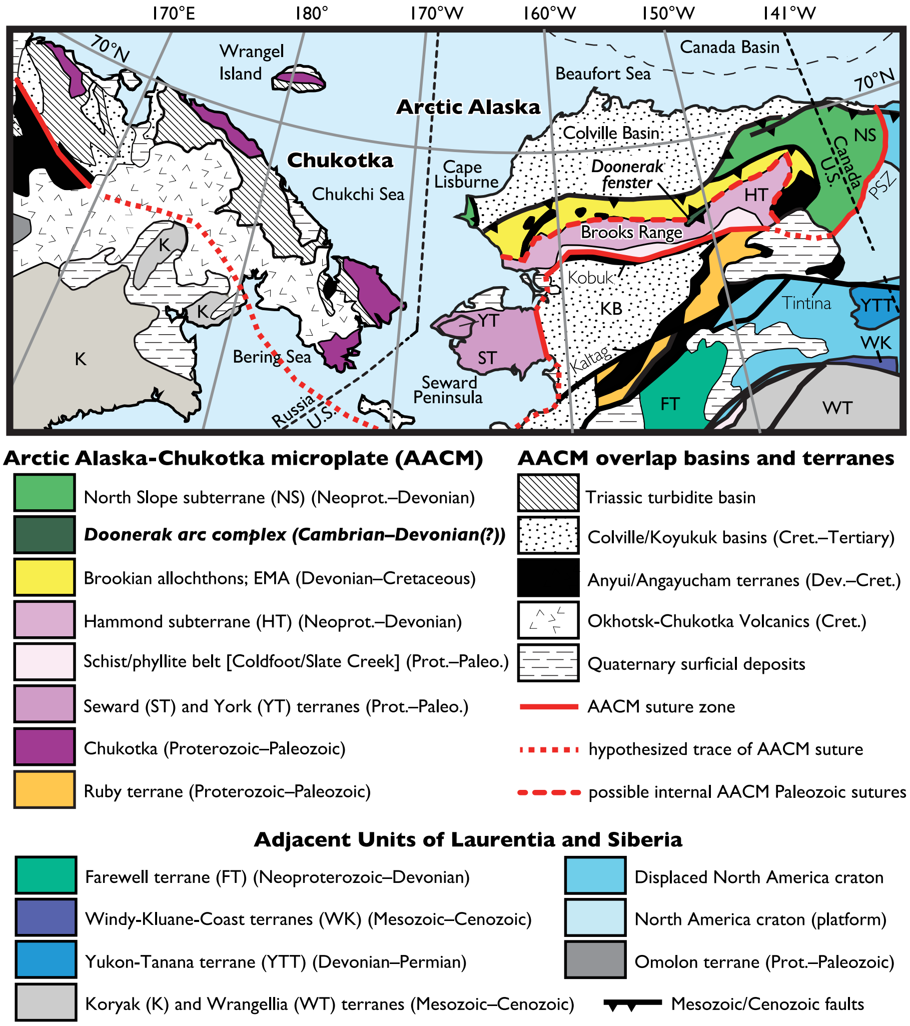

Figure 1. Key geological components of the composite Arctic Alaska–Chukotka microplate (AACM) after Mull (1982), Miller et al. (2006), Amato et al. (2009), and Moore et al. (1994, 2015). The Doonerak fenster is located within the central Brooks Range and shares affinities with the North Slope subterrane of Arctic Alaska. Note the hypothesized internal suture within the Arctic Alaska–Chukotka microplate, including the boundary between the North Slope and other Paleozoic components, as marked by the Doonerak arc complex. KB—Koyukuk Basin, Dev.—Devonian, Cret.—Cretaceous, Neoprot.—Neoproterozoic, Jur.—Jurassic, Prot.—Proterozoic, PSZ—Porcupine shear zone, Paleo.—Paleozoic, EMA—Endicott Mountains Allochthon.

reconstructions of the Arctic (Miller et al., 2006) and key paleogeographic links among circum-Arctic paleocontinents (Dumoulin et al., 2002, 2014; Blodgett et al., 2002; Amato et al., 2009, 2014; Macdonald et al., 2009; Cocks and Torsvik, 2011; Strauss et al., 2013; Cox et al., 2015). The Arctic Alaska–Chukotka microplate also preserves a rich history of tectonic events that may constrain the nature and geographic extent of the Grenville, Timanian, Caledonian-Appalachian, and Ellesmerian orogenic belts in the Arctic (Gee and Pease, 2004; Amato et al., 2009; Colpron and Nelson, 2009, 2011; Beranek et al., 2010, 2013a; Miller et al., 2011; Pease, 2011; Anfinson et al., 2012a, 2012b; Lorenz et al., 2012; Strauss et al., 2013; Hadlari et al., 2014; Malone et al., 2014; Till et al., 2014a, 2014b; Ershova et al., 2015, 2016; Johnson et al., 2016).

Neoproterozoic–Devonian sedimentary and metamorphic rocks of the Arctic Alaska–Chukotka microplate may be separated into at least two distinct pre-Mississippian basement domains based on igneous and detrital zircon geochronological data, paleobiological affinities of fossil assemblages, and stratigraphic correlations (Strauss et al., 2013; Till et al., 2014a, and references therein): a northeastern region (in present coordinates) characterized by Laurentian affinity platformal and basinal strata that are commonly included in the North Slope subterrane (Strauss et al., 2013; Cox et al., 2015; McClelland et al., 2015a; Lane et al., 2015; Johnson et al., 2016) and a southwestern area dominated by mostly metamorphosed sedimentary rocks with affinities to Siberia and Baltica that are assigned to other subterranes within the Arctic Alaska–Chukotka microplate (Fig. 1; Kos'ko et al., 1993; Patrick and McClelland, 1995; Natal'in et al., 1999; Blodgett et al., 2002; Dumoulin et al., 2002, 2014; Amato et al., 2009, 2014; Miller et al., 2006, 2010, 2011; Till et al., 2014a, 2014b; Akinin et al., 2015). The precise boundary between these two broadly defined pre-Mississippian basement domains of the Arctic Alaska–Chukotka microplate and its tectonic significance are poorly understood; however, previous workers have highlighted Ordovician–Devonian arc-related rocks of the Doonerak fenster (Figs. 1 and 2) in the central Brooks Range of Alaska as a plausible location for a major internal suture within the Arctic Alaskan portion of the Arctic Alaska–Chukotka microplate (Mull, 1982; Grantz et al., 1991; Dumoulin et al., 2000; Strauss et al., 2013). In particular, Strauss et al. (2013) proposed that the early Paleozoic Apoon assemblage of the

Figure 2. Simplified geologic map of the Doonerak fenster, central Brooks Range of Alaska, after Dillon et al. (1986), Mull et al. (1987a), Oldow et al. (1987a), Moore et al. (1997), Julian and Oldow (1998), and Seidensticker and Oldow (1998). (A) Major map units in the central Brooks Range after Dillon et al. (1986) and Moore et al. (1997). The black box shows the rough outline of the inset map of the Doonerak fenster (B) and the cross-section line (A–A′) shown in Figure 3. Note that the cross section extends further north out of the figure frame. The localities with previous age data are shown as circled numbers—these data are presented in Table 1. (B) Geologic map of study area traverse (after Julian, 1989; Seidensticker and Oldow, 1998; our mapping) showing the sample locations (yellow stars) and major map units in the Apoon assemblage. Dhf—Devonian Hunt Fork Shale; Ddrp—Devonian Dietrich River phyllite; CTe—Carboniferous–Triassic Endicott Group undivided; Pzc—Paleozoic Apoon assemblage unit Pzc; Pzp—Paleozoic Apoon assemblage unit Pzp; Pza/Pzv—Paleozoic Apoon assemblage units Pzv and Pza; Ptcp—Paleozoic Trembley Creek phyllite; conod.—conodont; brachs—brachiopods.

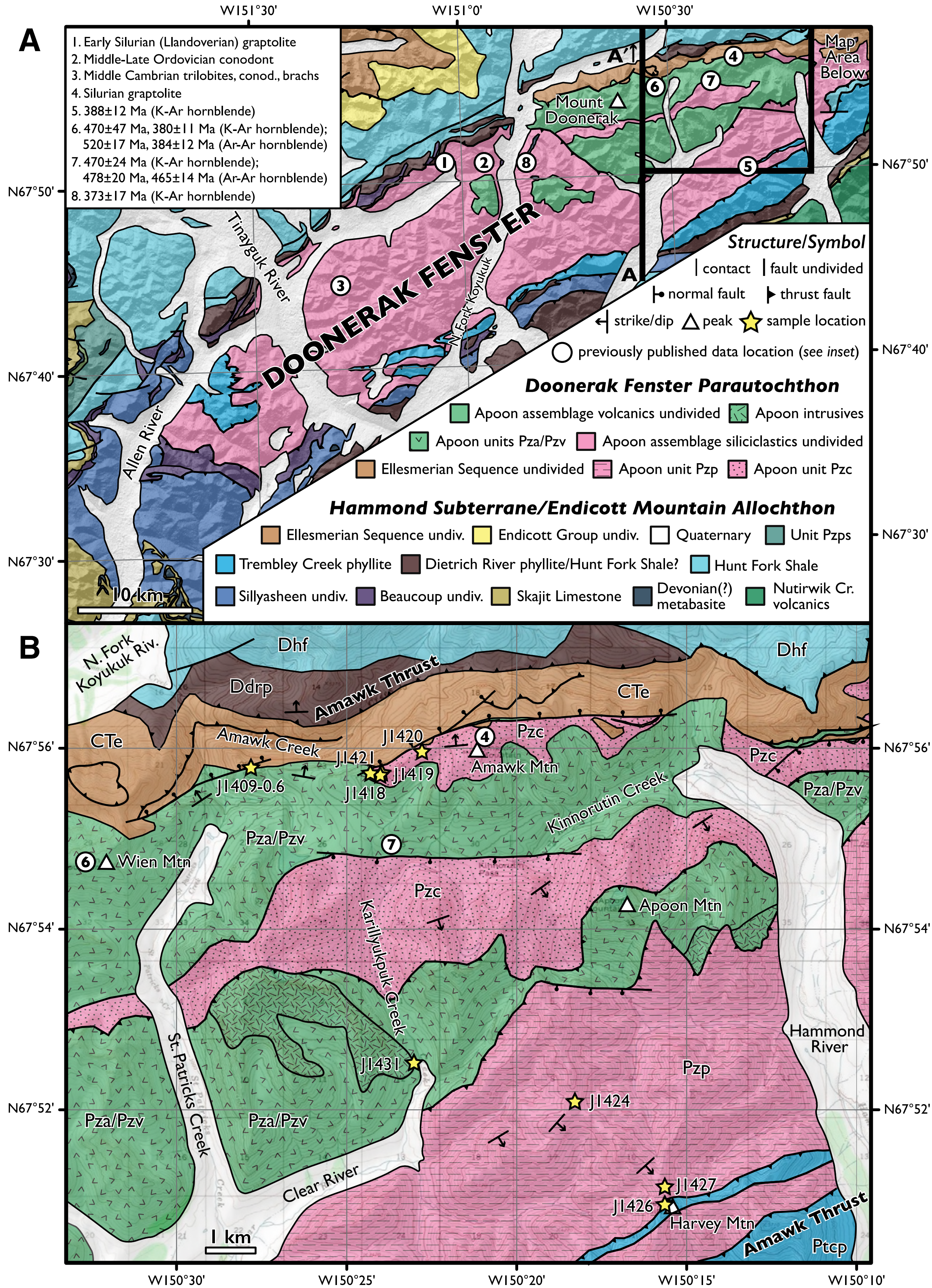
A
W151°30'
W151°0'
W150°30'
1. Early Silurian (Llandoverian) graptolite
2. Middle-Late Ordovician conodont
3. Middle Cambrian trilobites, conod., brachs
4. Silurian graptolite
5. 388±12 Ma (K-Ar hornblende)
6. 470±47 Ma, 380±11 Ma (K-Ar hornblende); 520±17 Ma, 384±12 Ma (Ar-Ar hornblende)
7. 470±24 Ma (K-Ar hornblende); 478±20 Ma, 465±14 Ma (Ar-Ar hornblende)
8. 373±17 Ma (K-Ar hornblende)
A'
A
Mount Doonerak
Map Area Below
N67°50'
N67°40'
N67°30'
Tinayguk River
N. Fork Koyukuk
DOONERAK FENSTER
Allen River
10 km
Structure/Symbol
contact
fault undivided
normal fault
thrust fault
strike/dip
peak
sample location
previously published data location (see inset)
Doonerak Fenster Parautochthon
Apoon assemblage volcanics undivided
Apoon intrusives
Apoon units Pza/Pzv
Apoon assemblage siliciclastics undivided
Ellesmerian Sequence undivided
Apoon unit Pzp
Apoon unit Pzc
Hammond Subterrane/Endicott Mountain Allochthon
Ellesmerian Sequence undiv.
Endicott Group undiv.
Quaternary
Unit Pzps
Trembley Creek phyllite
Dietrich River phyllite/Hunt Fork Shale?
Hunt Fork Shale
Sillyasheen undiv.
Beaucoup undiv.
Skajit Limestone
Devonian(?) metabasite
Nutirwik Cr. volcanics
B
N. Fork Koyukuk Riv.
Dhf
Ddrp
Amawk Thrust
CTe
Amawk Creek
J1420
J1421
J1419
J1418
J1409-0.6
Pzc
Amawk Mtn
Pza/Pzv
Kinnorutin Creek
Wien Mtn
Apoon Mtn
Karillyukpuk Creek
J1431
Pzp
J1424
J1427
J1426
Harvey Mtn
Hammond River
St. Patricks Creek
Clear River
Ptcp
1 km
N67°56'
N67°54'
N67°52'
W150°30'
W150°25'
W150°20'
W150°15'
W150°10'

Doonerak fenster evolved independently and in a similar tectonic setting to the age-equivalent M'Clintock arc of the Pearya terrane (Trettin, 1987) of Ellesmere Island, Canada, prior to Arctic Alaska–Chukotka microplate amalgamation in Devonian time. In this context, the Apoon assemblage may provide a key link to early Paleozoic arc magmatism associated with the closure of the northernmost Iapetus Ocean. Here, we present the first U-Pb and Lu-Hf isotopic analyses on zircon from early Paleozoic mafic igneous rocks and sedimentary units of the Apoon assemblage to assess the tectonic and paleogeographic setting of this poorly understood arc complex.

GEOLOGIC SETTING OF THE DOONERAK FENSTER

The E-W–trending Brooks Range of northern Alaska and Yukon borders the southern edge of the Canada Basin and represents a north-vergent fold-and-thrust belt of Middle Jurassic to Tertiary age (Fig. 1; Mull, 1982; Oldow et al., 1987a; Grantz et al., 1991; Moore et al., 1994). The ~1000-km-long Brookian orogen is characterized by a southern hinterland of polydeformed metamorphic rocks and a northern foreland belt dominated by allochthonous thrust sheets and a mildly deformed foreland basin (Moore et al., 1994, 2015, and references therein). The Doonerak fenster (Brosgé and Reiser, 1971) is a NE-SW–trending, doubly plunging antiform in the central Brooks Range (Figs. 1, 2, and 3) that exposes the structurally lowest level of the Brookian orogen (Dutro et al., 1976; Mull et al., 1987a; Oldow et al., 1987a). The fenster is capped by the Amawk thrust (Figs. 2 and 3), which is the basal detachment of the Endicott Mountains allochthon, a foreland-dipping imbricate stack of thrust sheets composed of upper Paleozoic siliciclastic and carbonate rocks of the Endicott and Lisburne groups (Brosgé et al., 1962, 1979; Dutro et al., 1976; Mull, 1982; Mull et al., 1987a; Oldow et al., 1987a; Moore et al., 1994, 1997; Handschy, 1998; Phelps and Avé Lallement, 1998; Seidensticker and Oldow, 1998). Basement rocks of the Doonerak fenster are interpreted as correlative with pre-Mississippian units of the North Slope subterrane and as underlying the Brookian Colville foreland basin (Brosgé et al., 1974; Carter and Laufeld, 1975; Armstrong et al., 1976; Dutro et al., 1976; Mull, 1982; Mull et al., 1987a, 1987b; Moore et al., 1994). This correlation provides a critical constraint on allochthonous units in the fold-and-thrust belt and the Brookian parautochthon, requiring substantial N-vergent displacement of the Endicott Mountains allochthon of at least 80 km and perhaps totaling hundreds of kilometers (Mull, 1982; Mull et al., 1987b; Oldow et al., 1987a; Moore et al., 1994, 1997).

The Brooks Range has commonly been subdivided on the basis of differing pre-Mississippian lithotectonic assemblages (e.g., Mull, 1982; Jones et al., 1987; Silberling et al., 1992; Moore et al., 1994, 1997). Throughout this manuscript, we use the subterrane nomenclature highlighted by Moore et al. (1994, 1997) to delineate the approximate boundaries of distinct pre-Mississippian basement domains (Fig. 1). Although the true boundaries of the Neoproterozoic–early Paleozoic crustal fragments that comprise the Arctic Alaska–Chukotka microplate are unknown, we view this as the simplest and most consistent terminology to employ in Arctic Alaska until a new nomenclature is erected.

The early Paleozoic Apoon assemblage of the Doonerak fenster (Oldow et al., 1984; Julian, 1989; Julian and Oldow, 1998) is considered to be time-equivalent with pre-Mississippian rocks of the North Slope (Franklinian sequence of Lerand, 1973), based in part on recognition of a prominent sub-Mississippian unconformity beneath the Kekiktuk Conglomerate of the Endicott Group in both regions and similarities in the overlying upper Paleozoic to lower Mesozoic sedimentary succession (i.e., the Ellesmerian sequence; Fig. 4; Moore et al., 1994, and references therein). This regionally significant unconformity is attributed to contractional deformation and subsequent extension associated with the enigmatic Devonian–Mississippian Romanzof and Ellesmerian orogenies (Churkin, 1975; Brosgé et al., 1962; Reed, 1968; Dutro, 1970; Sable, 1977; Oldow et al., 1987b; Anderson et al., 1994; Moore et al., 1994; Lane, 2007). While most previous workers have discussed the Doonerak fenster in light of its Mesozoic–Tertiary significance, this locality may be equally important to our understanding of the early Paleozoic paleogeography and tectonics of the Arctic.

The Apoon assemblage is divided into four, fault-bounded lithological units for which the primary depositional and/or intrusive relationships remain uncertain (Fig. 4; Julian, 1989; Julian and Oldow, 1998). From north to south, these include an ~500-m-thick mafic to intermediate pyroclastic volcanic unit (Pza), an ~1.5-km-thick heterogeneous siliciclastic succession (Pzc), an ~400-m-thick mafic volcanic and volcaniclastic package with minor intrusive rocks (Pzv), and an ~3-km-thick fine-grained phyllite and slate unit with minor limestone and volcaniclastic strata (Pzp; Fig. 4). Although the Apoon volcanic rocks are slightly altered (Julian, 1989), geochemical data from both units Pzv and Pza yield compositional overlap between calc-alkaline arc basalts, island-arc tholeiites, and mid-ocean-ridge basalt (MORB) geochemical fields (Moore, 1987; Julian, 1989; Moore et al., 1997; Julian and Oldow, 1998). Herein, we refer to these units collectively as either the Apoon assemblage or Doonerak arc complex based on their widespread exposure near Mount Doonerak (Fig. 2).

Radiometric age constraints for the Apoon assemblage are limited to six hornblende K-Ar and $^{40}Ar/^{39}Ar$ ages from mafic sills and dikes (Fig. 2; Table 1; Dutro et al., 1976). These analyses yielded cooling ages that range from ca. 520 to 373 Ma and broadly cluster into two groups,

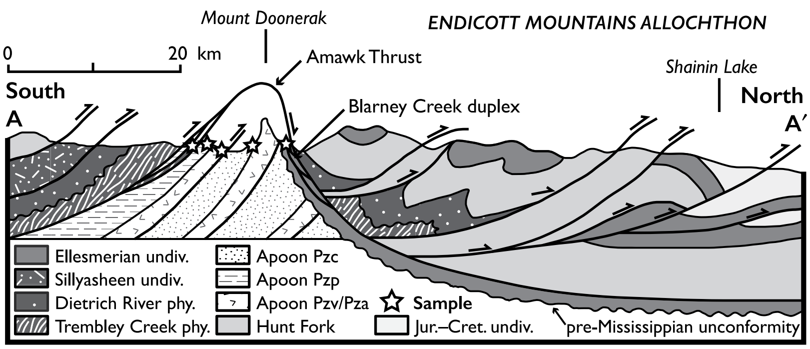

Figure 3. Highly simplified geological cross section of the Doonerak fenster from A to A′ (outlined in Fig. 2) illustrating the schematic position of sampled pre-Mississippian rocks within the fenster. Note the schematic Blarney Creek duplex (Oldow et al., 1984) in Ellesmerian sequence rocks of the footwall of the Amawk thrust. This cross section indicates the presence of a distinct pre-Mississippian unconformity between the Endicott Group and Apoon assemblage (see text for an explanation). Figure is modified after Dutro et al. (1976), Dillon et al. (1986), Mull et al. (1987b), Oldow et al. (1987a), Adams et al. (1997), Moore et al. (1997), and Julian and Oldow (1998).

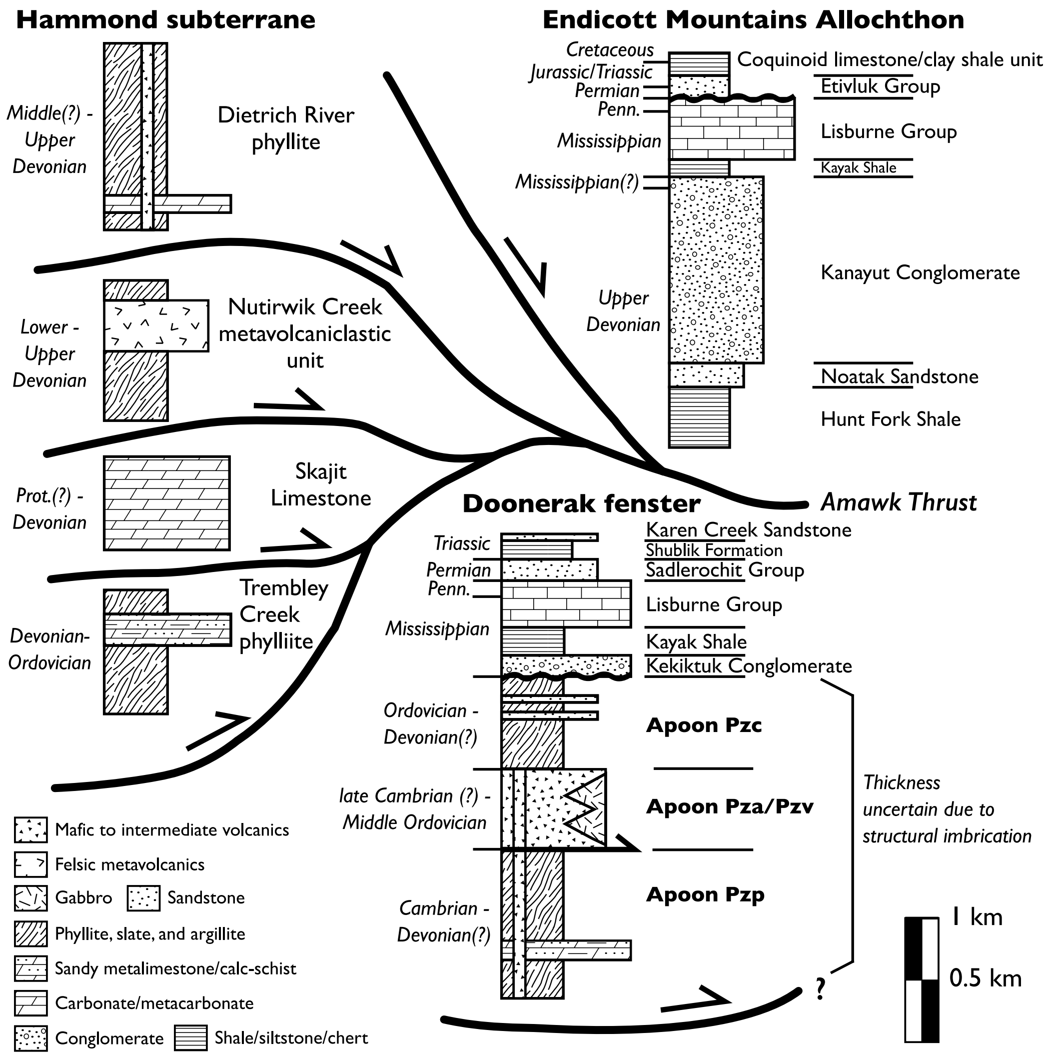

Figure 4. Simplified stratigraphic and structural relationships in the central Brooks Range, Alaska, among the Endicott Mountains allochthon, Doonerak fenster, and Hammond subterrane. Figure is modified after Moore et al. (1997) with stratigraphic nomenclature from Julian (1989), Julian and Oldow (1998), and Moore et al. (1997). Prot.—Proterozoic; Penn.—Pennsylvanian.

ca. 380 Ma and ca. 470 Ma, with one analysis yielding a 520 ± 17 Ma age (Dutro et al., 1976). Further age data from the siliciclastic and carbonate units of the Apoon assemblage are provided by geographically isolated paleontological collections (Fig. 2; Table 1). For reference, we use the time scale of Cohen et al. (2013; updated in 2015) throughout this manuscript to describe the age of different fossil assemblages or stratigraphic units. Repetski et al. (1987) reported Middle(?) Ordovician conodonts from siliceous volcaniclastic rocks, presumably of unit Pzv, and Lower Silurian (Llandoverian) graptolites and Silurian conodonts from a unit that lithologically resembles Pzc (Fig. 2; Table 1). Julian and Oldow (1998) also reported poorly preserved Silurian graptolites from unit Pzc near the summit of Amawk Mountain (Fig. 2; Table 1). Sandy meta-limestone units from the extreme southwestern part of the Doonerak fenster (presumably of unit Pzp) yielded early–middle Cambrian (Global Stage 4–5, Series 2–3) trilobites of Siberian affinity (Fig. 2; Table 1; Dutro et al., 1984a), as well as protoconodonts, hyolithids, and acrotretid brachiopods (Dutro et al., 1984a, 1984b). Based on these sparse geochemical, geochronological, and paleontological data, the Apoon assemblage is considered to represent the remnants of an early Paleozoic island-arc succession (Julian, 1989; Julian and Oldow, 1998); however, there are no early Paleozoic arc-related plutonic rocks preserved in the Brooks Range, and the true tectonic setting and polarity of this magmatic arc are currently unknown. As a result, the paleogeographic significance of the Doonerak arc within the greater context of the Arctic Alaska–Chukotka microplate and Arctic region remains uncertain (Dutro et al., 1976; Moore, 1987; Julian, 1989; Julian and Oldow, 1998).

The Endicott Group of the Doonerak fenster consists of the Upper Devonian(?)–Lower Mississippian Kekiktuk Conglomerate and Lower Mississippian Kayak Shale (Fig. 4; Armstrong et al., 1976). These dominantly siliciclastic rocks are regionally overlain by Lower Mississippian–Lower Pennsylvanian carbonate strata of the Lisburne Group, Permian siliciclastic rocks of the Sadlerochit Group, and Triassic sooty shale, limestone, and sandstone of the Shublik Formation and Karen Creek Sandstone

TABLE 1. PUBLISHED AGE CONSTRAINTS FOR THE APOON ASSEMBLAGE, DOONERAK FENSTER, BROOKS RANGE, ALASKA

Sample number	Age (Ma)	Method	Type	Latitude (°N)	Longitude (°W)	Citation	Number in Figure 2
Geochronology							
74ARr-11	388 ± 12	K-Ar	Hornblende	67 50.3′	150 17.6′	Dutro et al. (1976)	5
59ABe-478	470 ± 47	K-Ar	Hornblende	67 54.7′	150 32.6′	Dutro et al. (1976)	6
59ABe-478	520 ± 17	$^{40}Ar/^{39}Ar$	Hornblende	67 54.7′	150 32.6′	Dutro et al. (1976)	6
65ALe-1	380 ± 11	K-Ar	Hornblende	67 54.7′	150 32.6′	Dutro et al. (1976)	6
65ALe-1	384 ± 12	$^{40}Ar/^{39}Ar$	Hornblende	67 54.7′	150 32.6′	Dutro et al. (1976)	6
65ALe-6	470 ± 24	K-Ar	Hornblende	67 54.8′	150 24.1′	Dutro et al. (1976)	7
65ALe-6	478 ± 20	$^{40}Ar/^{39}Ar$	Hornblende	67 54.8′	150 24.1′	Dutro et al. (1976)	7
65ALe-6a	465 ± 14	$^{40}Ar/^{39}Ar$	Hornblende	67 54.8′	150 24.1′	Dutro et al. (1976)	7
58ARr-8A	373 ± 17	K-Ar	Hornblende	67 51.3′	150 51.0′	Dutro et al. (1976)	8
Biostratigraphy							
None given	Silurian	Graptolite	None Given	On map	On map	M. Churkin (personal commun.) *in* Julian and Oldow (1998)	4
81 Abe 52C USGS 9477-CO	Early–middle Cambrian (Global Stage 4–5)	Trilobite	*Kootenia* cf. *K. anabarensis* Lermontova, cf. *"Parehmania" lata* Chernysheva, and *Pagetia* sp.	On map	On map	Dutro et al. (1984a)	3
81 Abe 52A USGS 9475-CO	Middle Cambrian	Brachiopod	*Nisusia* sp. and *Linnarssonia* sp.	On map	On map	Dutro et al. (1984b)	3
81 Abe 52B USGS 9476-CO	Middle Cambrian	Conodont	*Westergaardodina* sp., hyolithids	On map	On map	Dutro et al. (1984b)	3
USGS 9473-CO	Middle-Late Ordovician (Arenigian–Caradocian)	Conodont	*Periodon* ramiform	67 51.5′	150 56′	Repetski et al. (1987)	2
83Br 781MC; 84ADu 5 (USGS 11447-SD)	Early Silurian (Llandoverian)	Graptolite	*Orthograptus* sp?, *Pristiograptus?* sp., *Monograptus* sp., *Monograptus(?)* sp.	67 51.2′	151 03′	Repetski et al. (1987)	1
83Br 781MC; 84ADu 5 (USGS 11447-SD)	Early Silurian (Llandoverian)	Conodont	*Dapsilodus*	67 51.2′	151 03′	Repetski et al. (1987)	1

(Fig. 4; Brosgé et al., 1962, 1974; Armstrong et al., 1976; Armstrong and Mamet, 1978; Dutro et al., 1976; Mull et al., 1987a; Adams et al., 1997; Dumoulin et al., 1997). Although the Kekiktuk Conglomerate of the Doonerak fenster region is assumed to be Late Devonian(?)–early Mississippian in age based on correlations with plant fossil–bearing strata in the NE Brooks Range (Brosgé et al., 1962), there are no direct age constraints on these strata from this specific region. A minimum age constraint for the Kekiktuk Conglomerate is provided by fossiliferous Lower Mississippian (Osagean) strata of the overlying Kayak Shale (Armstrong et al., 1976; Armstrong and Mamet, 1978; Dumoulin et al., 1997). To the north of the Doonerak fenster, the Endicott Group of the Endicott Mountains allochthon consists, in ascending order, of the Hunt Fork Shale, Noatak Sandstone, Kanayut Conglomerate, and Kayak Shale (Figs. 2, 3, and 4).

Pre-Mississippian metasedimentary and metavolcanic rocks of the Hammond and Coldfoot subterranes of the Arctic Alaska–Chukotka microplate are mostly exposed to the south of the Doonerak fenster and compose the metamorphic hinterland of the Brooks Range (Moore et al., 1994, 1997; Till et al., 2008, and references therein). Although little consensus exists over the primary stratigraphic order of these highly deformed rocks, the Hammond subterrane surrounding the Doonerak fenster has been independently subdivided into both nine informally named metaclastic and metacarbonate units (Dillon, 1989; Dumoulin and Harris, 1994; Moore et al., 1997) and seven distinct nappe sequences of the Skajit allochthon (Oldow et al., 1987a, 1998). The most characteristic stratigraphic unit of the Hammond subterrane is a largely dismembered Upper Proterozoic(?)–Middle Devonian metacarbonate, which was loosely referred to as the Skajit limestone (Brosgé et al., 1962; Brosgé and Reiser, 1964; Dillon et al., 1988; Dillon, 1989; Dumoulin and Harris, 1994). These metacarbonate rocks have been subsequently described and locally subdivided into distinct units of different age and depositional setting that appear to represent the remnants of a single, long-lived late Proterozoic(?)–Devonian carbonate platform succession (Dumoulin and Harris, 1994; Moore et al., 1997; Oldow et al., 1998; Dumoulin et al., 2002, 2014). Many of the metaclastic rocks of the Hammond subterrane were originally mapped as belonging to the heterogeneous Upper Devonian Beaucoup Formation (Dutro et al., 1976; Dillon et al., 1986, 1988; Dillon, 1989); however, subsequent work has subdivided these metasedimentary and metavolcanic rocks into a suite of Upper Ordovician–Upper Devonian lithological or lithotectonic successions because of their regional heterogeneity (Figs. 2 and 4; Oldow et al., 1987a, 1998; Moore et al., 1997). Here, we adopt the informal nomenclature of Moore et al. (1997) in our description of the metasedimentary units surrounding the Doonerak fenster (Figs. 2 and 4) and build upon previous sparse geochronological constraints with new U-Pb and $^{40}Ar/^{39}Ar$ data from the Hammond subterrane.

ANALYTICAL METHODS

U-Pb Zircon Geochronology and Lu-Hf Isotopic Analysis

Six samples from the Apoon assemblage (J1418, J1419, J1420, J1424, J1427, and J1431), two samples from the Kekiktuk Conglomerate of the Endicott Group (J1409-0.6 and J1421), and one sample from a thrust sliver of the Trembley Creek phyllite of the Hammond subterrane (J1426; Moore et al., 1997) were collected during the summer of 2014 for igneous and detrital zircon U-Pb geochronology and Hf isotope geochemistry (Fig. 2; Table 2). Standard mineral separation procedures were followed at the University of Iowa and Stanford University, which included crushing, sieving, water density and magnetic separation, and heavy liquid density separation.

Approximately 300–500 zircon grains were randomly selected from detrital samples and mounted in epoxy, ground to expose the grain interiors, and polished prior to cathodoluminescence (CL) and backscattered electron (BSE) imaging. A similar mounting procedure was

TABLE 2. GLOBAL POSITIONING SYSTEM (GPS) COORDINATES (IN DECIMAL DEGREES) OF GEOCHRONOLOGY SAMPLES, DOONERAK FENSTER, BROOKS RANGE, ALASKA

Sample name	Map unit	Location	Latitude (°N)	Longitude (°W)
J1409-0.6	Kekiktuk Conglomerate	Amawk Ridge	67.9296389	150.4688056
J1418	Apoon–Pzc	Amawk Ridge	67.9278889	150.4046111
J1419	Apoon–Pzc	Amawk Ridge	67.9279444	150.4046667
J1420	Apoon–Pzc	Amawk Ridge	67.9311389	150.38025
J1421	Kekiktuk Conglomerate	Amawk Ridge	67.927678	150.410278
J1424	Apoon–Pzp	Harvey Mountain	67.8686944	150.3073056
J1426	Trembley Creek phyllite	Harvey Mountain	67.8493333	150.2604722
CH14DW16	Trembley Creek phyllite	Harvey Mountain	67.8493333	150.2604722
J1427	Apoon–Pzp	Harvey Mountain	67.8508333	150.2606389
J1431	Apoon–Pzv	Karillyukpuk Creek	67.87675	150.3878056

Note: Pzc—heterogeneous siliciclastic succession; Pzp—fine-grained phyllite and slate unit with minor limestone and volcaniclastic strata; Pzv—mafic volcanic and volcaniclastic package with minor intrusive rocks.

applied to pristine grains selected from igneous sample J1431. CL imaging of zircon mounts at the University of Iowa used a Gatan Chroma CL2 unit mounted on a Hitachi S3400 scanning electron microscope (SEM). CL and BSE images collected at Stanford University used a JEOL 5600 SEM equipped with an in-house blue-filtered CL detector. These CL and BSE images were used to select spot locations to avoid inherited cores, complex zoning, or zones of possible metamictization.

U-Pb isotopic ratios and trace-element compositions for igneous sample J1431 were determined in situ on bulk-separated zircon on the sensitive high-resolution ion microprobe with reverse geometry (SHRIMP-RG) instrument at the U.S. Geological Survey–Stanford University Ion Probe Laboratory following procedures outlined by Barth and Wooden (2006, 2010). A separate aliquot of zircon from sample J1431 was also analyzed using laser ablation–inductively coupled plasma–mass spectrometry (LA-ICP-MS) at the University of Arizona LaserChron Center in order to select grains for Hf isotope geochemistry. U-Pb isotopic ratios for zircon from the remaining detrital samples were determined *in situ* using LA-ICP-MS at the University of Arizona LaserChron Center following methods outlined in Gehrels et al. (2006, 2008) and Gehrels and Pecha (2014). A subset of these detrital and igneous zircons from the same mounts was analyzed for Hf isotope geochemistry using high-resolution-ICP-MS (HR-ICP-MS) at the Arizona LaserChron Center following methods outlined by Gehrels and Pecha (2014). In each analysis, a 40-μm-diameter ablation site was centered over the previously excavated U-Pb analysis pit. Detailed descriptions of the SHRIMP-RG, LA-ICP-MS, and HR-ICP-MS analytical methods are provided in the GSA Data Repository.[1]

Reported uncertainties on the U-Pb isotopic data are at the 1σ level and include only measurement errors. Weighted mean SHRIMP-RG ^{207}Pb-corrected ^{206}Pb/^{238}U ages were calculated by utilizing a subset of concordant spot analyses. Individual spot ages are reported with internal uncertainty only, whereas weighted averages include an external uncertainty determined as the standard deviation of the standards within a given analytical session. During data reduction and prior to data filtering for the LA-ICP-MS analyses, ~5%–10% of analyses were rejected due to anomalous down-hole fractionation interpreted to reflect crossing internal age boundaries or metamict zones (Gehrels and Pecha, 2014). These background-corrected analytical data were then reduced from raw ratios to ^{206}Pb/^{238}U, ^{207}Pb/^{235}U, and ^{207}Pb/^{206}Pb ratios and ages using the AgeCalc macro and then assigned a ^{206}Pb/^{238}U "best age" if the result was younger than 900 Ma, or a ^{207}Pb/^{206}Pb "best age" if the ^{206}Pb/^{238}U result was older than 900 Ma. Following these data reduction steps, we excluded analyses from our plots based on the following criteria: (1) >10% uncertainty in ^{206}Pb*/^{238}U age, (2) >10% uncertainty in ^{206}Pb*/^{207}Pb* age, (3) >10% discordance or >5% reverse discordance on analyses with ^{206}Pb*/^{238}U ages older than 700 Ma, (4) analyses for which the 2σ error ellipse did not overlap with concordia, (5) >500 "counts per second (cps) ^{204}Pb intensity, (6) U concentrations >1000 ppm, and (7) U/Th >10. The data are presented on concordia diagrams and relative age-probability plots generated with Isoplot 3 (Ludwig, 2003).

^{40}Ar/^{39}Ar Geochronology

An ~20 cm^3 aliquot of sample CH14DW16 from the Trembley Creek phyllite (from the same location as J1426; Fig. 2; Table 2) was hand-crushed with a mortar and pestle at Stanford University. Muscovite was separated by electrostatic properties, sieved to various grain sizes, hand-selected to avoid contaminant phases and/or inclusions, and irradiated following detailed methods described in the GSA Data Repository (see footnote 1). Argon isotopic ratios were measured with a Nu instrument Noblesse multicollector mass spectrometer at Stanford University following methods outlined in Oze et al. (2017) and described in the GSA Data Repository (see footnote 1). Data reduction was performed with an in-house software package (AGECAL v. 12.2; Marty Grove). The raw data were corrected for procedural blank, detector gain, ion counter dead time, radioactive decay, and irradiation constants for neutron-induced argon, and the calculation of model ages assumed an atmospheric argon ratio of ^{40}Ar/^{36}Ar = 295.5 (McDougall and Harrison, 1999). Analytical errors propagated are 1σ standard deviations. Uncertainties in atmospheric ^{40}Ar/^{36}Ar composition and interfering nuclear reactions were not considered or propagated for individual steps but were included in the total errors associated with model ages.

FIELD OBSERVATIONS AND ANALYTICAL RESULTS

SHRIMP-RG U-Pb Geochronology

Coarse-grained leucogabbro in Apoon map unit Pzv (sample J1431) was sampled from a >200-m-thick, previously unrecognized intrusive body exposed on the west side of Karillyukpuk Creek near the confluence with Clear River (Fig. 2). The contact between this homogeneous gabbroic unit with volcanic rocks of unit Pzv is locally covered by talus (Fig. 5A); however, regional geochemical data support a petrogenetic connection between the plutonic and volcanic units, and one can recognize clear intrusive contacts at other localities (Fig. 2; Julian, 1989; Julian and Oldow, 1998). In thin section, sample J1431 mostly consists of partially altered subhedral plagioclase laths and elongate, prismatic, and euhedral augite with accessory intergranular hornblende, biotite, calcite, quartz, and opaques. Euhedral zircons in sample J1431 range from ~50 to 150 μm and have blocky to prismatic terminations with well-developed oscillatory zonation. No inherited components were apparent in the grains that were imaged with CL and analyzed for U-Pb geochronology. Excluding two analyses with high errors, the remaining six concordant analyses define a ^{207}Pb-corrected ^{206}Pb/^{238}U weighted mean age of 462 ± 8 Ma (2σ; Fig. 6). A separate aliquot of zircon

[1]GSA Data Repository item 2016366, including U-Pb SHRIMP-RG and LA-ICP-MS, ^{40}Ar-^{39}Ar MC-ICP-MS, and Lu-Hf HR-ICP-MS analytical methods and data tables, is available at http://www.geosociety.org/datarepository/2016 or by request to editing@geosociety.org.

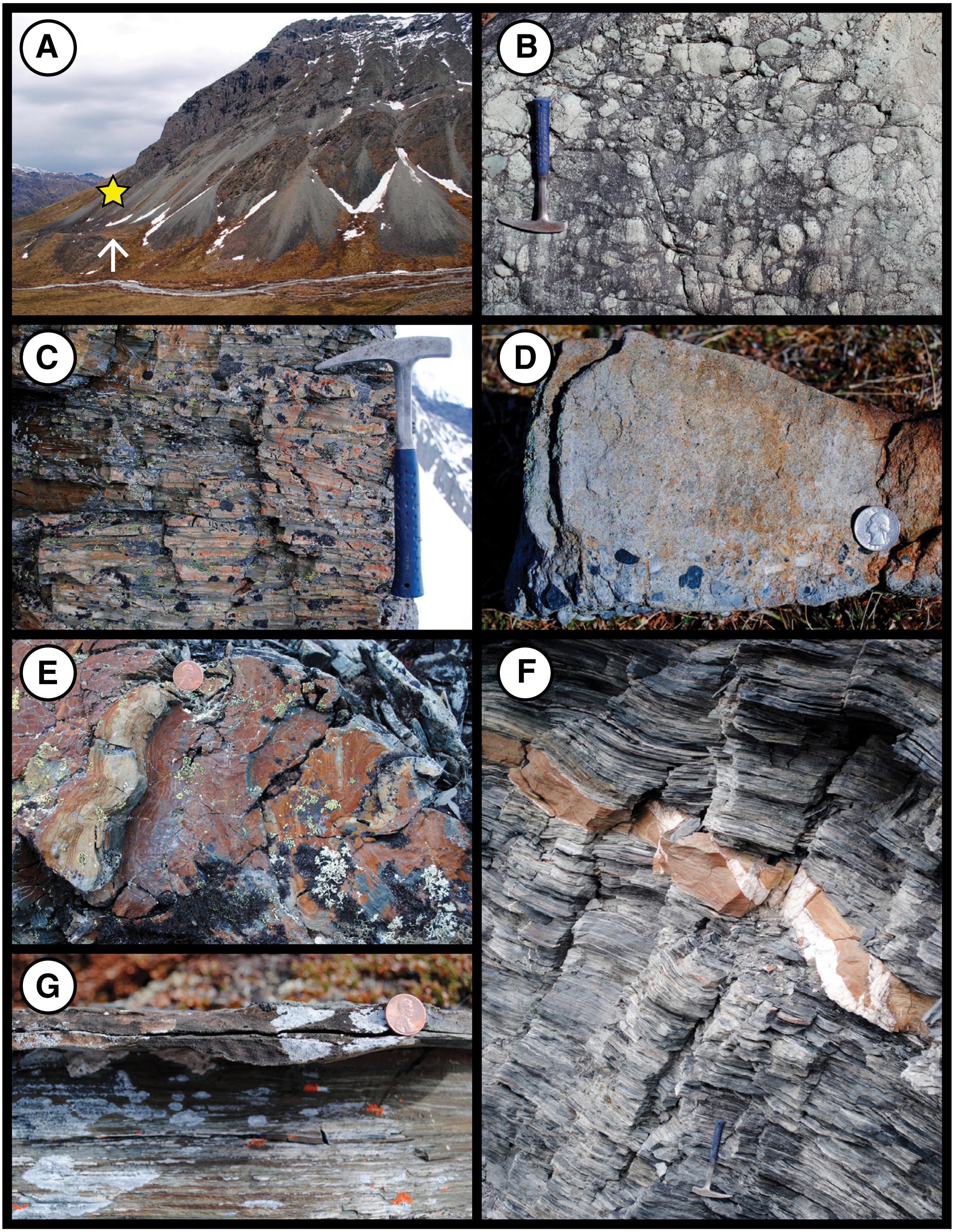
A
B
C
D
E
F
G

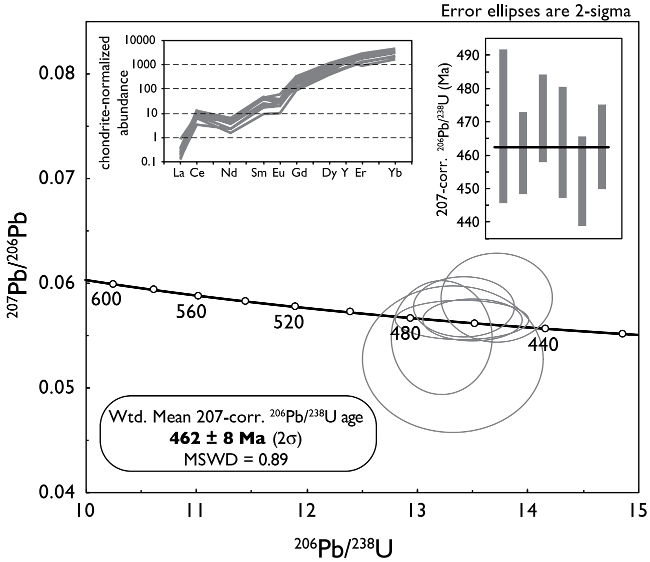

Figure 6. Tera-Wasserburg diagram for leucogabbro sample (J1431) in map unit Pzv of the Apoon assemblage along Karillyukpuk Creek, Doonerak fenster, Brooks Range, Alaska (see Fig. 2 for location). The upper-right inset shows a weighted mean best age plot for individual zircon analyses. The upper-left inset shows chondrite-normalized rare earth element (REE) abundances for individual zircon crystals assessed by sensitive high-resolution ion microprobe with reverse geometry (SHRIMP-RG). REE data were normalized using chondrite compositions of Sun and McDonough (1989). Error bars and ellipses are shown at the 2σ level. Plot was constructed with Isoplot 3.75 (Ludwig, 2003), and raw data are published in Tables DR4 and DR5 of the GSA Data Repository (see text footnote 1). MSWD—mean square of weighted deviates.

Figure 5. Selected photographs of geochronological samples and field relationships in the Doonerak fenster, central Brooks Range, Alaska. (A) Photograph of massive leucogabbro sampled for U-Pb sensitive high-resolution ion microprobe with reverse geometry (SHRIMP-RG) analysis from map unit Pzv (J1431) near the confluence of Karillyukpuk Creek and Clear River (Fig. 2). The arrow points to two tents for scale, and the yellow star denotes the sample location. (B) Massive, clast-supported volcaniclastic conglomerate of map unit Pza of the Apoon assemblage near Amawk Creek. Hammer for scale is 32 cm long. (C) Fractured planar and ripple cross-laminated volcaniclastic siltstone and fine-grained sandstone in map unit Pzc of the Apoon assemblage. Hammer for scale is 32 cm long. (D) Normal graded chert-pebble conglomerate of the basal Kekiktuk Conglomerate sampled for U-Pb detrital zircon geochronology (J1409-0.6) along Amawk Creek (Fig. 2). Quarter for scale is 2.4 cm in diameter. (E) Isoclinally folded lithic arenite sampled for U-Pb detrital zircon geochronology (J1420) from map unit Pzc of the Apoon assemblage on Amawk Mountain. Penny for scale is 1.9 cm in diameter. (F) Olive-green–colored massive tuffaceous horizon with calcite veins in penetratively deformed gray-black phyllite of map unit Pzp of the Apoon assemblage. Hammer for scale is 32 cm in length and is at the bottom of the photograph. (G) Starved ripple of volcaniclastic quartz wacke in massive phyllite of map unit Pzc. This horizon was sampled for U-Pb detrital zircon geochronology (J1419). Penny for scale is 1.9 cm in diameter.

from this sample that was analyzed by LA-ICP-MS is within error of this result (see GSA Data Repository [see footnote 1]; Table 1). Titanium concentrations from these zircons range from 10 to 55 ppm and show rare earth element (REE) patterns (Fig. 6) consistent with igneous zircon crystallization (e.g., Belousova et al., 2002; Hoskin and Schaltegger, 2003; Grimes et al., 2015).

LA-ICP-MS U-Pb Geochronology

The detrital zircon samples are separated into four groups according to map unit associations: Apoon assemblage units Pzc and Pzp (Julian, 1989), the Kekiktuk Conglomerate of the Endicott Group (Brosgé et al., 1962), and the informal Trembley Creek phyllite of the Hammond subterrane (Moore et al., 1997). The detrital zircon U-Pb data are presented as stacked histograms and relative probability plots in Figure 7. Stacked Wetherill concordia diagrams are provided in the GSA Data Repository (see footnote 1). Data from each sample are also presented in the context of metric multidimensional scaling (MDS) statistical analyses (Vermeesch, 2013) to facilitate evaluation of proposed lithological ties between different map units (Fig. 8). MDS utilizes the statistical effect size of the Kolmogorov-Smirnov test (i.e., dimensionless distances) as a measure of dissimilarity to produce a map of points where similar samples cluster together and dissimilar samples plot far apart (Vermeesch, 2013).

Apoon Assemblage—Unit Pzc

Map unit Pzc of the Apoon assemblage is dominated by thick exposures of black to gray-green phyllite and argillite with minor coarse-grained mafic volcaniclastic rocks (Fig. 4; Julian, 1989). The fine-grained strata contain a penetrative cleavage and are difficult to distinguish lithologically from map unit Pzp further to the south (Fig. 2). Dark-green to gray mafic volcaniclastic horizons are dominated by centimeter- to meter-thick beds of poorly sorted lithic arenite and wacke with minor matrix-supported conglomerate. Although many of the primary sedimentary structures in unit Pzc are obliterated by penetrative cleavage, one can still recognize distinct intervals that contain graded bedding, bedding-parallel burrows, erosional and channel-fill geometries, and prominent dune and ripple cross-lamination (Figs. 5C and 5G). In thin section, the volcaniclastic horizons consist of fine- to medium-grained and angular to subrounded mono- and polycrystalline quartz, sericitized feldspar, plagioclase, clinopyroxene, amphibole, epidote, zircon, and abundant opaque minerals. Lithic fragments in the coarser-grained strata are mainly composed of chert, mudstone, and plagioclase- and pyroxene-bearing volcanic clasts; rare metamorphic and coarse-grained mafic igneous clasts are also present in low abundance. Julian (1989) and Julian and Oldow (1998) reported point-counting data from 14 sandstone samples in unit Pzc, all of which fall within the dissected magmatic arc field as defined by qualitative assessment of quartz-feldspar-lithic (QFL) ternary diagrams (Dickinson and Suczek, 1979).

Samples J1418 and J1419 of unit Pzc were collected in close proximity to one another from fine- to coarse-grained volcaniclastic horizons on a prominent E-W–trending ridge above Amawk Creek (Fig. 2; Table 2). Sample J1418 is a dark-green to gray, sheared matrix-supported granule conglomerate. The majority of the lithic

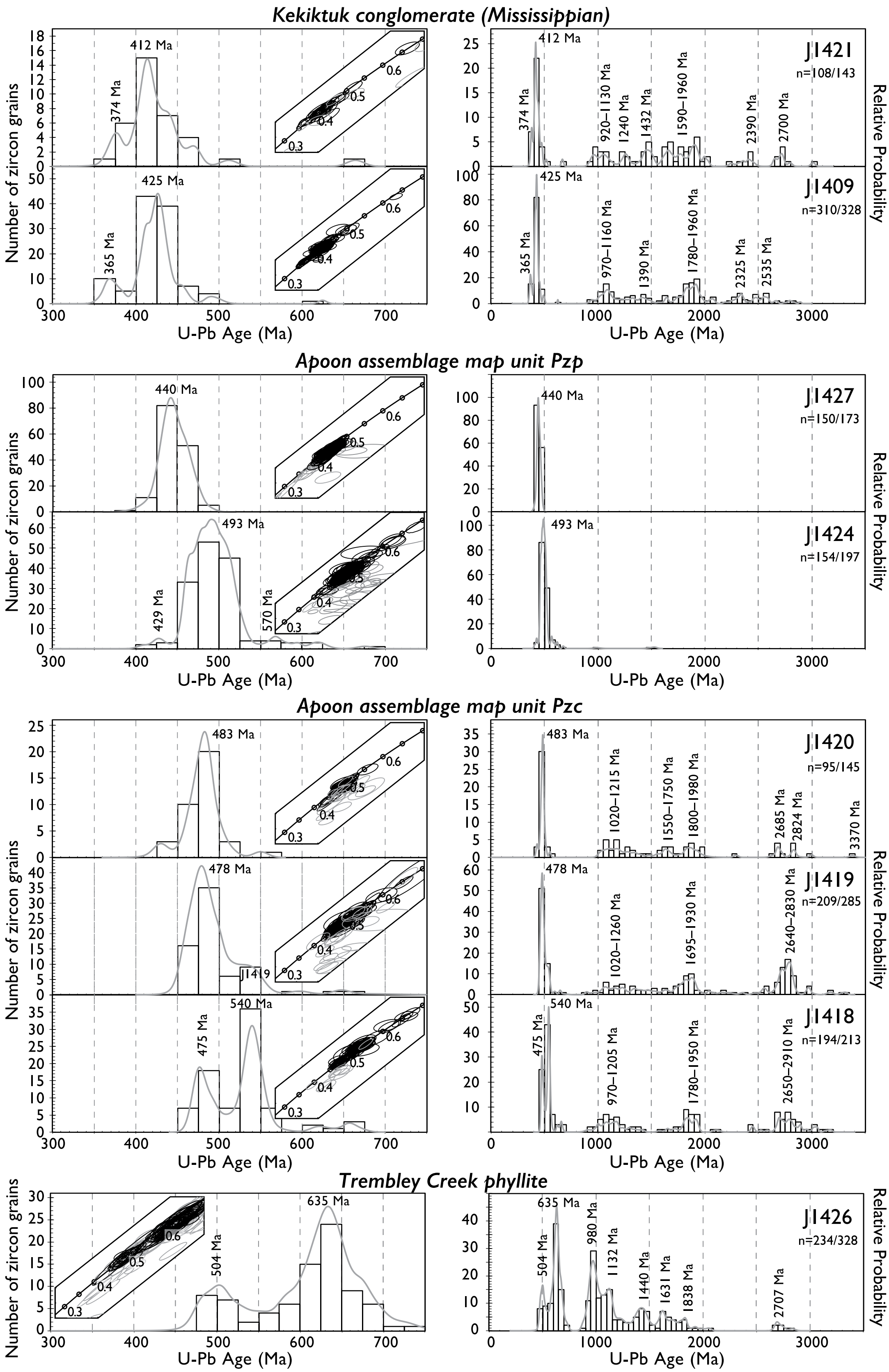
Kekiktuk conglomerate (Mississippian)
412 Ma
374 Ma
J1421
n=108/143
920–1130 Ma
1240 Ma
1432 Ma
1590–1960 Ma
2390 Ma
2700 Ma
425 Ma
365 Ma
J1409
n=310/328
970–1160 Ma
1390 Ma
1780–1960 Ma
2325 Ma
2535 Ma
Apoon assemblage map unit Pzp
440 Ma
J1427
n=150/173
493 Ma
429 Ma
570 Ma
J1424
n=154/197
Apoon assemblage map unit Pzc
483 Ma
J1420
n=95/145
1020–1215 Ma
1550–1750 Ma
1800–1980 Ma
2685 Ma
2824 Ma
3370 Ma
478 Ma
J1419
n=209/285
1020–1260 Ma
1695–1930 Ma
2640–2830 Ma
540 Ma
475 Ma
J1418
n=194/213
970–1205 Ma
1780–1950 Ma
2650–2910 Ma
Trembley Creek phyllite
635 Ma
504 Ma
J1426
n=234/328
980 Ma
1132 Ma
1440 Ma
1631 Ma
1838 Ma
2707 Ma
Number of zircon grains
Relative Probability
U-Pb Age (Ma)

Figure 7. Histograms and normalized probability distribution plots for detrital zircon data from the Doonerak fenster, central Brooks Range, Alaska (see Fig. 2 for sample locations). The right-hand plots show all of the data for each sample, whereas the left-hand plots are focused in on the younger age populations. The insets are zoomed-in Wetherill concordia plots that display the error ellipses for the youngest grains in each analysis (black ellipses are concordant analyses, and gray ellipses were excluded from probability plots and histograms based on our data-filtering procedures). A detailed description of the data-filtering procedure is provided in the Analytical Methods section. Also shown are the numbers of grains analyzed from each sample. Analyses are reported in Table 1 of the GSA Data Repository (see text footnote 1).

clasts are flattened in the foliation plane and composed of both plagioclase-bearing volcanic pebbles and subrounded shale chips. This sample also contains angular to subrounded mono- and polycrystalline quartz, chert, sericitized feldspar, clinopyroxene, metamorphic lithic fragments, and numerous opaque minerals. The matrix is dominated by chlorite, muscovite, white mica, calcite, and very fine-grained quartz and feldspar. Zircons from sample J1418 are ~30–170 μm in length and colorless to cloudy in color. Approximately half of the zircons are euhedral and the remainder are subrounded. U-Pb age populations from sample J1418 consist of major peaks with ranges of 480–470 (9%), 560–510 (25%), 1205–970 (13%), 1950–1780 (12%), and 2910–2650 Ma (15%). The youngest peak is centered around ca. 475 Ma, with the youngest zircon yielding an age of 468 ± 8 Ma (1σ; Fig. 7).

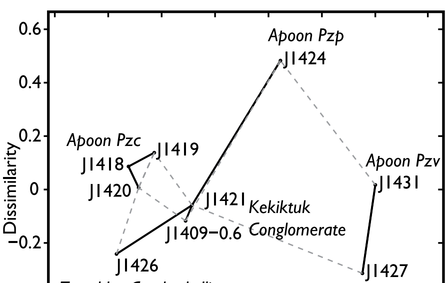

Figure 8. Metric multidimensional scaling (MDS) map (after Vermeesch, 2013) providing two-dimensional visualization of dimensionless Kolmogorov-Smirnov (K-S) distances between detrital zircon age spectra for all samples. Spatial proximity of points correlates with statistical similarity. Solid lines tie most similar neighbors, and dashed lines tie second most similar neighbors.

Sample J1419 is a light-green-gray, very fine- to fine-grained cross-laminated lithic arenite. This sample was collected from a horizon of discontinuous, ~2–4-cm-thick starved ripples within a massive fine-grained phyllitic interval (Fig. 5G). The sample is compositionally similar to J1418, but it contains a higher proportion of calcite cement. Zircons from sample J1419 are colorless to cloudy and range from ~40–125 μm in length. Typically, the cloudy zircons are rounded ellipsoids, while the clear grains are euhedral with prismatic tips. Zircon U-Pb age populations from sample J1419 consist of major peaks with ranges of 495–460 (24%), 540–510 (6%), 1260–1020 (9%), 1930–1695 (14%), and 2830–2640 Ma (22%). The youngest peak is centered around ca. 478 Ma, with the youngest zircon yielding an age of 458 ± 9 Ma (1σ; Fig. 7). Notably, both of these samples contain abundant Paleoproterozoic and Archean zircon age populations.

Sample J1420 was collected from map unit Pzc on the same E-W–trending ridgeline, ~300 m below the western summit of Amawk Mountain (Fig. 2; Table 2) and in close proximity to Silurian graptolite collections described in Julian and Oldow (1998). This sample consists of an ~10-cm-thick, isoclinally folded quartz lithic arenite (Fig. 5E) that is interbedded with black slate and minor phyllite. Sample J1420 is compositionally similar to samples J1418 and J1419, but it contains greater proportions of volcanic detritus and polycrystalline quartz. Zircons from sample J1420 are relatively small (20–80 μm in length) with rounded edges and few distinct euhedral grains. Major age populations from this sample have ranges of 485–460 (26%), 1215–1020 (15%), 1740–1550 (9%), 1980–1800 (14%), and 2830–2670 Ma (9%). The youngest peak is centered around ca. 483 Ma, with the youngest zircon yielding an age of 428 ± 10 Ma (1σ; Fig. 7). This sample also contains a prominent late Archean detrital zircon population.

Apoon Assemblage—Unit Pzp

Map unit Pzp of the Apoon assemblage outcrops throughout the southern half of the Doonerak fenster and is dominated by thick exposures of phyllite, slate, and argillite with minor intervals of argillaceous limestone, lithic wacke, and tuffaceous strata (Figs. 2 and 4; Julian, 1989). Fine-grained siliciclastic rocks in unit Pzp contain a penetrative foliation that is axial planar to isoclinal folds. The majority of the phyllitic strata are dark gray to black, with zones of abundant pyrite and iron oxides that weather reddish-brown; subtle grain-size variation is marked by intervals with crude parallel lamination and prominent shifts to lighter hues of gray and brown phyllite. Light-gray-green, ~10–60-cm-thick layers of altered tuff are interspersed throughout the monotonous phyllitic intervals and are characterized by abundant secondary calcite veins and sharp contacts with adjacent phyllitic strata (Fig. 5F). These horizons contain rarely preserved ash, lapilli, phenocryst-bearing volcanic fragments, fractured phenocrysts of plagioclase, and angular quartz grains with minor fine-grained secondary calcite, dolomite, albite, quartz, and white mica.

Near Harvey Mountain at the southern boundary of the Doonerak fenster (Fig. 2), unit Pzp is represented by a poorly exposed interval of interbedded phyllite, lithic wacke, and minor lithic pebble conglomerate. The coarser-grained strata comprise <5% of the local outcrop distribution and are thin- to medium-bedded with occasional bedding-parallel trace fossils, distinct normal graded beds with basal scour surfaces, and minor planar lamination and ripple cross-lamination. The coarser-grained strata compositionally resemble sandstone intervals described from map unit Pzc and consist of fine-grained sedimentary, metamorphic, and volcanic lithic fragments, mono- and polycrystalline quartz, alkali feldspar, plagioclase, and muscovite. Although these coarse-grained strata are structurally imbricated with the Trembley Creek phyllite of the Hammond subterrane (Fig. 2), they appear to be interbedded with, and genetically related, to the black to dark-gray phyllite of map unit Pzp.

Sample J1424 was collected from a light-gray-green, very fine-grained reworked tuffaceous horizon in the central portion of the Pzp map unit outcrop belt (Fig. 2; Table 2). This sample contains phenocryst-bearing volcanic fragments, angular and subrounded quartz grains, and immature sedimentary lithic fragments within a matrix of recrystallized calcite, quartz, and white mica. All of the clasts are flattened and oriented parallel to the penetrative foliation. Detrital zircons are predominately colorless to light brown and range from ~70–200 μm in length. Nearly all zircons are euhedral and oscillatory zoned in CL images. The age population from sample J1424 consists of a monotonic peak ranging from 530 to 450 Ma (88%; Fig. 7). The major peak is centered around ca. 493 Ma, with the youngest zircon yielding a U-Pb LA-ICP-MS age of 409 ± 7 Ma (1σ; Fig. 8). The youngest age population consists of four zircon crystals that range from ca. 430 to 410 Ma. This sample also contains two very small populations of older detrital zircons that range from 670 to 560 Ma (8%) and 1530 to 990 Ma (2%).

Sample J1427 was collected from the southern edge of the Doonerak fenster in the coarser-grained interval described above near Harvey Mountain (Fig. 2; Table 2). This sample consists of an ~20-cm-thick, fine- to medium-grained lithic wacke with angular quartz, feldspar, chert, and lithic fragments, coarse muscovite, and a very fine-grained matrix of white mica, chlorite, and quartz. Colorless and brown zircons from sample J1427 are euhedral and range in size from ~100–300 µm. The age population from sample J1427 consists of a single monotonic peak ranging from 490 to 410 Ma (Fig. 7). The peak is centered around ca. 441 Ma, with the youngest zircon yielding a U-Pb LA-ICP-MS age of 395 ± 11 Ma (1σ; Fig. 8). The youngest age population consists of six zircon crystals that range from ca. 415 to 395 Ma. This sample contains no older zircon crystals, with the oldest grain yielding an age of 489 ± 7 Ma (1σ).

Endicott Group—Kekiktuk Conglomerate

The Kekiktuk Conglomerate and overlying Endicott Group are only exposed along the northern edge of the Doonerak fenster (Fig. 2). These strata are deformed within the Blarney Creek duplex zone, which affects localized footwall rocks below the Amawk thrust (Mull et al., 1987a; Phelps and Avé Lallement, 1998; Seidensticker and Oldow, 1998). We examined the Kekiktuk Conglomerate on a prominent E-W–trending ridgeline directly above Amawk Creek (Fig. 2). Here, the Kekiktuk measures ~20.6 m thick and consists of a basal 0.6-m-thick, medium- to very coarse-grained and trough cross-bedded quartz arenite within minor clast-supported chert pebble conglomerate (Fig. 5D). Locally, the contact with the underlying Apoon volcanic rocks of unit Pza is covered in talus; however, we confidently identified *in situ* Apoon rocks within ~1.2 m of the basal conglomeratic horizon. These basal strata are overlain by a 7.5-m-thick covered interval, which passes up section into a 6.7-m-thick yellow-maroon to gray-green silicified slate and siltstone unit that contains poorly preserved plant fossils. These fine-grained strata are overlain by 2.8 m of moderately sorted and thick-bedded chert cobble conglomerate interbedded with medium- to coarse-grained chert arenite and minor gray-green shale. These strata contain abundant mudcracks, shale rip-up clasts, dune-scale cross-stratification, and abundant secondary quartz veins. The conglomeratic horizons are clast-supported and appear to be channelized, grading abruptly up section into 2.7 m of recessive gray-green argillite and phyllite within minor matrix-supported chert and quartz wacke. This fine-grained interval locally passes up section into another channelized, 2.1–4.3-m-thick, clast-supported chert pebble conglomerate with similar sedimentary structures to the lower horizon. The Kekiktuk Conglomerate appears to be abruptly overlain by jet-black phyllitic shale of the basal Kayak Shale, although the contact between the two units is covered where we examined it.

Sample J1409-0.6 comes from the uppermost 5 cm of the basal chert pebble conglomerate unit (Fig. 5D). In thin section, this sample is almost exclusively composed of subrounded to well-rounded grains of monocrystalline quartz and chert with minor shale lithic fragments, zircon, muscovite, clay minerals, opaques, calcite, and silica cement. The quartz grains are commonly recrystallized with diffuse grain boundaries and locally display undulose extinction and embayed grain margins. Zircons from sample J1409-0.6 are ~70–120 µm in length and equant to euhedral with a minor population of subrounded grains. Detrital zircon age populations from sample J1409-0.6 consist of major peaks with ranges of 389–360 (5%), 450–400 (27%), 1160–970 (11%), 1490–1350 (5%), 1960–1780 (17%), and 2590–2400 Ma (7%). The youngest peaks are centered around ca. 367 and ca. 426 Ma, with the youngest zircon yielding a U-Pb LA-ICP-MS age of 360 ± 8 Ma (1σ; Fig. 7).

Sample J1421 comes from an isolated outcrop of the Kekiktuk Conglomerate along the western ridgeline of Amawk Mountain in close proximity to the Apoon Pzc samples (Fig. 2; Table 2). This silicified chert wacke was sampled from a conspicuous interval of isoclinally folded, purple, maroon, and green phyllite and slate that appears to underlie the prominent chert pebble conglomerate at the base of our coarsely measured section of the Kekiktuk Conglomerate near Amawk Creek. Mull et al. (1987a) and Seidensticker and Oldow (1998) also described a very similar fine-grained and discontinuous lower unit of the Kekiktuk Conglomerate and noted that it locally contains intensely sheared chert pebble conglomerate that rests directly on black slate and phyllite of the Apoon assemblage. Compositionally, this sample consists of very fine- to fine-grained, subrounded to subangular monocrystalline quartz and chert with a prominent matrix consisting of opaques, calcite, white mica, and clay minerals. All of the primary minerals are strongly flattened and oriented parallel to the main tectonic foliation. Sample J1421 contains colorless subrounded zircon ranging from ~30 to 160 µm in length. The detrital zircons from sample J1421 contain similar age populations to those of sample J1409-0.6, with ranges of 400–368 (6%), 450–410 (21%), 1140–920 (7%), 1490–1430 (7%), 1910–1630 (22%), and 2750–2350 Ma (9%). The youngest peaks are centered around ca. 365 and ca. 425 Ma, with the youngest zircon yielding a U-Pb LA-ICP-MS age of 368 ± 7 Ma (1σ; Fig. 7).

Trembley Creek Phyllite

In the southernmost part of the Doonerak fenster, Apoon map unit Pzp is in fault contact with a prominent tectonic sliver of hanging-wall rocks of the Endicott Mountains allochthon (Figs. 2 and 3). This ~500-m-thick package of Hammond subterrane rocks was mapped but unnamed by Brosgé and Reiser (1964, 1971) and then correlated later by Dutro et al. (1976) to the widespread and heterogeneous Upper Devonian Beaucoup Formation. Dillon et al. (1986, 1988) later separated out these strata as map unit "Dw" of the Devonian "Whiteface Mountain unit," noting a subtle lithological contrast but broad age equivalency with rocks of the Beaucoup Formation in the immediate hanging wall of the Amawk thrust. More recently, Moore et al. (1997) separated out these strata from the Beaucoup Formation because of their distinctive micaceous arenite composition in the otherwise fine-grained deposits of the Beaucoup Formation and reallocated them to the informal Trembley Creek phyllite, a name that we adopt herein (Figs. 2 and 4). There are no formal descriptions of the Trembley Creek phyllite besides basic lithological descriptions in map legends (Dillon et al., 1986; Moore et al., 1997); the only age constraint comes from unpublished detrital white mica $^{40}Ar/^{39}Ar$ ages of ca. 450 Ma (Moore et al., 1997), providing a rough maximum age constraint.

The Trembley Creek phyllite outcrop belt near Harvey Mountain (Fig. 2) consists of light-gray to orange-brown weathering, thin- to thick-bedded calcareous sandstone, micaceous quartz wacke, and calc–mica schist with minor purple and green phyllite, all of which contain a strong foliation. These deformed strata contain poorly preserved cross-bedding and local erosional scours, but most of the primary sedimentary features are not preserved. Sample J1426 consists predominantly of calc–mica schist with a poorly sorted, immature sedimentary protolith composed of angular to subangular grains of calcite, quartz, alkali feldspar, and muscovite with minor chert, shale, and metamorphic lithic fragments. Detrital zircons from sample J1426 can be divided into two populations based on size: large (120–300 µm) euhedral zircon and small (25–75 µm) angular to subrounded zircon. Both the large and small populations contain zircon with metamict textures in CL. Detrital zircon U-Pb age populations from sample J1426 are strikingly different from the other sample sets in this study and consist of major peaks with ranges of 530–490 (7%), 680–540 (26%), 1070–920 (25%), 1170–1090 (8%), 1480–1360 (8%), 1670–1590 (6%), and 2770–2640 Ma (2%). The youngest peaks are centered around ca. 630 and 504 Ma, with the youngest zircon yielding a U-Pb LA-ICP-MS age of 480 ± 9 Ma (1σ; Fig. 7). The geochronological data from sample J1426 are also distinct from other samples in that they exhibit both a moderate degree of discordance and contain an abundance of grains having high U/Th ratios. Forty-four grains exhibit U/Th ratios >10, a characteristic commonly attributed to metamorphic zircon (e.g., Rubatto, 2002). Although more than 30 of these are concordant, analyses with elevated U/Th ratios are interpreted to reflect the effects of metamorphism and are therefore excluded from consideration (Fig. 7).

Zircon Hf Isotope Geochemistry

Apoon Assemblage

Lu-Hf isotopic measurements were performed on 97 zircon crystals from the Apoon assemblage of the Doonerak fenster (Fig. 9; GSA Data Repository [see footnote 1]). Forty-eight analyses from two samples (J1419 and J1420) of unit Pzc of the Apoon assemblage targeted a broad range of ca. 3320–465 Ma age populations (Fig. 9): Zircon crystals with U-Pb ages younger than 1000 Ma (35% of the analyses) have $\varepsilon_{Hf(t)}$ values that generally exceed +7, Proterozoic zircon crystals yield widely dispersed $\varepsilon_{Hf(t)}$ values that range from –26 to +12 (excluding a single erroneous analysis that plotted well above the depleted mantle curve), and Archean zircons yielded a narrow range of $\varepsilon_{Hf(t)}$ values between −10 and +4. Hafnium isotopes from unit Pzp of the Apoon assemblage were measured on 39 zircon grains from two samples (J1424 and J1427) focusing on U-Pb ages between ca. 622 and 409 Ma (Fig. 9). The Lu-Hf isotopic compositions of these young Neoproterozoic–Silurian grains fall within a narrow range, with most of the analyses (23 of 39 analyses; 59%) yielding $\varepsilon_{Hf(t)}$ values between +8 and +13. A small subset of three Ordovician (ca. 460 Ma) grains plots just below the chondritic uniform reservoir (CHUR) trendline (Fig. 9) but does not exceed $\varepsilon_{Hf(t)}$ values <–4. Finally, Lu-Hf isotopic data from 10 analyses on zircons from the leucogabbro of unit Pzv (sample J1431) yielded a very narrow range of positive $\varepsilon_{Hf(t)}$ values between +10 and +13 (Fig. 9).

Endicott Group—Kekiktuk Conglomerate

Forty-three Lu-Hf isotopic measurements were performed on zircon grains from two samples (J1409-0.6 and J1421) of the Kekiktuk Conglomerate (Fig. 9; GSA Data Repository [see footnote 1]). The youngest population of Devonian zircon grains (ca. 400–360 Ma; 21% of analyses) yielded negative $\varepsilon_{Hf(t)}$ values between −16 and −7. In contrast, older Ordovician–Silurian zircon crystals (ca. 460–420 Ma; 25% of analyses) showed positive $\varepsilon_{Hf(t)}$ values ranging from +3 and +12. Mesoproterozoic zircon from the Kekiktuk Conglomerate yielded mostly positive $\varepsilon_{Hf(t)}$ values ranging from −2 to +8, while the Paleoproterozoic age populations showed a wider range of $\varepsilon_{Hf(t)}$ values from −13 to +9 (Fig. 9). No Archean zircons were analyzed for Lu-Hf isotopes from the Kekiktuk Conglomerate.

Trembley Creek Phyllite

The Lu-Hf isotopic data from 36 zircon grains in sample J1426 of the Trembley Creek phyllite display a diverse range of both positive and negative $\varepsilon_{Hf(t)}$ values (Fig. 9; GSA Data Repository [see footnote 1]). Neoproterozoic and early Paleozoic zircons (ca. 980–480 Ma; 52% of analyses) showed moderately negative $\varepsilon_{Hf(t)}$ values ranging from −5 and +1, with one Ediacaran outlier recording an $\varepsilon_{Hf(t)}$ value of +9.9 (Fig. 9). Prominent Mesoproterozoic zircon age populations (ca. 1450–1040 Ma; 22% of the analyses) yielded positive $\varepsilon_{Hf(t)}$ values ranging from +2 to +9, whereas Paleoproterozoic and Archean grains display a range of more depleted $\varepsilon_{Hf(t)}$ values from −13 to +0.5 (Fig. 9).

$^{40}Ar/^{39}Ar$ Geochronology

The $^{40}Ar/^{39}Ar$ step-heating spectrum for sample CH14DW16 of the Trembley Creek phyllite is shown in Figure 10. Model ages calculated from gas aliquots released during individual steps range from ca. 267 Ma at the lowest temperature and rapidly converge toward ca. 465 Ma at the highest temperature, giving a total gas age (TGA) of 465 Ma. The majority of the gas released during heating yielded an Ordovician age and is consistent with Ordovician growth of mica or complete cooling into argon-retentive temperatures at that time. More complex partially retentive histories are permissible, so the most parsimonious interpretation is simply that mica growth is constrained as older than the terminal release model age of ca. 465 Ma. The curvature in model ages at low-temperature steps in sample CH14DW16 is consistent with partial diffusive loss due to a reheating event that is constrained as younger than the initial release model age of ca. 267 Ma.

DISCUSSION

Age and Significance of the Apoon Assemblage, Doonerak Fenster

The main lithological components, sedimentological and petrological characteristics, and volcanic geochemistry of the Apoon assemblage are typical of a volcanic arc setting (Dutro et al., 1976; Mull et al., 1987a; Julian, 1989; Julian and Oldow, 1998). These data are further supported by the new U-Pb geochronology and Hf isotope geochemistry presented herein, which record multiple phases of juvenile early Paleozoic arc volcanism in the Apoon assemblage (ca. 540–510, 495–475, and 460–440 Ma; Figs. 7 and 9). The recognition that both map units Pzp and Pzc host Cambrian–Devonian(?) reworked tuffaceous horizons and volcaniclastic rocks (Figs. 5 and 7) indicates that the Apoon assemblage was deposited in a long-lived, synvolcanic depocenter.

The apparent stratigraphic architecture of the Apoon assemblage includes a basal Cambrian or older fine-grained sedimentary unit (basal part of unit Pzp), an Upper Cambrian (Furongian)–Middle Ordovician juvenile volcanic arc sequence (units Pza and Pzv), and an Upper Cambrian (Furongian)–Upper Silurian or Lower Devonian(?) sedimentary and volcaniclastic succession (unit Pzc and part of unit Pzp). Although the exact age range of these units is unknown, the updated stratigraphy implies that the Doonerak arc experienced discrete pulses of tectonic subsidence and oceanic arc magmatism and indicates a more complex history than previous interpretations of a single Ordovician–Silurian coeval arc/back-arc system (e.g., Julian and Oldow, 1998).

The structural and stratigraphic architecture of the oldest rocks in the Apoon assemblage was not examined in this study and remains poorly understood. Critically, the middle Cambrian trilobite faunas from what is presumably map unit Pzp (Fig. 2; Dutro et al., 1984a, 1984b) are strikingly similar to fossil collections described from the nearby Snowden Mountain area of the Hammond subterrane (Palmer et al., 1984); these paleontological similarities, combined with local lithological differences with other Pzp outcrops throughout the Doonerak fenster, have led to the suggestion that these fossiliferous rocks are not part of the Apoon assemblage but belong instead to an allochthonous tectonic sliver derived from Hammond subterrane rocks in the hanging wall of the Amawk thrust (T.E. Moore, 2016, personal commun.). This interpretation creates important ambiguity regarding the age and significance of the oldest units in the Apoon assemblage and potentially severs

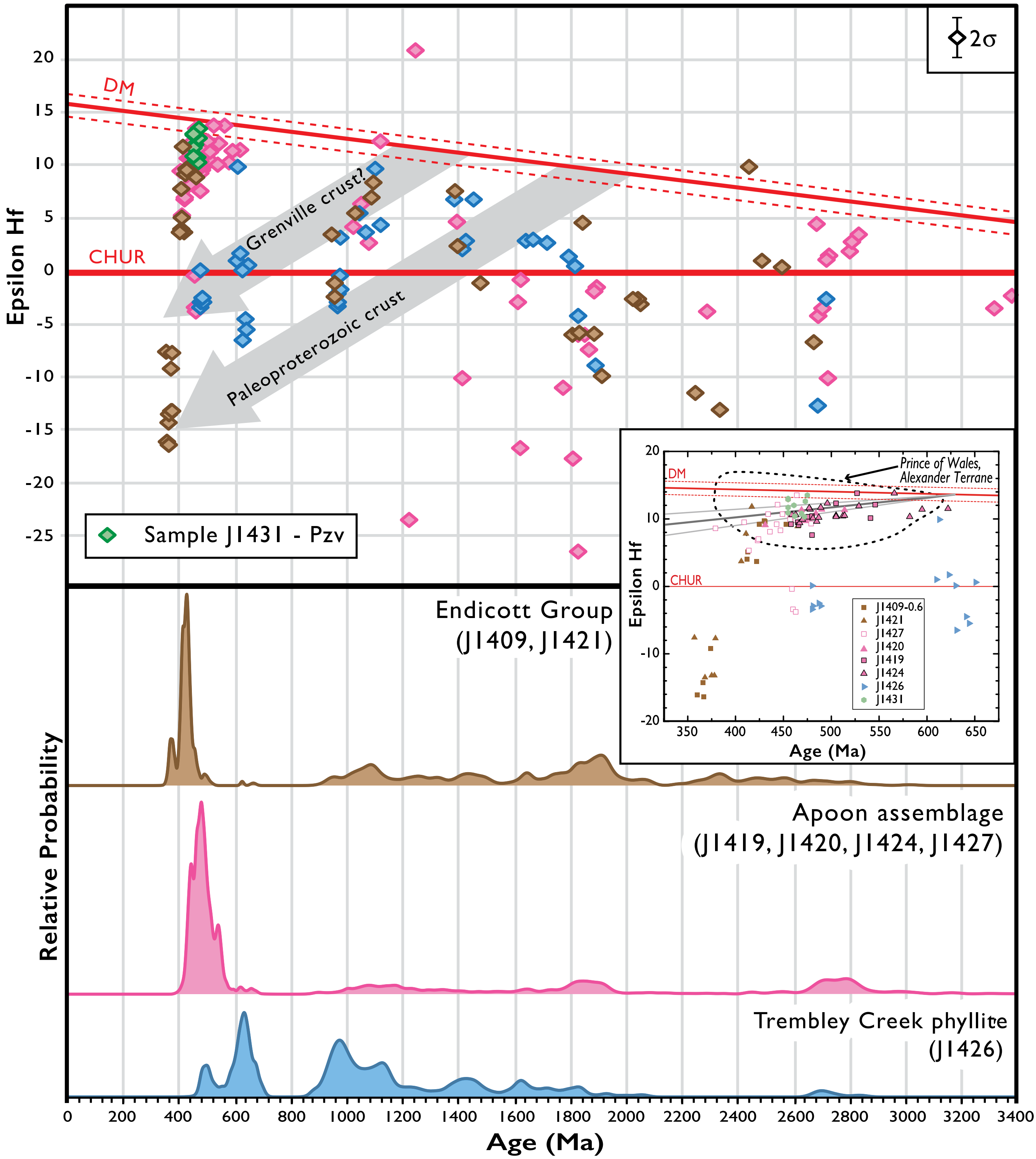

Figure 9. Hf isotope compositions of detrital and igneous zircons from the Doonerak fenster of the central Brooks Range, Alaska. Lower curves show normalized composite age distribution plots of detrital zircons from samples in the Apoon assemblage (pink), Kekiktuk Conglomerate (brown), and Trembley Creek phyllite (blue). There is no vertical exaggeration. Upper plot shows Hf isotope analyses from these same U-Pb samples (with matching colors), except for the analyses from sample J1431, a leucogabbro from Apoon map unit Pzv (Fig. 6), which are shown in green and not included in the age curves. DM—depleted mantle (Vervoort and Blichert-Toft, 1999), CHUR—chondritic uniform reservoir (Bouvier et al., 2008). The gray arrows were calculated based on average crustal evolution trajectories assuming present-day $^{176}Lu/^{177}Hf = 0.0115$ (Vervoort and Patchett, 1996; Vervoort et al., 1999). Inset shows a zoomed-in view of Neoproterozoic–early Paleozoic Hf isotopic data from the Apoon assemblage, Trembley Creek, and Kekiktuk Conglomerate with different symbols representing different samples (see legend and Fig. 7). Shown for reference is the outline (dashed line) of Hf isotopic data from the Prince of Wales region of the Alexander terrane (White et al., 2016, and references therein).

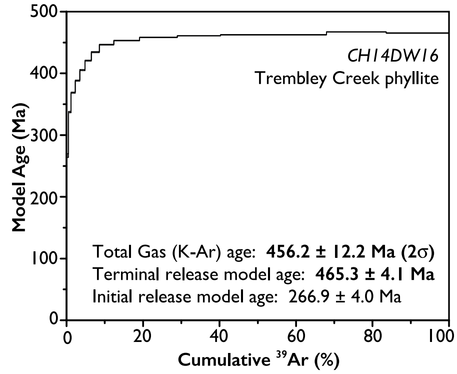

Figure 10. $^{40}Ar/^{39}Ar$ model age spectra for detrital muscovite from the Trembley Creek phyllite. Sample location is the same as J1426 as shown in Figure 2. Individual release step ages are plotted against cumulative percentage of ^{39}Ar released. Uncertainties in model ages are shown at the 2σ level. Raw data are reported in Table DR3 of the GSA Data Repository (see text footnote 1).

purported paleobiogeographic links between the Doonerak arc and the Siberian craton (e.g., Palmer et al., 1984; Blodgett et al., 2002; Dumoulin et al., 2002).

The new 462 ± 8 Ma U-Pb SHRIMP-RG zircon age from leucogabbro intruding volcanic and volcaniclastic rocks of map unit Pzv (Figs. 2 and 5A) is consistent with previously reported ca. 470 Ma K-Ar and $^{40}Ar/^{39}Ar$ ages on hornblende from dikes and sills in map unit Pza (Fig. 2; Table 1; Dutro et al., 1976). These data provide an important geochronological link between the two imbricated volcanic belts of the Apoon assemblage (Pza and Pzv) and support previous claims that these map units are coeval (Dutro et al., 1976; Mull et al., 1987a; Moore, 1987; Julian, 1989; Julian and Oldow, 1998). Based on their lithologic and petrographic characteristics, the volcaniclastic turbidites in map unit Pzc were most likely derived from proximal Apoon volcanic rocks (Julian, 1989; Julian and Oldow, 1998); therefore, we suggest the significant ca. 490–475 Ma age population in these strata (Fig. 7), coupled with the 462 ± 8 Ma age of the leucogabbro, brackets a major phase of Apoon volcanism in the Upper Cambrian (Furongian) through Middle Ordovician. Collectively, the Apoon Lu-Hf isotopic dataset is dominated by highly juvenile Cambrian–Silurian $\varepsilon_{Hf(t)}$ values ranging from +7 to +12 (Fig. 9), which indicate that this early Paleozoic volcanism was isolated from continental influence and potentially generated in an intra-oceanic arc setting. If the fossiliferous Middle Cambrian strata described above are deemed allochthonous, this would indicate that the oldest rocks in the Apoon assemblage are instead represented by these ca. 490–460 Ma arc volcanics. An earlier phase of ca. 540–510 Ma juvenile arc magmatism is inferred from zircon populations in the volcaniclastic strata of map unit Pzc; however, as described herein, these zircon populations are most likely allochthonous due to their association with older cratonic detritus (Fig. 7).

The deposition of units Pzc and Pzp in an Upper Cambrian (Furongian)–Upper Silurian or Lower Devonian(?) juvenile back-arc or forearc setting is supported herein by paleontological, sedimentological, geochemical, and geochronological evidence (Julian, 1989; Julian and Oldow, 1998). The abundance of fine-grained slate, argillite, and phyllite interbedded with minor tuffaceous horizons and volcaniclastic turbidites suggests these units were dominated by suspension deposition in a low-energy setting punctuated by episodes of volcanism and volcaniclastic sedimentation. However, the Pzc and Pzp successions appear to differ in age and provenance (Figs. 7 and 8). For example, samples from volcaniclastic horizons in unit Pzc contain abundant detrital zircon with U-Pb age populations ca. 540–510, 1260–970, 1980–1695, 2910–2640, and 3315–3020 Ma; these data contrast with the unimodal ca. 490 and 441 Ma U-Pb age populations of unit Pzp. These profound disparities in zircon age populations are also supported by clear petrological differences, such as the ubiquity of poorly sorted volcanic and metamorphic detritus in unit Pzc.

There are several ways to interpret the new U-Pb data from the Apoon assemblage, the most parsimonious of which indicates that map units Pzp and Pzc record fundamentally different phases or loci of sedimentation within the Doonerak arc complex. Based on the volcanogenic nature of the sampled strata, map unit Pzp appears to record ca. 490–440 Ma distal back-arc or forearc sedimentation (Fig. 7); however, both of the samples from this unit also contain small zircon populations as young as ca. 430–395 Ma, which suggest they may represent Early Devonian (Lochkovian) or younger volcaniclastic or epiclastic horizons characterized by abundant inheritance. Despite this, no Devonian fossils have been recovered from the Apoon assemblage to date, and the youngest zircon populations in all of the samples show signs of substantial Pb-loss (Fig. 7; GSA Data Repository [see footnote 1]); therefore, until future work contradicts or substantiates these results, we interpret the peak age of the youngest significant age population in the probability distribution plots (Fig. 7) as a conservative maximum depositional age for these tuffaceous and volcaniclastic strata.

Early Paleozoic Tectonism Recorded in the Apoon Assemblage

Map unit Pzc records the influx of coarse-grained sedimentary, igneous, and metamorphic detritus characterized by exotic ca. 3315–510 Ma zircon age populations (Figs. 7 and 9) into the Doonerak arc complex. We interpret this change in provenance to record juxtaposition of the juvenile Doonerak arc with an unknown crustal fragment of continental affinity in a collisional or strike-slip setting. The large populations of ca. 1260–970, 1980–1695, 2910–2640, and 3315–3020 Ma zircons in unit Pzc support a typical Laurentian basement signature for this exotic crustal fragment; however, the distinct Tonian (ca. 980–950 Ma) and Ediacaran–Cambrian (ca. 560–510 Ma) zircon populations, as well as the cosmopolitan nature of these Proterozoic and Archean basement provinces (e.g., Andersen, 2014), create ambiguity in the determination of a specific source region, or this implies there were several juxtaposed crustal fragments.

The exact age of this tectonism is also poorly constrained; based on the youngest peak age populations in samples from unit Pzc, this event must have been Early Ordovician or younger in age (Fig. 7). As highlighted already, however, the petrological and sedimentological characteristics of these volcaniclastic strata provide support for derivation from volcanic rocks of the Apoon assemblage (units Pzv and Pza), indicating that localized uplift and erosion of the Doonerak arc occurred during this event. A post–Middle Ordovician age for this tectonism is supported by the presence of trace zircon crystals as young as ca. 428 Ma in the Pzc volcaniclastic strata (sample J1420), as well as the close proximity of these samples to graptolite-bearing Silurian slate near the summit of Amawk Mountain (Fig. 2). A similar stratigraphic relationship is also recognized along strike to the west, where Silurian slate was found interbedded with volcaniclastic strata that are lithologically identical to unit Pzc (Fig. 2; Repetski et al., 1987). These data suggest this collision or strike-slip juxtaposition is most likely Early Silurian (Wenlock) or younger in age. In the following sections, we outline a number of scenarios to explain how these geochronological data fit into a regional tectonic framework that is consistent with proposed paleogeographic reconstructions of the Doonerak arc in early Paleozoic time.

In the southernmost part of the Doonerak fenster, fine-grained strata of map unit Pzp are cut by a number of diabase dikes and sills, one of which was dated with K-Ar and $^{40}Ar/^{39}Ar$ geochronology on hornblende at 388 ± 12 Ma (Fig. 2; Dutro et al., 1976). These Middle Devonian (Eifelian?) mafic rocks occur as isolated bodies that are too small to show on the geological map (Fig. 2); however, it appears as though they may be widespread throughout the fenster and cut many (if not all) of the Apoon map units and rocks of the Hammond subterrane (Dutro et al., 1976; Julian, 1989; Moore et al., 1997). We suggest these mafic rocks provide an important link to Early–Middle Devonian magmatism associated with the establishment of the Ambler arc and the eventual opening of the Devonian–Jurassic Angayucham Ocean (e.g., Dillon et al., 1980; Hitzman et al., 1986; Moore et al., 1997; Raterman et al., 2006). This suggests that the pre-Mississippian basement domains of the Doonerak arc complex and Hammond subterrane were juxtaposed at this time.

Age and Significance of the Endicott Group, Doonerak Fenster

Our field observations of the Kekiktuk Conglomerate are consistent with previous work that describes a significant disconformity between the Apoon assemblage and overlying Endicott Group within the Doonerak fenster (Armstrong et al., 1976; Mull et al., 1987a; Moore et al., 1994, 1997; Adams et al., 1997; Dumoulin et al., 1997; Julian and Oldow, 1998). This interpretation is further substantiated by the U-Pb detrital zircon geochronology presented herein, which records a prominent shift in provenance across this critical stratigraphic boundary (Figs. 7 and 8). Samples J1409-0.6 and J1421 of the Kekiktuk Conglomerate, which are indistinguishable in MDS space (Fig. 8), record fundamental petrological similarities with the Kekiktuk Conglomerate of the NE Brooks Range (Nilsen, 1981; Moore and Nilsen, 1984; Mull et al., 1987a; Adams et al., 1997; Julian, 1989) and yield detrital zircon age populations consistent with equivalent strata in the North Slope subsurface (Gottlieb et al., 2014). The Kekiktuk samples from the Doonerak fenster host prominent populations of Middle–Late Devonian (ca. 385–360 Ma) zircons, which were most likely sourced from Devonian granitic rocks exposed throughout the NE Brooks Range of Alaska and Yukon (Sable, 1977; Dillon et al., 1980; Mortensen and Bell, 1991; Dumoulin, 2001; Lane, 2007).

The Lu-Hf isotopic data from the Kekiktuk Conglomerate record two distinct compositional clusters in Paleozoic U-Pb age populations (Fig. 9). The youngest age population (ca. 385–360 Ma) yields highly evolved $\varepsilon_{Hf(t)}$ values that may be interpreted to reflect derivation from reworked Paleoproterozoic crust or complex admixtures of juvenile Paleozoic and older crustal sources (Fig. 9). The second cluster of Paleozoic zircons (ca. 460–405 Ma) has intermediate to moderately juvenile $\varepsilon_{Hf(t)}$ values, which could reflect either local recycling of Apoon assemblage rocks and/or contribution from mixed sedimentary and volcanic sources in pre-Mississippian strata of the NE Brooks Range, such as the synorogenic Clarence River group (Johnson et al., 2016). The age spectra and $\varepsilon_{Hf(t)}$ values of Proterozoic and Archean zircons from the Kekiktuk Conglomerate closely resemble the Lu-Hf isotopic composition of similar-age zircon in the Apoon assemblage (Fig. 9); however, these data may equally reflect recycling of distal North Slope pre-Mississippian rocks, which is also consistent with previous sedimentological and geochronological studies of the Kekiktuk Conglomerate throughout the central and NE Brooks Range (e.g., Nilsen, 1981; Moore and Nilsen, 1984; Gottlieb et al., 2014).

Regional Implications for Devonian Orogenesis in the Brooks Range

The geochronological correlation between the Kekiktuk Conglomerate in the Doonerak fenster and the NE Brooks Range supports a model of widespread, S-directed fluvial-deltaic sedimentation over deformed pre-Mississippian basement domains of the North Slope subterrane and Doonerak arc following contractional deformation associated with the Romanzof and/or Ellesmerian orogenies (e.g., Moore et al., 1994; Lane, 2007; Strauss et al., 2013). However, previous workers have argued that all of the penetrative deformation in the Apoon assemblage is related to younger Brookian contraction, with no evidence for older Romanzof or Ellesmerian structural fabrics within the Doonerak fenster (Oldow et al., 1984; Julian and Oldow, 1998; Seidensticker and Oldow, 1998). Notably, the Ellesmerian sequence in the Doonerak fenster records a more distal paleoenvironmental position with respect to the NE Brooks Range (Armstrong et al., 1976; Armstrong and Mamet, 1978; Kelley and Brosgé, 1995; Adams et al., 1997; Dumoulin et al., 1997), which could be a result of detachment of the Apoon assemblage at depth and northward translation during Brookian shortening (e.g., Seidensticker and Oldow, 1998). Therefore, the Apoon assemblage may have escaped pre-Mississippian Romanzof–Ellesmerian deformation because it occupied a different structural position within the orogen(s) (Oldow et al., 1984; Julian, 1989; Julian and Oldow, 1998). Regional documentation of S-vergent structures in pre-Mississippian rocks of the NE Brooks Range (Oldow et al., 1987a; Lane, 2007) supports such a model because it restores the Apoon assemblage away from the projected hinterland of the Romanzof-Ellesmerian orogen; however, the majority of structural studies in the NE Brooks Range record N-vergent kinematics for these Devonian collisional events (e.g., Hanks, 1989; Wallace and Hanks, 1990; Mull and Anderson, 1991; Moore et al., 1994; Cole et al., 1999; Houseknecht and Connors, 2016; Johnson et al., 2016). This places the hypothetically undeformed Apoon assemblage within the projected hinterland of the Romanzof-Ellesmerian orogen, a situation that is structurally untenable. Alternatively, pre-Mississippian rocks of the Apoon assemblage and North Slope subterrane may have evolved independently in the early Paleozoic with subsequent juxtaposition by strike-slip deformation prior to overlap by the Endicott Group (Julian, 1989; Strauss et al., 2013; McClelland et al., 2015b).

Age and Significance of the Trembley Creek Phyllite, Hammond Subterrane

The Trembley Creek phyllite is mapped at several localities flanking the southern edge of the Doonerak fenster, including a distinguishable tectonic sliver imbricated with rocks of the Apoon assemblage (Figs. 2 and 3; Brosgé and Reiser, 1964, 1971; Dutro et al., 1976; Dillon et al., 1986, 1988; Julian and Oldow, 1998; Phelps and Avé Lallement, 1998; Seidensticker and Oldow, 1998). The presence of ca. 460 Ma detrital muscovite in our sample from the Trembley Creek phyllite (Fig. 10) confirms a broad stratigraphic link with correlative rocks along the Dalton Highway corridor, where Moore et al. (1997) reported similar $^{40}Ar/^{39}Ar$ detrital white mica ages. We interpret the coarse-grained muscovite as detrital due to the strong petrologic contrast with the surrounding fine-grained matrix, the presence of mechanically broken and/or rounded edges on some grains, and the alignment of detrital grains in a foliation that is a result of depositional stacking rather than metamorphic growth or structural alignment. Although not discussed further herein, the $^{40}Ar/^{39}Ar$ muscovite cooling ages from the Trembley Creek phyllite (Fig. 10) suggest that pre-Mississippian rocks in and around the Doonerak fenster did not reach temperatures greater than ~425 °C (Harrison et al., 2009).

Based on regional structural and stratigraphic relationships in the central Brooks Range, Moore et al. (1997) interpreted the Trembley Creek phyllite to be Devonian or older in age; the U-Pb and ^{40}Ar-^{39}Ar data presented herein provide a maximum depositional age of roughly ca. 490–465 Ma (Figs. 7 and 9), which suggests this unit could be as old as Middle Ordovician (Darriwilian). The most striking feature of the Trembley Creek U-Pb and Lu-Hf datasets is the profoundly different provenance signature from structurally adjacent rocks of the Apoon assemblage (Figs. 7 and 8). In particular, sample J1426 yielded prominent ca. 680–520 and 980–920 Ma zircon age populations that are rare in the Apoon assemblage (Fig. 7) and practically nonexistent in pre-Mississippian strata of the NE Brooks Range, except in younger synorogenic strata of the Clarence River group (Strauss et al., 2013; McClelland et al., 2015a; Lane et al., 2015; Johnson et al., 2016). The only other detrital zircon geochronology that exists from the Hammond subterrane comes from unpublished datasets described by Moore et al. (2007) and Till and Dumoulin (2013), both of which reported similar results to the data presented herein.

Detrital zircon U-Pb data from pre-Mississippian metasedimentary units in the Seward and York terranes of Seward Peninsula, Alaska, and the Chukotka Peninsula and Wrangel Island of NE Russia (Fig. 1), which are most likely correlative with the Hammond subterrane (e.g., Dumoulin et al., 2002, 2014; Miller et al., 2010; Till et al., 2014a), yielded U-Pb age populations that are indistinguishable from those of the Trembley Creek phyllite (Amato et al., 2009, 2014; Miller et al., 2010, 2011; Till et al., 2014a). The Hammond subterrane and Seward terrane also host plutonic and volcanic rocks ranging from ca. 970 to 540 Ma that broadly match many of the major age populations within the Trembley Creek sample (e.g., Amato et al., 2014, and references therein). Thus, the new U-Pb geochronological data presented here not only confirm a strong link in provenance between the Hammond and Seward/Chukotka regions of the Arctic Alaska–Chukotka microplate, but also support the existence of a significant pre-Mississippian tectonic boundary between Neoproterozoic–early Paleozoic basement domains of the Hammond and North Slope subterranes (Strauss et al., 2013).

Provenance and Paleogeographic Implications of the Trembley Creek Phyllite

Attempts to identify the source and significance of late Neoproterozoic detritus in metasedimentary units of Seward and Chukotka have recently focused on proposed magmatic and provenance links to the ca. 615–550 Ma Timanide orogen of Baltica (Amato et al., 2009; Colpron and Nelson, 2009, 2011; Miller et al., 2011; Till et al., 2014a, 2014b; Akinin et al., 2015). The Timanides are discontinuously exposed from the southern Ural Mountains of Russia northwestward to the Varanger Peninsula of Norway and extend northeastward into the Polar Urals, Novaya Zemlya, Severnaya Zemlya, and the Taimyr Peninsula of Arctic Russia (Puchkov, 1997; Gee and Pease, 2004; Kuznetsov et al., 2007, 2010; Lorenz et al., 2007, 2013; Pease and Scott, 2009; Corfu et al., 2010). Timanian magmatism and deformation, which may have locally lasted through the latest Cambrian (Bogolepova and Gee, 2004; Lorenz et al., 2007), record convergence between Baltica and either the composite microcontinent of Arctida or multiple independent peri-Baltican crustal fragments (Roberts and Siedlecka, 2002; Pease et al., 2008; Kuznetsov et al., 2007, 2010, and references therein). Ediacaran(?)–early Paleozoic foreland and hinterland basins of the Timanian orogen on Baltica record detrital zircon U-Pb age populations ca. 750–470 and 3200–1850 Ma, with small contributions of ca. 1250–900 and 1650–1480 Ma zircons (Kuznetsov et al., 2007, 2010; Lorenz et al., 2013; Andresen et al., 2014; Gee et al., 2014, 2015; Slama and Pedersen, 2015, and references therein). The $\varepsilon_{Hf(t)}$ compositions of Neoproterozoic–Cambrian zircons in proximal Timanian basins are moderately juvenile ($\varepsilon_{Hf[t]}$ = −2 to +10; Kuznetsov et al., 2010; Andresen et al., 2014), although data from hypothesized distal foreland deposits yield more diverse $\varepsilon_{Hf(t)}$ values ranging from −27 to +18 (Bingen et al., 2005; Kristoffersen et al., 2014; Slama and Pedersen, 2015). These data are broadly similar to those reported herein from the Trembley Creek phyllite, except for an apparent contrast in the abundance of Tonian–Mesoproterozoic zircon age populations and a much smaller range of $\varepsilon_{Hf(t)}$ values in Neoproterozoic–Cambrian zircon from Alaska.

Similarities in Timanian-age magmatic rocks and/or sedimentary detritus have also been identified in a variety of other circum-Arctic and Cordilleran terranes. For example, Timanian links have been proposed for the Southwest terrane of Svalbard (Majka et al., 2008, 2014, 2015; Mazur et al., 2009), the Alexander terrane of Alaska and Yukon (Beranek et al., 2012, 2013a, 2013b; Tochilin et al., 2014; White et al., 2016), the De Long and New Siberian Islands of Arctic Russia (Ershova et al., 2015, 2016), and the Sierran-Klamath terranes of California (Grove et al., 2008; Colpron and Nelson, 2009, 2011). As a result, many paleogeographic reconstructions restore the Arctic Alaska–Chukotka microplate and these associated crustal fragments to the Baltican side of the northern Iapetus Ocean during the latest Neoproterozoic and early Paleozoic (Colpron and Nelson, 2009, 2011; Miller et al., 2011; Beranek et al., 2013a, 2013b; Till et al., 2014a, 2014b; Ershova et al., 2015, 2016).

Recent studies have also identified Ediacaran igneous rocks and detrital zircon populations in Laurentian sedimentary successions from northern Greenland (Le Boudec et al., 2014; Morris et al., 2015; Rosa et al., 2016). Although most of this Ediacaran magmatism is concentrated in allochthonous thrust sheets and/or peri-Laurentian terranes (e.g., Svalbard and Pearya), Le Boudec et al. (2014) and Morris et al. (2015) reported significant populations of ca. 650–620 Ma zircon in early–middle Cambrian (Cambrian Global Stages 2–3) autochthonous strata of northern Greenland. Rosa et al. (2016) proposed that Ediacaran magmatism in northern Greenland may support a northwestward continuation of the Ediacaran Timanian orogenic belt toward the Laurentian margin; however, many of these “exotic” Ediacaran magmatic rocks and zircon age populations broadly overlap in age with poorly understood extensional tectonism along the northern margin of Laurentia associated with the breakup of Rodinia (e.g., Surlyk and Hurst, 1984; Henriksen and Higgins, 1998; Dewing et al., 2008). Moreover, the conspicuously broad age range (ca. 700–500 Ma) of magmatic rocks associated with the Timanian orogen and our fundamental lack of detailed Ediacaran paleogeographic models for the circum-Arctic (e.g., Malone et al., 2014; Cawood et al., 2015, 2016) complicate assumptions that all Neoproterozoic magmatism in the circum-Arctic is derived from Baltica. These uncertainties accentuate a need for more rigorous assessment of Neoproterozoic age populations in sedimentary deposits of circum-Arctic and Cordilleran terranes.

The significant ca. 1020–900 Ma detrital zircon age population in the Trembley Creek phyllite is difficult to explain with a direct link to the Timanides because magmatism of this age is rare in the exposed hinterland of the orogen (Kuznetsov et al., 2007, 2010, and references therein). Despite this, many workers still assume that smaller Mesoproterozoic detrital and xenocrystic zircon populations in Timanian foreland deposits are derived from unexposed Timanian basement sources (e.g., Lorenz et al., 2007; Andresen et al., 2014; Slama and Pedersen, 2015). As an alternative, early Neoproterozoic magmatism is common in North-East Greenland, Svalbard, and Pearya (e.g., Trettin et al., 1987; Peucat et al., 1989; Gee et al., 1995; Strachan et al., 1995; Kalsbeek et al., 2000; Watt et al., 2000; Watt and Thrane, 2001; Johansson et al., 2004; Pettersson et al., 2009; Kirkland et al., 2011; Majka et al., 2014, 2015; Malone et al., 2014), as well as throughout the Sveconorwegian orogen of southwestern Baltica (Bingen et al., 2008; Bingen and Solli, 2009, and references therein) and even within the Arctic Alaska–Chukotka microplate (e.g., Amato et al., 2014). Magmatism of this age has generally been attributed to either northward continuation of the Grenville-Sveconorwegian orogen between Baltica and Laurentia (e.g., Lorenz et al.,

2012) or pre- to syn-Caledonian long-distance strike-slip transport from the Appalachians and British Caledonides (e.g., Harland, 1997; Pettersson et al., 2010; Kirkland et al., 2006, 2008, 2011). Instead, Cawood et al. (2010, 2015) argued that much of this magmatism occurred *in situ* and is related to a coeval but distinctly different tectonic event called the Valhalla orogeny. Although this model relies heavily on paleomagnetic data to support a 90° clockwise rotation of Baltica away from Laurentia during the Grenville–Sveconorwegian orogen (Cawood and Pisarevsky, 2006), it does account for the subduction-related geochemistry that characterizes the Neoproterozoic (Tonian) magmatic rocks of North-East Greenland, Svalbard, and Pearya (Gee et al., 1995; Kalsbeek et al., 2000; Johansson et al., 2004, 2005; Kirkland et al., 2006, 2008, 2011; Cawood et al., 2010; Malone et al., 2014).

Independent of the paleogeographic reconstruction of these Tonian–Mesoproterozoic orogenic belts, many of these peri-Laurentian crustal fragments also host late Neoproterozoic magmatic and deformational events (e.g., Kirkland et al., 2006, 2008, 2011; Majka et al., 2008, 2014, 2015; Cawood et al., 2010, 2015; Malone et al., 2014). Therefore, we argue that Ediacaran magmatism in the circum-Arctic was likely inherited from a complex paleogeographic framework that does not necessarily require a direct link with the Timanide convergent margin of Baltica. Although speculative, the presence of a Neoproterozoic fringing arc system along the outboard northeastern Greenland margin of Laurentia during the breakup of Rodinia not only provides a viable explanation for regional magmatic and subsidence patterns (e.g., Cawood et al., 2010, 2015, 2016; Malone et al., 2014), but also a reasonable paleogeographic link to the active continental margins of Siberia, Baltica, and Gondwana (Amato et al., 2009; Cawood et al., 2010, 2015, 2016; Malone et al., 2014). Therefore, although the Arctic Alaska–Chukotka microplate may have been situated in proximity to the Timanides during the late Neoproterozoic–early Paleozoic (Miller et al., 2011; Beranek et al., 2012, 2013a, 2013b), it is equally permissible that portions of this composite crustal fragment remained outboard of the Laurentian margin in an intra-oceanic arc setting similar to the Pearya terrane or Southwest terrane of Svalbard (Malone et al., 2014). In this model, the extensive Neoproterozoic fringing arc systems of Siberia, Baltica, and Laurentia may have generated juvenile basement fragments that seeded the Ediacaran–Ordovician arc systems now scattered throughout the circum-Arctic and Cordilleran terranes.

Linking Ordovician–Silurian Arc Magmatism in the Arctic and Implications for Regional Paleogeography

Taconic–Caledonian Orogenic Events in the Arctic and North American Cordillera

Latest Ediacaran–early Paleozoic passive-margin sedimentation along the northeastern margin of Laurentia and western margin of Baltica was terminated by diachronous closure of the Iapetus Ocean during the Taconic–Caledonian orogenic cycle (e.g., McKerrow et al., 2000). These Cambrian–Devonian tectonic events are well calibrated in the Appalachians and Scandinavian Caledonides (van Staal et al., 2010; van Staal and Barr, 2012; Chew and Strachan, 2014; Corfu et al., 2014, and references therein), but little is known about coeval tectonism in the circum-Arctic region (e.g., Pease, 2011). The main phase of Caledonian deformation in the Scandinavian and Greenland Caledonides, the Scandian event (ca. 435–425 Ma), involved oblique westward subduction of Baltica beneath Laurentia (Gee, 1975; Gee and Sturt, 1985; Roberts, 2003; Higgins and Leslie, 2008; Corfu et al., 2014, and references therein). Evidence for Scandian deformation occurs as far north as the Svalbard archipelago, where widespread ca. 430–420 Ma compressional deformation, magmatism, and metamorphism are recorded in the Northwest and Northeast terranes (Harland, 1997; Johansson et al., 2004; Myhre et al., 2009; Pettersson et al., 2009). The end of regional Scandian deformation in Scandinavia is reportedly marked by a transition to regional Early–Middle Devonian (ca. 400–380 Ma) ductile extension and Late Devonian–Mississippian (ca. 365–300 Ma) sinistral transpression (Andersen, 1998; Tucker et al., 2004; Fossen, 2010; and many others). However, simultaneous sinistral and dextral strike-slip deformation coeval with ultrahigh-pressure metamorphism in North-East Greenland clearly indicates that contraction in the Caledonian orogen persisted through ca. 350 Ma, with exhumation of the North-East Greenland eclogite province recorded by detritus in Mississippian siliciclastic strata (Sartini-Rideout et al., 2006; Gilotti and McClelland, 2008; Gilotti et al., 2014; Hallett et al., 2014; McClelland et al., 2016). The late phases of the Caledonian orogeny in Svalbard are recorded by the emplacement of local ca. 400 Ma post-tectonic granitic plutons and the widespread development of Late Silurian–Devonian sinistral transtensional basins with syn- to postorogenic siliciclastic debris (e.g., Gee and Page, 1994; Harland, 1997; Gee and Teben'kov, 2004). The northern trace of the Caledonian orogen and hypothesized suture between Baltica and Laurentia likely intersects the Lomonosov Ridge where it was subsequently dismembered during the Mesozoic–Cenozoic opening of the Arctic Ocean.

The Scandinavian Caledonides contain discontinuously exposed pre-Scandian ophiolitic and magmatic arc complexes that overlap in age with the multi-phase Taconic orogeny (e.g., Harland and Gayer, 1972; Furnes et al., 1985; Andersen and Andresen, 1994; Pedersen and Dunning, 1997; Yoshinobu et al., 2002; Slagstad et al., 2011, 2014; and many others). For example, geochemical and geochronological data from suprasubduction zone ophiolites in the Trondheim region of central Norway record a protracted history of ca. 497–467 Ma peri-Laurentian oceanic and continental arc magmatism (Slagstad et al., 2014, and references therein). Scattered remnants of late Cambrian–Late Ordovician (ca. 495–450 Ma) island-arc fragments and immature spreading centers are also preserved in the Karmøy, Bømlo, and Gullfjellet ophiolite sequences of southwestern Norway (e.g., Pedersen and Hertogen, 1990; Pedersen and Dunning, 1997), as well as throughout a relatively continuous belt of Caledonide nappes extending from central Norway (e.g., Helgeland Nappe Complex; Yoshinobu et al., 2002; Barnes et al., 2007; McArthur et al., 2014, and references therein) to the Ofoten–Tromsø region of northern Norway (e.g., Ofoten, Niingen, Lyngsfjellet, Tromsø, and Nakkedal nappes; Corfu et al., 2003; Augland et al., 2014a, 2014b, and references therein). Recent work has documented peri-Baltican or peri-Laurentian oceanic arc fragments within the Kalak and Seve nappe complexes of the Middle and Lower allochthons (e.g., Corfu et al., 2011; Root and Corfu, 2012), which were long thought to represent imbricated segments of the outer continental margin of Baltica (e.g., Sturt et al., 1978; Gee et al., 1985; Andréasson et al., 1998). These pre-Scandian oceanic slivers and juvenile arc fragments record a protracted history of intra-Iapetus island-arc magmatism, back-arc extension, and microcontinent accretion presumably outboard of the northeastern Laurentian margin (Corfu et al., 2014, and references therein).

Evidence of early Paleozoic convergent margin tectonism is also widespread along the northern margin of Laurentia (e.g., Thorsteinsson and Tozer, 1970; Trettin, 1987; Trettin et al., 1991a, 1991b; Higgins et al., 1991). Passive margin sedimentation in the Franklinian Basin of northern Greenland and Ellesmere Island was abruptly terminated by the arrival of Lower Silurian–Lower Devonian (ca. 440–410 Ma) flysch of the Peary Land Group and Danish River and Fire Bay formations, which was coincident with the Scandic phase of the Caledonian orogeny (Hurst and Surlyk, 1984; Higgins et al., 1991; Trettin, 1987, 1991, 1998; Trettin et al., 1991a, 1991b; Dewing et al., 2008; Anfinson et al., 2012a, 2012b; Hadlari et al., 2014; Beranek et al., 2015). The Pearya terrane hosts Early–Middle Ordovician (ca. 481–465 Ma) arc magmatism and deformation associated with the M'Clintock orogeny (Trettin, 1987), which has been attributed to both intra-arc deformation (Trettin, 1987; Klaper, 1992; Trettin, 1992) and outboard terrane amalgamation prior to accretion onto the Laurentian margin (von Gosen et al., 2012; McClelland et al., 2012). The M'Clintock orogeny is synchronous with the Taconic 2 and 3 events of the Appalachians and British Caledonides (e.g., van Staal and Barr, 2012) and has been linked regionally to similar Early Ordovician tectonism in the Vestgötabreen Complex (Eidembreen event) of Svalbard's Southwest terrane (Trettin, 1987; Dallmeyer et al., 1990; Gee and Page, 1994; Labrousse et al., 2008; Gee and Teben'kov, 2004; von Gosen et al., 2012; McClelland et al., 2012; Gasser and Andresen, 2013; Kośmińska et al., 2014; Majka et al., 2015). Subduction-related mafic rocks of the Richarddalen Complex of west-central Svalbard also record ca. 460 Ma high-pressure metamorphism that matches M'Clintock deformation (Gromet and Gee, 1998) and suggests that Pearya and various components of Svalbard may have been part of the same intra-arc collision outboard of Laurentia prior to peak Scandian deformation (e.g., von Gosen et al., 2012; McClelland et al., 2012; Gasser and Andresen, 2013; Kośmińska et al., 2014; Majka et al., 2015). More recently, bedrock samples of amphibolite, garnet-bearing gneiss, and augen-orthogneiss dredged from submarine outcrops along the Chukchi Borderland of the Canada Basin have yielded similar late Cambrian–Early Ordovician (ca. 520–470 Ma) and Late Ordovician–Silurian (ca. 465–420 Ma) metamorphic and magmatic ages, potentially linking portions of the Chukchi Borderland to Pearya and western Svalbard prior to the opening of the Amerasian Basin (Brumley et al., 2015).

Temporally overlapping early Paleozoic magmatism and tectono-thermal events are also recorded in the Alexander terrane of Alaska and NW Canada and the Sierran-Klamath terranes of northern California, both of which have hypothesized paleogeographic ties to the Iapetus realm (Wright and Wyld, 2006; Grove et al., 2008; Colpron and Nelson, 2009, 2011; Beranek et al., 2013a, 2013b; White et al., 2016, and references therein). The eastern Klamath (Redding, Trinity, and Yreka subterranes) and northern Sierran terranes contain Ediacaran (ca. 612–550 Ma) basement fragments and early Paleozoic (ca. 480–410 Ma) subduction-related magmatic rocks and synorogenic strata that have generally been regarded as displaced remnants of oceanic island arcs (Wallin and Metcalf, 1998; Wright and Wyld, 2006; Grove et al., 2008; Lindsley-Griffin et al., 2008, and references therein). Paleomagnetic, biogeographic, and detrital zircon geochronological studies from various units in the Sierran-Klamath terranes solidify correlations with the Alexander terrane and support the formation of these early Paleozoic oceanic arc fragments within the northern Iapetus in close proximity to Mesoproterozoic–Paleoproterozoic and Ediacaran source regions (e.g., Grove et al., 2008; Lindsley-Griffin et al., 2008; and many others). Although initial models favored transport of the Sierran-Klamath terranes in a Caribbean/Scotia-type plate-tectonic system along the southern margin of Laurentia (Wright and Wyld, 2006), recent work favors a similar tectonic setting along the northern margin of Laurentia (Colpron and Nelson, 2009, 2011; Beranek et al., 2012, 2013a, 2013b).

The Alexander terrane consists of three distinct geographic components, including the Prince of Wales Island region in southeast Alaska, the Saint Elias Mountains region of Yukon, British Columbia, and southeast Alaska, and the Banks Island region of west-central British Columbia (Cecil et al., 2011; Beranek et al., 2012; Tochilin et al., 2014; White et al., 2016, and references therein). The Prince of Wales Island area is composed of a basal Ediacaran–Cambrian (ca. 595–530 Ma) volcanic arc sequence (Wales Group), which is separated by a significant late Cambrian–Early Ordovician unconformity (Wales orogeny) from the overlying Ordovician–Silurian (ca. 490–420 Ma) magmatic arc sequence of the Descon Formation (Churkin and Eberlein, 1977; Eberlein et al., 1983; Gehrels and Saleeby, 1987; Gehrels et al., 1996; Cecil et al., 2011; White et al., 2016). Juvenile plutonic and volcanic arc rocks and associated synorogenic strata of the Descon Formation were locally tectonized and metamorphosed in the Late Silurian–Early Devonian Klakas orogeny and regionally overlain by molasse of the Lower Devonian Karheen Formation (Gehrels and Saleeby, 1987). These proximal arc-related rocks apparently transition northward into age-equivalent early Paleozoic mixed siliciclastic and carbonate strata exposed in the Banks Island region (e.g., Tochilin et al., 2014) and a distinct sequence of Cambrian–Ordovician mafic volcanic rocks and Ordovician–Devonian carbonate and siliciclastic strata in the Saint Elias Mountains region (Dodds and Campbell, 1992; Dodds et al., 1993; Mihalynuk et al., 1993; Beranek et al., 2012, 2013a, 2013b); however, the exact stratigraphic ties between these different regions are still poorly constrained, and syntheses of detrital zircon U-Pb and Lu-Hf isotopic datasets record prominent compositional differences in coeval early Paleozoic volcanic and sedimentary units (White et al., 2016). Although the Alexander terrane has a diverse history of disparate paleogeographic reconstructions (e.g., Gehrels and Saleeby, 1987; Bazard et al., 1995; Gehrels et al., 1996; Butler et al., 1997; Soja and Antoshkina, 1997; Blodgett et al., 2002; Soja and Krutikov, 2008), most workers now favor an origin near Baltica with hypothetical links to the northern Caledonides (Colpron and Nelson, 2009, 2011; Miller et al., 2011; Beranek et al., 2013a, 2013b; Tochilin et al., 2014; White et al., 2016).

Paleogeographic and Tectonic Significance of the Doonerak Arc

Based on limited data from the central Brooks Range, some workers have proposed links between the arc-related Apoon assemblage and Cambrian–Silurian magmatic and metamorphic events in the Caledonides and circum-Arctic region (Natal'in et al., 1999; Dumoulin et al., 2000; Colpron and Nelson, 2009, 2011; Beranek et al., 2013a, 2015; Strauss et al., 2013; Till et al., 2014a). The new geochronological and stratigraphic data presented herein enable us to significantly refine tectonic models for the Doonerak arc in this early Paleozoic paleogeographic framework. First, the juvenile Hf isotopic signature of the Apoon volcanics is consistent with an oceanic arc setting similar to the Prince of Wales Island region of the Alexander terrane, the Sierran–Klamath terranes, and many of the peri-Laurentian arc fragments preserved in the northern Scandinavian Caledonides (e.g., Augland et al., 2014b; Slagstad et al., 2014; Tochilin et al., 2014; White et al., 2016). Furthermore, the 462 ± 8 Ma age from the Apoon assemblage overlaps with the Taconic 3 event of the Appalachians and localized Middle Ordovician magmatic and metamorphic ages in the Southwest terrane of Svalbard (Dallmeyer et al., 1990; Gromet and Gee, 1998), Pearya (Trettin, 1987; Trettin, 1992; McClelland et al., 2012), and the Chukchi Borderland (Brumley et al., 2015). Finally, the profound change of provenance within map unit Pzc of the Apoon assemblage records an enigmatic tectonic event within the Doonerak arc that may to overlap with the timing of the Klakas orogeny of the Alexander terrane (Gehrels and Saleeby, 1987), the onset of synorogenic sedimentation in the Franklinian Basin (Hurst and Surlyk, 1984; Higgins et al., 1991; Trettin et al., 1991a, 1991b; Trettin, 1998; Patchett et al., 1999), and the hypothesized accretion of Pearya to the Laurentian margin (Trettin, 1987). Below, we outline two reasonable paleogeographic scenarios for the early Paleozoic tectonic setting of the

Doonerak arc complex based on these data and preliminary correlations, both of which assume that the pre-Mississippian basement domains of Doonerak, Hammond, and the North Slope were independent tectonic entities prior to their amalgamation sometime during the Silurian–Devonian (Fig. 11).

Building upon current circum-Arctic models that restore the Hammond, Seward, York, and Chukotka portions of the Arctic Alaska–Chukotka microplate and the Alexander terrane to the peripheral margin of Baltica during the late Neoproterozoic–early Paleozoic (Colpron and Nelson, 2009, 2011; Miller et al., 2011; Beranek et al., 2012, 2013a, 2013b; Till et al., 2014a; White et al., 2016), one plausible reconstruction is that the Doonerak arc was linked to the Alexander terrane in an intra-oceanic arc setting outboard of the leading edge of Baltica (Fig. 11A). Protracted Middle Ordovician–Early Devonian convergence of this peri-Baltican arc system with the northernmost extension of the Taconic arc system (e.g., Pearya, Southwest terrane of Svalbard, and portions of the Scandinavian Upper and Uppermost allochthons) would have ultimately sealed the northern edge of the Iapetus Ocean and may be evidenced by the Klakas orogeny and unnamed tectonic event within the Doonerak arc. Localized uplift and erosion of these colliding arc terranes may have internally provided diverse Tonian–Silurian detritus to the Banks Island and Saint Elias Mountains regions of the Alexander terrane (White et al., 2016), as well as externally to the retroarc foreland Franklinian Basin (Anfinson et al., 2012a; Hadlari et al., 2014; Beranek et al., 2015). In particular, Ediacaran–Silurian zircon populations with distinctly juvenile $\varepsilon_{Hf(t)}$ compositions in the Franklinian Basin (e.g., Anfinson et al., 2012b) may have been directly sourced from the Doonerak and Prince of Wales Island arc complexes (among others). Continued westward (in present coordinates) migration of this convergent margin system along a major sinistral strike-slip system near the northern Laurentian margin (e.g., Sweeney, 1982; Trettin, 1987; McClelland et al., 2012, 2015b; Strauss et al., 2013; Johnson et al., 2016) would have eventually facilitated the displacement of the Alexander terrane and the Sierran-Klamath terranes into the paleo-Pacific realm (Colpron and Nelson, 2009, 2011; McClelland et al., 2012, 2015b), while the Doonerak arc was trapped within the complex collisional zone between different segments of the Arctic Alaska–Chukotka microplate (e.g., Hammond and Seward terranes) and the distal Laurentian margin (e.g., North Slope

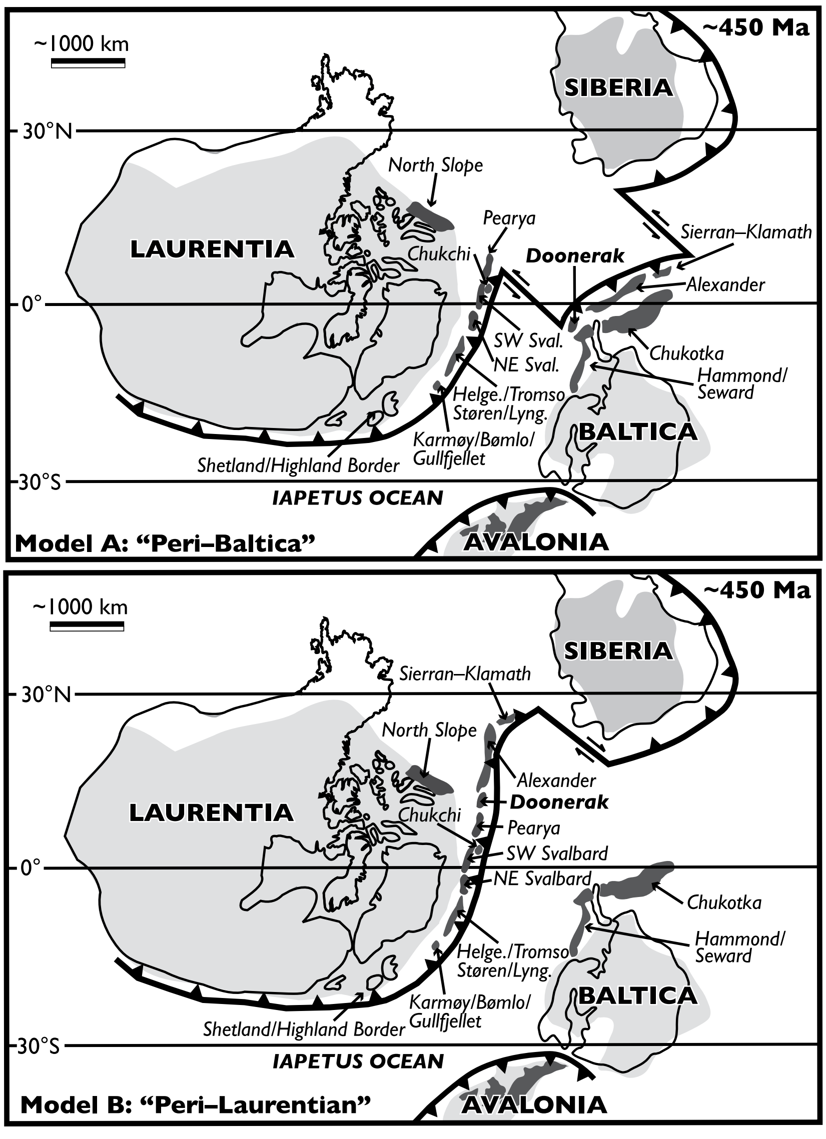

Figure 11. Schematic paleogeographic reconstructions of circum-Arctic paleocontinents and terranes/microcontinents in the Late Ordovician (ca. 450 Ma). Latitudinal positions of Laurentia, Siberia, and Baltica are based upon reconstructions from Cocks and Torsvik (2005, 2007, 2011, and references therein), and the geometry of circum-Arctic terranes is based on the rough geometry of modern outcrop distributions. Note that Tertiary shortening from the Eurekan orogen of Ellesmere Island is schematically restored along the northern margin of Laurentia. In both reconstructions, the positions of Cambrian–Ordovician ophiolites and subduction zone complexes exposed within the uppermost nappes of the Caledonian orogen are restored to the Laurentian margin (see text for discussion). The North Slope subterrane of Arctic Alaska is kept on the peri-Laurentian margin following Strauss et al. (2013), Cox et al. (2015), and Johnson et al. (2016). Note that in both of these scenarios, the Alexander terrane could be separated into two distinct segments instead of one continuous terrane (e.g., van Staal et al., 2010). (A) Paleogeographic model that restores the Doonerak arc complex to a similar tectonic setting as the Alexander terrane and exotic portions of the Arctic Alaska–Chukotka microplate along the convergent margin of Baltica. In order for this reconstruction to be viable, there must be subduction polarity reversal during arc-arc collision in order to ensure Baltica is on the lower plate during Scandian contraction. (B) Paleogeographic model that restores the Doonerak arc complex (and other circum-Arctic terranes) to the northern segment of the peri-Laurentian Taconic orogenic system. This model would also require an episode of subduction polarity reversal in order to accrete the Pearya terrane and Doonerak arc complex to the NE margin of Laurentia. See text for model assumptions and implications. Helge.—Helgeland; Lyng.—Lyngsfjellet; Sval.—Svalbard.

subterrane). In this scenario, the Doonerak arc marks a fundamental suture between peri-Baltican and peri-Laurentian portions of the Taconic–Caledonian orogen, similar to the Red Indian Line of the Appalachians, which marks a boundary between peri-Gondwanan and peri-Laurentian terranes (Williams et al., 1988).

While this model is appealing because it proposes a Caledonian suture in the Arctic Alaska–Chukotka microplate and provides an explanation for the disparities in stratigraphic architecture and provenance between the Hammond and North Slope basement domains, it suffers from a lack of convincing data that Doonerak and Alexander represent unambiguous peri-Baltican crustal fragments. For example, if Ediacaran magmatic ages or detrital zircon populations in the circum-Arctic are not definitively linked to the Timanide orogen (see earlier discussion), no component of these datasets unambiguously confirms paleogeographic links to the margin of Baltica. Although many workers have highlighted key paleontological ties between these terranes and the Siberian and Baltican cratons (e.g., Blodgett et al., 2002; Dumoulin et al., 2002, and references therein), many of these faunal assemblages are from Late Ordovician–Devonian strata and may simply reflect geographic proximity to these circum-Arctic cratons. Given the potential ambiguity in characterizing source regions for the Tonian–Ediacaran provenance data described here from the Hammond subterrane, it is worth considering other tectonic models that explore peri-Laurentian origins for exotic terranes previously considered unambiguously tied to Baltica.

In a more radical tectonic model acknowledging the permissibility of peripheral Neoproterozoic arc- and rift-related magmatism near the NE Laurentian margin during the breakup of Rodinia (e.g., Malone et al., 2014; Cawood et al., 2015, 2016), the Doonerak arc and Prince of Wales Island region of the Alexander terrane may have formed part of the northern peri-Laurentian Taconic arc system (Fig. 11B). Hypothetically, this early Paleozoic arc system would have been built upon different juvenile arc terranes and/or rifted peri-Laurentian crustal fragments (e.g., Pearya, Chukchi, the Southwest terrane of Svalbard, and portions of the Upper and Uppermost allochthons of Scandinavia) that were inherited from a complex paleogeography associated with the Cryogenian–Ediacaran fragmentation of Rodinia. In this model, protracted Middle Ordovician(?)–Early Devonian tectonism in the Doonerak arc and Alexander terrane (e.g., Klakas orogeny) may have been related to intra-arc deformational events (e.g., van Staal et al., 2010; McClelland et al., 2012; Augland et al., 2014a, 2014b; Corfu et al., 2014; Slagstad et al., 2014; Majka et al., 2014, 2015) and/or enigmatic collision(s) between peri-Laurentian and peri-Baltican fringing arc systems. The U-Pb detrital zircon geochronology and Lu-Hf isotopic data from map unit Pzc of the Apoon assemblage support the juxtaposition of this oceanic arc with a Laurentian-affinity continental fragment—this could indicate uplift and erosion of a peri-Laurentian terrane (e.g., Pearya) or closure of a marginal ocean basin between the Doonerak arc and Franklinian Basin of northeastern Laurentia. The Scandian arrival of Baltica into the west-dipping Caledonian subduction zone may have ultimately generated the necessary geodynamic conditions to initiate the conversion of the northern margin of Laurentia into a major sinistral transform margin, which ultimately facilitated circum-Arctic transcurrent displacements of Cordilleran terranes (e.g., Sweeney, 1982; Colpron and Nelson, 2009, 2011; Mazur et al., 2009; von Gosen et al., 2012; McClelland et al., 2012, 2015b; Gasser and Andresen, 2013).

This peri-Laurentian model for the Doonerak arc complex would support restoration of the Hammond subterrane (and potentially other portions of the Arctic Alaska–Chukotka microplate) to either the peri-Laurentian realm or the peripheral margin of Baltica (Fig. 11B). It also brings up the possibility that different segments of the Alexander terrane (e.g., Prince of Wales Island vs. Saint Elias Mountains) were only juxtaposed in the Klakas orogeny (van Staal et al., 2010), potentially explaining the significant stratigraphic and geochronological discrepancies between the two regions. For example, the Klakas orogeny could represent the collision between a peri-Baltican arc system composed of the Saint Elias Mountains segment of the Alexander terrane (lower plate) with a peri-Laurentian segment of the Taconic arc system represented by the Prince of Wales Island region of the Alexander terrane (upper plate) prior to (or coincident with) regional Scandian deformation. The localized uplift and erosion of this diverse northern segment of the Taconic orogenic belt may have also provided Tonian–Silurian detritus (Anfinson et al., 2012a, 2012b; Hadlari et al., 2014; Beranek et al., 2015) to the retroarc foreland Franklinian Basin and to many of the terranes now dispersed throughout the North American Cordillera. The eventual conversion of the northern margin of Laurentia into a major sinistral strike-slip system would have also facilitated the translation of the Alexander and Sierran-Klamath terranes into Panthalassa, leaving the Doonerak arc complex behind as a remnant of this early Paleozoic multiphase transpressional orogen.

CONCLUSIONS

While most studies have described the Doonerak fenster of the central Brooks Range, Alaska, in light of its Mesozoic–Tertiary significance in the Brookian orogen, this locality may be equally important to our understanding of early Paleozoic paleogeography and tectonics in the Arctic. The new U-Pb and Lu-Hf isotopic data presented herein from the Cambrian–Devonian(?) Apoon assemblage of the Doonerak fenster, combined with previously published geologic, geochronologic, and biostratigraphic data, provide fundamental new insights into the magmatic and tectonic evolution of the Arctic Alaska–Chukotka microplate and other circum-Arctic terranes. The first-order conclusions of this study are as follows:

(1) Although structural deformation in the central Brooks Range still precludes a clear assessment of facies and age relationships within the early Paleozoic Apoon assemblage, the new U-Pb and Lu-Hf isotopic data elucidate new stratigraphic links between disparate map units within the Doonerak fenster.

(2) U-Pb (SHRIMP-RG) and Hf isotopic analyses on zircon from a leucogabbro in map unit Pzv of the Apoon assemblage yield a ^{207}Pb-corrected ^{206}Pb/^{238}U age of 462 ± 8 Ma (2σ; Fig. 6), confirming previous reports of ca. 470 Ma K-Ar and ^{40}Ar-^{39}Ar ages on hornblende from arc-related volcanic rocks in the Doonerak fenster (Dutro et al., 1976). These igneous zircons also yield highly juvenile $\varepsilon_{Hf(t)}$ isotopic values (up to +13), providing evidence for Middle Ordovician juvenile arc magmatism in the Brooks Range.

(3) Recognition that both map units Pzp and Pzc of the Apoon assemblage host Cambrian(?)–Upper Silurian or Lower Devonian(?) reworked tuffaceous horizons and volcaniclastic rocks (Figs. 4 and 7) implies that the Apoon assemblage was deposited within a long-lived, synvolcanic depocenter. Definitive components of this intra-oceanic arc system include an Upper Cambrian (Furongian)–Middle Ordovician volcanic arc sequence and an Upper Cambrian (Furongian)–Silurian or Early Devonian(?) back-arc or fore-arc succession. The Apoon assemblage contains a distinct Middle Ordovician or younger sedimentary succession that contains both reworked juvenile arc detritus and exotic continental siliciclastic, volcanic, and metamorphic material, perhaps recording evidence for tectonic juxtaposition of the Doonerak arc with one or more unknown crustal fragments.

(4) Detrital zircons analyzed using LA-ICP-MS from volcaniclastic and tuffaceous strata of the Apoon assemblage yield a spectrum of unimodal and polymodal age populations,

including prominent age groups of ca. 490–420, 540–510 Ma, 1250–960, 1500–1380, 1945–1750, and 2830–2650 Ma. Lu-Hf isotopic data from the ca. 490–420 Ma age population are highly juvenile, implying a lack of crustal assimilation during Ordovician–Silurian arc magmatism. The older detrital zircon age populations are all concentrated in volcaniclastic strata of map unit Pzc of the Apoon assemblage.

(5) U-Pb detrital zircon data from the Kekiktuk Conglomerate record striking petrological and geochronological similarities with equivalent strata in the NE Brooks Range. This clear stratigraphic, petrologic, and geochronologic correlation supports a model of widespread S-directed Mississippian fluvial-deltaic sedimentation across the North Slope and Doonerak arc basement domains despite differing Romanzof–Ellesmerian structural histories. This may reflect strike-slip juxtaposition of the North Slope and Hammond subterranes and Doonerak arc prior to overlap by the early Mississippian and younger Endicott Group.

(6) The Trembley Creek phyllite of the Hammond subterrane hosts a profoundly different provenance signature from structurally adjacent rocks of the Apoon assemblage, including large populations of ca. 680–520 and 980–920 Ma zircons (Fig. 7). The new U-Pb geochronological data presented here not only confirm a strong link in provenance between the Hammond and Seward/Chukotka regions of the Arctic Alaska–Chukotka microplate, but also support the existence of a significant pre-Mississippian tectonic boundary between basement domains of the Hammond and North Slope subterranes.

(7) The U-Pb geochronological and Lu-Hf isotopic data suggest a potential link between the Doonerak arc of Arctic Alaska and other early Paleozoic arc terranes of the Caledonides, circum-Arctic, and North American Cordillera, including the Prince of Wales Island region of the Alexander terrane. We present two different models (peri-Baltican or peri-Laurentian) that propose a connection between the Doonerak arc and Taconic–Caledonian arc magmatism along the fringes of the Iapetus Ocean (Fig. 11).

ACKNOWLEDGMENTS

Strauss, Ward, and Johnson were each supported by Geological Society of America graduate student research grants. McClelland was funded by the National Science Foundation (NSF) Tectonics Program (EAR-1049368). Strauss was also supported by the Department of Earth and Planetary Sciences at Harvard University, the Department of Earth Sciences at Dartmouth College, and the NSF Tectonics Program (EAR-1624131). Hoiland acknowledges support from a Stanford McGee Grant and a NSF Graduate Research Fellowship under grant number DGE-4747. We thank Loic Labrousse, Nicolas Lemmonier, and Sarah Roeske for help with helicopter logistics; Nancy Brandt at Toolik Research Station and Dana Truffer-Moudra at Polar Field Services for logistical support; Jobe Chakuchin at the National Park Service for providing access to Gates of the Arctic National Park; Marty Grove for collection of $^{40}Ar/^{39}Ar$ data at Stanford University; Matt Coble and the Stanford-USGS Micro Analysis Center for providing instrument time, technical support, and scientific guidance in acquiring ion microprobe data; and Daniel Alberts, Intan Yokelson, Mark Pecha, and Nicky Giesler for help at the Arizona LaserChron Center. The LaserChron Center is supported by NSF grant EAR-1338583. Zircon imaging utilized equipment of the University of Iowa Central Microscopy Research Facilities purchased with funding from NSF grant EAR-1038684 and National Institute of Health (NIH) grant S10-RR022498-01. We thank Gil Mull for providing copies of his field notes from the Doonerak fenster and for numerous discussions of Brooks Range geology. Tom Moore provided a copy of Bill Brosge's unpublished field map from the Doonerak fenster and constructive criticism on a preliminary version of this manuscript. Julie Dumoulin, Luke Beranek, and Associate Editor Cees van Staal also provided helpful feedback and editorial support.

REFERENCES CITED

Adams, K.E., Mull, C.G., and Crowder, R.K., 1997, Permian deposition in the north central Brooks Range, Alaska: Constraints for tectonic reconstructions: Journal of Geophysical Research, v. 102, no. B9, p. 20,727–20,748, doi:10.1029/97JB00950.

Akinin, V.V., Gottlieb, E.S., Miller, E.L., Polsunenkov, G.O., Stolbov, N.M., and Sobolev, N.N., 2015, Age and composition of basement beneath the De Long archipelago, Arctic Russia, based on zircon U-Pb geochronology and O-Hf isotopic systematics from crustal xenoliths in basalts of Zhokhov Island: Arktos, v. 1, p. 9.

Amato, J.M., Toro, J., Miller, E.L., Gehrels, G.E., Farmer, G.L., Gottlieb, E.S., and Till, A.B., 2009, Late Proterozoic–Paleozoic evolution of the Arctic Alaska–Chukotka terrane based on U-Pb igneous and detrital zircon ages: Implications for Neoproterozoic paleogeographic reconstructions: Geological Society of America Bulletin, v. 121, p. 1219–1235, doi:10.1130/B26510.1.

Amato, J.M., Aleinikoff, J.N., Akinin, V.V., McClelland, W.C., and Toro, J., 2014, Age, chemistry, and correlations of Neoproterozoic–Devonian igneous rocks of the Arctic Alaska–Chukotka terrane: An overview with new U-Pb ages, *in* Dumoulin, J.A., and Till, A.B., eds., Reconstruction of a Late Proterozoic to Devonian Continental Margin Sequence, Northern Alaska: Its Paleogeographic Significance and Contained Base-Metal Sulfide Deposits: Geological Society of America Special Paper 506, p. 29–57, doi:10.1130/2014.2506(02).

Andersen, T.B., 1998, The stratigraphy of the Magerøy Supergroup: North Norway: Norges Geologiske Undersøkelse, v. 285, p. 333–351.

Andersen, T.B., 2014, The detrital zircon record: Supercontinents, parallel evolution—Or coincidence?: Precambrian Research, v. 244, p. 279–287, doi:10.1016/j.precamres.2013.10.013.

Andersen, T.B., and Andresen, A., 1994, Stratigraphy, tectonostratigraphy and the accretion of outboard terranes in the Caledonides of Sunnhordland, west Norway: Tectonophysics, v. 231, p. 71–84, doi:10.1016/0040-1951(94)90122-8.

Anderson, A.V., Wallace, W.K., and Mull, C.G., 1994, Depositional record of a major tectonic transition in northern Alaska: Middle Devonian to Mississippian rift-basin margin deposits, upper Kongakut River region, eastern Brooks Range, Alaska, *in* Thurston, D.K., and Fujita, K., eds., 1992 Proceedings of the International Conference on Arctic Margins: Anchorage, Alaska, U.S. Department of the Interior, Minerals Management Service, p. 71–76.

Andréasson, P.G., Svenningsen, O.M., and Albrecht, L., 1998, Dawn of Phanerozoic orogeny in the North Atlantic tract: Evidence from the Seve-Kalak superterrane, Svandinavian Caledonides: GFF, v. 120, p. 159–172, doi:10.1080/11035899801202159.

Andresen, A., Agyie-Dwarko, N.Y., Kristoffersenm, M., and Hanken, N.-M., 2014, A Timanian foreland basin setting for the late Neoproterozoic–early Palaeozoic cover sequences (Dividal Group) of northeastern Baltica, *in* Corfu, F., Gasser, D., and Chew, D.W., eds., New Perspectives on the Caledonides of Scandinavia and Related Areas: Geological Society of London Special Publication 390, p. 157–175, doi:10.1144/SP390.29.

Anfinson, O.A., Leier, A.L., Embry, A.F., and Dewing, K., 2012a, Detrital zircon geochronology and provenance of the Neoproterozoic to Late Devonian Franklinian Basin, Canadian Arctic Islands: Geological Society of America Bulletin, v. 124, p. 415–430, doi:10.1130/B30503.1.

Anfinson, O.A., Leier, A.L., Gaschnig, R., Embry, A.F., and Dewing, K., 2012b, U-Pb and Hf isotopic data from Franklinian Basin strata: Insights into the nature of Crockerland and the timing of accretion, Canadian Arctic Islands: Canadian Journal of Earth Sciences, v. 49, p. 1316–1328, doi:10.1139/e2012-067.

Armstrong, A.K., and Mamet, B.L., 1978, Microfacies of the Carboniferous Lisburne Group, Endicott Mountains, Arctic Alaska, *in* Stelck, C.R., and Chatterton, B.D.E., eds., Western and Arctic Canadian Biostratigraphy: Geological Association of Canada Special Paper 18, p. 333–394.

Armstrong, A.K., Mamet, B.L., Brosgé, W.P., and Reiser, H.N., 1976, Carboniferous section and unconformity at Mount Doonerak, Brooks Range, northern Alaska: American Association of Petroleum Geologists Bulletin, v. 60, p. 962–972.

Augland, L., Andresen, A., Corfu, F., Agyei-Dwarko, N., and Larionov, A., 2014a, The Bratten–Landegode gneiss complex: A fragment of Laurentian continental crust in the Uppermost Allochthon of the Scandinavian Caledonides, *in* Corfu, F., Gasser, D., and Chew, D.W., eds., New Perspectives on the Caledonides of Scandinavia and Related Areas: Geological Society of London Special Publication 390, p. 633–654, doi:10.1144/SP390.1.

Augland, L., Andresen, A., Gasser, D., and Steltenpohl, M.G., 2014b, Early Ordovician to Silurian evolution of exotic terranes in the Scandinavian Caledonides of the Ofoten–Troms area—Terrane characterization and correlation based on new U-Pb zircon ages and Lu-Hf isotopic data, *in* Corfu, F., Gasser, D., and Chew, D.W., eds., New Perspectives on the Caledonides of Scandinavia and Related Areas: Geological Society of London Special Publication 390, p. 655–678, doi:10.1144/SP390.19.

Barnes, C.G., Frost, C.D., Yoshinobu, A.S., McArthur, K., Barnes, M.A., Allen, C.M., Nordgulen, Ø., and Prestvik, T., 2007, Timing of sedimentation, metamorphism, and plutonism in the Helgeland Nappe Complex, north-central Norwegian Caledonides: Geosphere, v. 3, p. 683–703, doi:10.1130/GES00138.1.

Barth, A.P., and Wooden, J.L., 2006, Timing of magmatism following initial convergence at a passive margin, southwestern U.S. Cordillera, and ages of lower crustal magma sources: The Journal of Geology, v. 114, no. 2, p. 231–245, doi:10.1086/499573.

Barth, A.P., and Wooden, J.L., 2010, Coupled elemental and isotopic analysis of polygenetic zircons from granitic rocks by ion microprobe, with implications for melt evolution and the sources of granitic magmas: Chemical Geology, v. 277, p. 149–159, doi:10.1016/j.chemgeo.2010.07.017.

Bazard, D.R., Butler, R.F., Gehrels, G.E., and Soja, C.M., 1995, Early Devonian paleomagnetic data from the Lower Devonian Karheen Formation suggest Laurentia-Baltica connection for the Alexander terrane: Geology, v. 23, p. 707–710, doi:10.1130/0091-7613(1995)023<0707:EDPDFT>2.3.CO;2.

Belousova, E.A., Walters, S., Griffin, W.L., O'Reilly, S.Y., and Fisher, N.J., 2002, Zircon trace-element compositions as indicators of source rock type: Contributions to Mineralogy and Petrology, v. 143, p. 602–622, doi:10.1007/s00410-002-0364-7.

Beranek, L.P., Mortensen, J.K., Lane, L.S., Allen, T.L., Fraser, T.A., Hadlari, T., and Zantvoort, W.G., 2010, Detrital zircon geochronology of the western Ellesmerian clastic wedge, northwestern Canada: Insights on Arctic tectonics and the evolution of the northern Cordilleran miogeocline: Geological Society of America Bulletin, v. 122, no. 11–12, p. 1899–1911, doi:10.1130/B30120.1.

Beranek, L.P., van Staal, C.R., Gordee, S.M., McClelland, W.C., Israel, S., and Mihalynuk, M., 2012, Tectonic significance of Upper Cambrian–Middle Ordovician mafic volcanic rocks on the Alexander terrane, Saint Elias Mountains, northwestern Canada: The Journal of Geology, v. 120, no. 3, p. 293–314, doi:10.1086/664788.

Beranek, L.P., van Staal, C.R., McClelland, W.C., Israel, S.A., and Mihalynuk, M.G., 2013a, Baltican crustal provenance for Cambrian–Ordovician sandstones of the northern Alexander terrane, North American Cordillera: Journal of the Geological Society of London, v. 170, p. 7–18, doi:10.1144/jgs2012-028.

Beranek, L.P., van Staal, C.R., McClelland, W.C., Israel, S.A., and Mihalynuk, M.G., 2013b, Detrital zircon Hf isotopic compositions indicate a northern Caledonian connection for the Alexander terrane: Lithosphere, v. 5, no. 2, p. 163–168, doi:10.1130/L255.1.

Beranek, L.P., Pease, V., Hadlari, T., and Dewing, K., 2015, Silurian flysch successions of Ellesmere Island, Arctic Canada, and their significance to northern Caledonian palaeogeography and tectonics: Journal of the Geological Society of London, v. 172, no. 2, p. 201–212, doi:10.1144/jgs2014-027.

Bingen, B., and Solli, A., 2009, Geochronology of magmatism in the Caledonian and Sveconorwegian belts of Baltica: Synopsis for detrital zircon provenance studies: Norsk Geologisk Tidsskrift, v. 89, p. 267–290.

Bingen, B., Griffin, W.L., Torsvik, T.H., and Saeed, A., 2005, Timing of late Neoproterozoic glaciation of Baltica constrained by detrital zircon geochronology in the Hedmark Group, south-east Norway: Terra Nova, v. 17, p. 250–258, doi:10.1111/j.1365-3121.2005.00609.x.

Bingen, B., Nordgulen, Ø., and Viola, G., 2008, A four-phase model for the Sveconorwegian orogeny, SW Scandinavia: Norsk Geologisk Tidsskrift, v. 88, p. 43–72.

Blodgett, R.B., Rohr, D.M., and Boucot, A.J., 2002, Paleozoic links among some Alaskan accreted terranes and Siberia based on megafossils, *in* Miller, E.L., Grantz, A., and Klemperer, S.L., eds., Tectonic Evolution of the Bering Shelf–Chukchi Sea–Arctic Margin and Adjacent Landmasses: Geological Society of America Special Paper 360, p. 273–290, doi:10.1130/0-8137-2360-4.273.

Bogolepova, O.K., and Gee, D.G., 2004, Early Palaeozoic unconformity across the Timanides, NW Russia, *in* Gee, D.G., and Pease, V., eds., The Neoproterozoic Timanide Orogen of Eastern Baltica: Geological Society of London Memoir 30, p. 145–157, doi:10.1144/GSL.MEM.2004.030.01.13.

Bouvier, A., Vervoort, J.D., and Patchett, P.J., 2008, The Lu-Hf and Sm-Nd isotopic composition of CHUR: Constraints from unequilibrated chrondrites and implications for the bulk composition of terrestrial planets: Earth and Planetary Science Letters, v. 273, p. 48–57, doi:10.1016/j.epsl.2008.06.010.

Brosgé, W.P., and Reiser, H.N., 1964, Geologic Map and Section of the Chandalar Quadrangle, Alaska: U.S. Geological Survey Miscellaneous Geologic Investigations Map I-375, scale 1:250,000.

Brosgé, W.P., and Reiser, H.N., 1971, Preliminary Bedrock Geologic Map, Wiseman and Eastern Survey Pass Quadrangles, Alaska: U.S. Geological Survey Open-File Map 71–56, scale 1:250,000.

Brosgé, W.P., Dutro, J.T., Jr., Mangus, M.D., and Reiser, H.N., 1962, Paleozoic sequence in eastern Brooks Range, Alaska: American Association of Petroleum Geologists Bulletin, v. 46, p. 174–198.

Brosgé, W.P., Reiser, H.N., and Tailleur, I.L., 1974, Pennsylvanian Beds in Lisburne Group, South-Central Brooks Range: U.S. Geological Survey Circular 700, 41 p.

Brosgé, W.P., Reiser, H.N., Dutro, J.T., Jr., and Detterman, R.L., 1979, Bedrock Geologic Map of the Philip Smith Mountains Quadrangle, Alaska: U.S. Geological Survey Survey Miscellaneous Field Studies Map MF-897B, scale 1:250,000.

Brumley, K., Miller, E.L., Konstantinou, A., Grove, M., Meisling, K.E., and Mayer, L.A., 2015, First bedrock samples dredged from submarine outcrops in the Chukchi Borderland, Arctic Ocean: Geosphere, v. 11, no. 1, p. 76–92, doi:10.1130/GES01044.1.

Butler, R.F., Gehrels, G.E., and Bazard, D.R., 1997, Paleomagnetism of Paleozoic strata of the Alexander terrane, southeastern Alaska: Geological Society of America Bulletin, v. 109, no. 10, p. 1372–1388, doi:10.1130/0016-7606(1997)109<1372:POPSOT>2.3.CO;2.

Carter, C., and Laufeld, S., 1975, Ordovician and Silurian fossils in well cores from North Slope of Alaska: American Association of Petroleum Geologists Bulletin, v. 59, p. 457–464.

Cawood, P.A., and Pisarevsky, S.A., 2006, Was Baltica right-way-up or upside-down in the Neoproterozoic?: Journal of the Geological Society of London, v. 163, no. 5, p. 753–759, doi:10.1144/0016-76492005-126.

Cawood, P.A., Strachan, R., Cutts, K., Kinny, P.D., Hand, M., and Pisarevsky, S., 2010, Neoproterozoic orogeny along the margin of Rodinia: Valhalla orogen, North Atlantic: Geology, v. 38, no. 2, p. 99–102, doi:10.1130/G30450.1.

Cawood, P.A., Strachan, R.A., Merle, R.E., Millar, I.L., Loewy, S.L., Dalziel, I.W.D., Kinny, P.D., Jourdan, F., Nemchin, A.A., and Connelly, J.N., 2015, Neoproterozoic to early Paleozoic extensional and compressional history of East Laurentian margin sequences: The Moine Supergroup, Scottish Caledonides: Geological Society of America Bulletin, v. 127, no. 3–4, p. 349–371, doi:10.1130/B31068.1.

Cawood, P.A., Strachan, R.A., Pisarevsky, S.A., Gladkochub, D.P., and Murphy, J.B., 2016, Linking collisional and accretionary orogens during Rodinia assembly and breakup: Implications for models of supercontinent cycles: Earth and Planetary Science Letters, v. 449, p. 118–126, doi:10.1016/j.epsl.2016.05.049.

Cecil, M.R., Gehrels, G., Ducea, M.N., and Patchett, P.J., 2011, U-Pb-Hf characterization of the central Coast Mountains batholith: Implications for petrogenesis and crustal architecture: Lithosphere, v. 3, no. 4, p. 247–260, doi:10.1130/L134.1.

Chew, D.M., and Strachan, R.A., 2014, The Laurentian Caledonides of Scotland and Ireland, *in* Corfu, F., Gasser, D., and Chew, D.W., eds., New Perspectives on the Caledonides of Scandinavia and Related Areas: Geological Society of London Special Publication 390, p. 45–91, doi:10.1144/SP390.16.

Chian, D., Jackson, H.R., Hutchinson, D.R., Shimeld, J.W., Oakey, G.N., Lebedeva-Ivanova, N., Li, Q., Saltus, R.W., and Mosher, D.C., 2016, Distribution of crustal types in Canada Basin, Arctic Ocean: Tectonophysics, v. 691, p. 8–30.

Churkin, M., Jr., 1975, Basement rocks of Barrow Arch, Alaska, and circum-Arctic Paleozoic mobile belts: American Association of Petroleum Geologists Bulletin, v. 59, no. 3, p. 451–456.

Churkin, M., Jr., and Eberlein, G.D., 1977, Ancient borderland terranes of the North American Cordillera: Correlations and microplate tectonics: Geological Society of America Bulletin, v. 88, p. 769–786, doi:10.1130/0016-7606(1977)88<769:ABTOTN>2.0.CO;2.

Churkin, M., Jr., Whitney, J.W., and Rogers, J.F., 1985, The North American–Siberian connection, a mosaic of craton fragments in a matrix of oceanic terranes, *in* Howell, D.G., ed., Tectonostratigraphic Terranes of the Circum-Pacific Region, Earth Science Series 1: Houston, Texas, Circum–Pacific Council for Energy and Mineral Resources, p. 79–84.

Cocks, L.R.M., and Torsvik, T.H., 2005, Baltica from the late Precambrian to mid-Palaeozoic times: The gain and loss of a terrane's identity: Earth-Science Reviews, v. 72, p. 39–66, doi:10.1016/j.earscirev.2005.04.001.

Cocks, L.R.M., and Torsvik, T.H., 2007, Siberia, the wandering northern terrane, and its changing geography through the Palaeozoic: Earth-Science Reviews, v. 82, p. 29–74, doi:10.1016/j.earscirev.2007.02.001.

Cocks, L.R.M., and Torsvik, T.H., 2011, The Palaeozoic geography of Laurentia and western Laurussia: A stable craton with mobile margins: Earth-Science Reviews, v. 106, p. 1–51, doi:10.1016/j.earscirev.2011.01.007.

Cohen, K.M., Finney, S.C., Gibbard, P.L., and Fan, J.-X., 2013 (updated 2015), The ICS International Chronostratigraphic Chart: Episodes, v. 36, p. 199–204.

Cole, F., Bird, K.J., Mull, C.G., Wallace, W.K., Sassi, W., Murphy, J.M., and Lee, M., 1999, A balanced cross section and kinematic and thermal model across the northeastern Brooks Range mountain front, Arctic National Wildlife Refuge, Alaska, *in* ANWR Assessment Team, The Oil and Gas Resource Potential of the Arctic National Wildlife Refuge 1002 Area, Alaska: U.S. Geological Survey Open-File Report 98–34, CD-ROM, p. SM1–SM42.

Colpron, M., and Nelson, J.L., 2009, A Palaeozoic Northwest Passage: Incursion of Caledonian, Baltican and Siberian terranes into eastern Panthalassa, and the early evolution of the North American Cordillera: Geological Society of London Special Publication 318, p. 273–307, doi:10.1144/SP318.10.

Colpron, M., and Nelson, J.L., 2011, A Paleozoic Northwest Passage and the Timanian, Caledonian, and Uralian connections to some exotic terranes in the North American Cordillera, *in* Spencer, A.M., Embry, A.F., Gautier, D.L., Stoupakova, A.V., and Sorensen, K., eds., Arctic Petroleum Geology: Geological Society of London Memoir 35, p. 463–484.

Corfu, F., Ravna, E.J.K., and Kullerud, K., 2003, A Late Ordovician U-Pb age for the Tromsø Nappe eclogites, Uppermost Allochthon of the Scandinavian Caledonides: Contributions to Mineralogy and Petrology, v. 145, p. 502–513, doi:10.1007/s00410-003-0466-x.

Corfu, F., Svensen, H., Neumann, E.-R., Nakrem, H.A., and Planke, S., 2010, U-Pb and geochemical evidence for a Cryogenian magmatic arc in central Novaya Zemyla, Arctic Russia: Terra Nova, v. 22, p. 116–124, doi:10.1111/j.1365-3121.2010.00924.x.

Corfu, F., Gerber, M., Andersen, T.B., Torsvik, T.H., and Ashwal, L.D., 2011, Age and significance of Grenvillian and Silurian orogenic events in the Finnmarkian Caledonides, northern Norway: Canadian Journal of Earth Sciences, v. 48, p. 419–440, doi:10.1139/E10-043.

Corfu, F., Andersen, T., and Gasser, D., 2014, The Scandinavian Caledonides: Main features, conceptual advances, and critical questions, *in* Corfu, F., Gasser, D., and Chew, D.W., eds., New Perspectives on the Caledonides of Scandinavia and Related Areas: Geological Society of London Special Publication 390, p. 9–43, doi:10.1144/SP390.25.

Cox, G.M., Strauss, J.V., Halverson, G.P., Schmitz, M.A., McClelland, W.C., Stevenson, R.S., and Macdonald, F.A., 2015, Kikiktat volcanics of Arctic Alaska—Melting of harzburgitic mantle associated with the Franklin large igneous province: Lithosphere, v. 7, no. 3, p. 275–295, doi:10.1130/L435.1.

Dallmeyer, R.D., Peucat, J.J., Hirajima, T., and Ohta, Y., 1990, Tectonothermal chronology within a blueschist-eclogite complex, west-central Spitsbergen, Svalbard: Evidence from ^{40}Ar/^{39}Ar and Rb/Sr mineral ages: Lithos, v. 24, p. 291–304, doi:10.1016/0024-4937(89)90049-2.

Dewing, K., Mayr, U., Harrison, J.C., and de Freitas, T., 2008, Upper Neoproterozoic to Lower Devonian stratigraphy of northeast Ellesmere Island, *in* Mayr, U., ed., Geology of Northeast Ellesmere Island Adjacent to Kane Basin and Kennedy Channel, Nunavut: Geological Survey of Canada Bulletin 592, p. 31–108.

Dickinson, W.R., and Suczek, C.A., 1979, Plate tectonics and sandstone compositions: American Association of Petroleum Geologists Bulletin, v. 63, p. 2164–2182.

Dillon, J.T., 1989, Structure and stratigraphy of the southern Brooks Range and northern Koyukuk Basin near the Dalton Highway, *in* Mull, C.G., and Adams, K.E., eds., Dalton Highway, Yukon River to Prudhoe Bay, Alaska: Bedrock Geology of the Eastern Koyukuk Basin, Central Brooks Range, and East-Central Arctic Slope: Alaska Division of Geological and Geophysical Surveys Guidebook 7, v. 2, p. 157–187.

Dillon, J.T., Pessel, G.H., Chen, J.A., and Veach, N.C., 1980, Middle Paleozoic magmatism and orogenesis in the Brooks Range, Alaska: Geology, v. 8, p. 338–343, doi:10.1130/0091-7613(1980)8<338:MPMAOI>2.0.CO;2.

Dillon, J.T., Brosge, W.P., and Dutro, J.T., Jr., 1986, Generalized Geologic Map of the Wiseman Quadrangle, Alaska: U.S. Geological Survey Open-File Report 86–219, scale 1:250,000.

Dillon, J.T., Harris, A.G., Dutro, J.T., Jr., Solie, D.N., Blum, J.D., Jones, D.L., and Howell, D.G., 1988, Preliminary

Geologic Map and Section of the Chandalar D-6 and Parts of the Chandalar C-6 and Wiseman C-1 and D-1 Quadrangles, Alaska: Alaska Division of Geological and Geophysical Surveys Report of Investigation 88-5, 1 sheet, scale 1:63,360, doi:10.14509/2453.

Dodds, C.J., and Campbell, R.B., 1992, Overview, Legend, and Mineral Deposit Tabulations for Geology of SW Kluane Lake (115G and F[E1/2]), Mount Saint Elias (115B and C[E1/2]), SW Dezadeash (115A), NE Yakutat (114O), and Tatschenshini (114P) Map Areas, Yukon Territory and British Columbia: Geological Survey of Canada Open-Files 2188–2192, 85 p.

Dodds, C.J., Campbell, R.B., Read, P.B., Orchard, M.J., Tozer, E.T., Bamber, E.W., Pedder, A.E.H., Norford, B.S., McLaren, D.J., Harker, P., McIver, E., Norris, A.W., Ross, C.A., Chatterton, B.D.E., Copper, G.A., Flower, R.H., Haggart, J.W., Uyeno, T.T., and Irwin, S.E.B., 1993, Macrofossil and Conodont Data from SW Kluane Lake (115G and F[E1/2]), Mount Saint Elias (115B and C[E1/2]), SW Dezadeash (115A), NE Yakutat (114O), and Tatschenshini (114P) Map Areas, Yukon Territory and British Columbia: Geological Survey of Canada Open-File 2731, 137 p.

Dumoulin, J.A., 2001, Lithologies of the basement complex (Devonian and older) in the National Petroleum Reserve, Alaska, *in* Houseknecht, D.W., ed., NPRA Core Workshop: Petroleum Plays and Systems in the National Petroleum Reserve, Alaska: Society for Sedimentary Geology (SEPM) Core Workshop 21, p. 201–214.

Dumoulin, J.A., and Harris, A.G., 1994, Depositional Framework and Regional Correlation of Pre-Carboniferous Metacarbonate Rocks of the Snowden Mountain Area, Central Brooks Range, Northern Alaska: U.S. Geological Survey Professional Paper 1545, 74 p.

Dumoulin, J.A., Watts, K.F., and Harris, A.G., 1997, Stratigraphic contrasts and tectonic relationships between Carboniferous successions in the Trans-Alaska Crustal Transect corridor and adjacent areas, northern Alaska: Journal of Geophysical Research, v. 102, no. B9, p. 20,709–20,726, doi:10.1029/97JB02350.

Dumoulin, J.A., Harris, A.G., Bradley, D.C., and de Freitas, T.A., 2000, Facies patterns and conodont biogeography in Arctic Alaska and the Canadian Arctic Islands: Evidence against juxtaposition of these areas during early Paleozoic time: Polarforschung, v. 68, p. 257–266.

Dumoulin, J.A., Harris, A.G., Gagiev, M., Bradley, D.C., and Repetski, J.E., 2002, Lithostratigraphic, conodont, and other faunal links between Lower Paleozoic strata in northern and central Alaska and northeastern Russia, *in* Miller, E.L., Grantz, A., and Klemperer, S.L., eds., Tectonic Evolution of the Bering Shelf–Chukchi Sea–Arctic Margin and Adjacent Landmasses: Geological Society of America Special Paper 360, p. 291–312, doi:10.1130/0-8137-2360-4.291.

Dumoulin, J.A., Harris, A.G., and Repetski, J.E., 2014, Carbonate rocks of the Seward Peninsula, *in* Dumoulin, J.A., and Till, A.B., eds., Reconstruction of a Late Proterozoic to Devonian Continental Margin Sequence, Northern Alaska: Its Paleogeographic Significance and Contained Base-Metal Sulfide Deposits: Geological Society of America Special Paper 506, p. 59–110.

Dutro, J.T., Jr., 1970, Pre-Carboniferous carbonate rocks, northeastern Alaska, *in* Adkison, W.L., and Brosge, W.P., eds., Proceedings of the Geological Seminar on North Slope of Alaska: Los Angeles, American Association of Petroleum Geologists, Pacific Section, p. M1–M7.

Dutro, J.T., Jr., Brosgé, W.P., Lanphere, M.A., and Reiser, H.N., 1976, Geologic significance of Doonerak structural high, central Brooks Range, Alaska: American Association of Petroleum Geologists Bulletin, v. 60, p. 952–961.

Dutro, J.T., Jr., Palmer, A.R., Repetski, J.E., and Brosgé, W.P., 1984a, The Doonerak anticlinorium revisited, *in* Coonrad, W.L., and Elliot, R.L., eds., The U.S. Geological Survey in Alaska—Accomplishments during 1981: U.S. Geological Survey Circular 868, p. 17–19.

Dutro, J.T., Jr., Palmer, A.R., Repetski, J.E., and Brosgé, W.P., 1984b, Middle Cambrian fossils from the Doonerak anticlinorium, central Brooks Range, Alaska: Journal of Paleontology, v. 58, p. 1364–1371.

Eberlein, G.D., Churkin, M., Jr., Carter, C., Berg, H.C., and Ovenshine, A.T., 1983, Geology of the Craig Quadrangle, Alaska: U.S. Geological Survey Open-File Report 83–91, 52 p., 4 sheets, scale 1:250,000.

Ershova, V.B., Prokopiev, A.V., Khudoley, A.K., Sobolev, N.N., and Petrov, E.O., 2015, Detrital zircon ages and provenance of the Upper Paleozoic successions of Kotel'ny Island (New Siberian Islands archipelago): Lithosphere, v. 7, no. 1, p. 40–45, doi:10.1130/L387.1.

Ershova, V.B., Lorenz, H., Prokopiev, A.V., Sobolev, N.N., Khudoley, A.K., Petrov, E.O., Estrada, S., Sergeev, S., Larionov, A., and Thomsen, T.B., 2016, The De Long Islands: A missing link in unraveling the Paleozoic paleogeography of the Arctic: Gondwana Research, v. 35, p. 305–322, doi:10.1016/j.gr.2015.05.016.

Fossen, H., 2010, Extensional tectonics in the North Atlantic Caledonides: A regional view, *in* Law, R.D., Butler, R.W.H., Holdsworth, R.E., Krabbendam, M., and Strachan, R.A., eds., Continental Tectonics and Mountain Building: The Legacy of Peach and Horne: Geological Society of London Special Publication 335, p. 767–793, doi:10.1144/SP335.31.

Furnes, H., Ryan, P.D., Grenne, T., Roberts, D., Sturt, B.A., and Prestvik, T., 1985, Geological and geochemical classification of the ophiolitic fragments in the Scandinavian Caledonides, *in* Gee, D.G., and Sturt, B.A., eds., The Caledonide Orogen—Scandinavia and Related Areas: Chichester, UK, Wiley, p. 657–669.

Gasser, D., and Andresen, A., 2013, Caledonian terrane amalgamation of Svalbard: Detrital zircon provenance of Mesoproterozoic to Carboniferous strata from Oscar II Land, western Spitsbergen: Geological Magazine, v. 150, p. 1103–1126, doi:10.1017/S0016756813000174.

Gee, D.G., 1975, A tectonic model for the central part of the Scandinavian Caledonides: American Journal of Science, v. 275, p. 468–515.

Gee, D.G., and Page, L.M., 1994, Caledonian terrane assembly on Svalbard: New evidence from $^{40}Ar/^{39}Ar$ dating in Ny Friesland: American Journal of Science, v. 294, p. 1166–1186, doi:10.2475/ajs.294.9.1166.

Gee, D.G., and Pease, V., eds., 2004, The Neoproterozoic Timanide Orogen of Northeast Baltica: Geological Society of London Memoir 30, 251 p.

Gee, D.G., and Sturt, B.A., eds., 1985, The Caledonide Orogen—Scandinavia and Related Areas: Chichester, UK, John Wiley and Sons, 1266 p.

Gee, D.G., and Teben'kov, A.M., 2004, Svalbard: A fragment of the Laurentian margin, *in* Gee, D.G., and Pease, V., eds., The Neoproterozoic Timanide Orogen of Eastern Baltica: Geological Society of London Memoir 30, p. 191–206, doi:10.1144/GSL.MEM.2004.030.01.16.

Gee, D.G., Kumpulainen, R., Roberts, D., Stephens, M.B., and Zachrisson, E., 1985, Scandinavian Caldedonides, Tectonostratigraphic Map: Sveriges Geologiska Undersokning 35, scale 1:2,000,000.

Gee, D., Johansson, Å., Ohta, Y., and Tebenkov, A., 1995, Grenvillian basement and a major unconformity within the Caledonides of Nordaustlandet, Svalbard: Precambrian Research, v. 70, no. 3–4, p. 215–234, doi:10.1016/0301-9268(94)00041-O.

Gee, D.G., Fossen, H., Henriksen, N., and Higgins, A.K., 2008, From the early Paleozoic platforms of Baltica and Laurentia to the Caledonide orogen of Scandinavia and Greenland: Episodes, v. 31, p. 44–51.

Gee, D.G., Janak, M., Majka, J., Robinson, P., and van Roermund, H., 2013, Subduction along and within the Baltoscandian margin during closure of the Iapetus Ocean and Baltica-Laurentia collision: Lithosphere, v. 5, no. 2, p. 169–178, doi:10.1130/L220.1.

Gee, D.G., Ladenberger, A., Dahlqvist, P., Majka, J., Be'eri-Shlevin, Y., Frei, D., and Thomson, T., 2014, The Baltoscandian margin detrital zircon signatures of the central Scandes, *in* Corfu, F., Gasser, D., and Chew, D.W., eds., New Perspectives on the Caledonides of Scandinavia and Related Areas: Geological Society of London Special Publication 390, p. 131–155, doi:10.1144/SP390.20.

Gee, D.G., Andréasson, P.-G., Lorenz, H., Frei, D., and Majka, J., 2015, Detrital zircon signatures of the Baltoscandian margin along the Arctic Circle Caledonides in Sweden: Precambrian Research, v. 265, p. 40–56, doi:10.1016/j.precamres.2015.05.012.

Gehrels, G.E., and Pecha, M., 2014, Detrital zircon U-Pb geochronology and Hf isotope geochemistry of Paleozoic and Triassic passive margin strata of western North America: Geosphere, v. 10, no. 1, p. 49–65, doi:10.1130/GES00889.1.

Gehrels, G.E., and Saleeby, J.B., 1987, Geologic framework, tectonic evolution, and displacement history of the Alexander terrane: Tectonics, v. 6, p. 151–173, doi:10.1029/TC006i002p00151.

Gehrels, G.E., Butler, R.F., and Bazard, D.R., 1996, Detrital zircon geochronology of the Alexander terrane, southeastern Alaska: Geological Society of America Bulletin, v. 108, p. 722–734, doi:10.1130/0016-7606(1996)108<0722:DZGOTA>2.3.CO;2.

Gehrels, G.E., Valencia, V., and Pullen, A., 2006, Detrital zircon geochronology by laser-ablation multicollector ICP-MS at the Arizona LaserChron Center, *in* Loszewski, T., ed., Geochronology: Emerging Opportunities, Paleontology Society Short Course: Paleontology Society Papers 12, p. 67–76.

Gehrels, G.E., Valencia, V., and Ruiz, J., 2008, Enhanced precision, accuracy, efficiency, and spatial resolution of U-Pb ages by laser ablation–multicollector–inductively coupled plasma–mass spectrometry: Geochemistry Geophysics Geosystems, v. 9, p. Q03017, doi:10.1029/2007GC001805.

Gilotti, J.A., and McClelland, W.C., 2008, Geometry, kinematics, and timing of extensional faulting in the Greenland Caledonides—A synthesis, *in* Higgins, A.K., Gilotti, J.A., and Smith, M.P., eds., The Greenland Caledonides: Evolution of the Northeast Margin of Laurentia: Geological Society of America Memoir 202, p. 251–271, doi:10.1130/2008.1202(10).

Gilotti, J.A., McClelland, W.C., and Wooden, J.L., 2014, Zircon captures exhumation of an ultrahigh-pressure terrane, North-East Greenland Caledonides: Gondwana Research, v. 25, p. 235–256, doi:10.1016/j.gr.2013.03.018.

Gottlieb, E.S., Meisling, K.E., Miller, E.L., and Mull, C.G., 2014, Closing the Canada Basin: Detrital zircon geochronology relationships between the North Slope of Arctic Alaska and the Franklinian mobile belt of Arctic Canada: Geosphere, v. 10, no. 6, p. 1366–1384, doi:10.1130/GES01027.1.

Grantz, A., Moore, T.E., and Roeske, S.M., 1991, Continent-ocean transect A-3: Gulf of Alaska to Arctic Ocean: Geological Society of America Centennial Continent/Ocean Transect 15, 72 p., 3 sheets, scale 1:500,000.

Grimes, C.B., Wooden, J.L., Cheadle, M.J., and John, B.E., 2015, "Fingerprinting" tectono-magmatic provenance using trace elements in zircon: Contributions to Mineralogy and Petrology, v. 170, p. 46, doi:10.1007/s00410-015-1199-3.

Gromet, L.P., and Gee, D.G., 1998, An evaluation of the age of high-grade metamorphism in the Caldedonides of Biskayerhalvoya: GFF, v. 120, p. 199–208, doi:10.1080/11035899801202199.

Grove, M., Gehrels, G.E., Cotkin, S.J., Wright, J.E., and Zou, H., 2008, Non-Laurentian cratonal provenance of Late Ordovician eastern Klamath blueschists and a link to the Alexander terrane, *in* Wright, J.E., and Shervais, J.W., eds., Ophiolites, Arcs and Batholiths: A Tribute to Cliff Hopson: Geological Society of America Special Paper 438, p. 223–250, doi:10.1130/2008.2438(08).

Hadlari, T., Davis, W.J., and Dewing, K., 2014, A pericratonic model for Pearya terrane as an extension of the Franklinian margin of Laurentia, Canadian Arctic: Geological Society of America Bulletin, v. 126, p. 182–200, doi:10.1130/B30843.1.

Hallett, B.W., McClelland, W.C., and Gilotti, J.A., 2014, The timing of strike-slip deformation along the Storstrømmen shear zone, Greenland Caledonides: U-Pb zircon and titanite geochronology: Geoscience Canada, v. 41, p. 19–45, doi:10.12789/geocanj.2014.41.038.

Handschy, J.W., 1998, Regional stratigraphy of the Brooks Range and North Slope, Arctic Alaska, *in* Oldow, J.S., and Avé Lallemant, H.G., eds., Architecture of the Central Brooks Range Fold and Thrust Belt, Arctic Alaska: Geological Society of America Special Paper 324, p. 1–8, doi:10.1130/0-8137-2324-8.1.

Hanks, C.L., 1989, Preliminary Geology of the Pre-Mississippian Rocks of the Aichilik and Egaksrak River Areas, Northeastern Brooks Range, Alaska:

Alaska Division of Geological and Geophysical Surveys Public Data File 89-1a, 18 p.
Harland, W.B., 1997, The Geology of Svalbard: Geological Society of London Memoir 17, 521 p.
Harland, W.B., and Gayer, R.A., 1972, The Arctic Caledonides and earlier oceans: Geological Magazine, v. 109, p. 289–314, doi:10.1017/S0016756800037717.
Harrison, T.M., Célérier, J., Aikman, A.B., Hermann, J., and Heizler, M.T., 2009, Diffusion of ^{40}Ar in muscovite: Geochimica et Cosmochimica Acta, v. 73, p. 1039–1051, doi:10.1016/j.gca.2008.09.038.
Henriksen, N., and Higgins, A.K., 1998, Early Palaeozoic basin development of North Greenland—Part of the Franklinian Basin: Polarforschung, v. 68, p. 131–140.
Higgins, A.K., and Leslie, A.G., 2008, Architecture and evolution of the East Greenland Caledonides—An introduction, *in* Higgins, A.K., Gilotti, J.A., and Smith, M.P., eds., The Greenland Caledonides: Evolution of the Northeast Margin of Laurentia: Geological Society of America Memoir 202, p. 29–53, doi:10.1130/2008.1202(02).
Higgins, A.K., Ineson, J.R., Pell, J.S., Surlyk, F., and Sonderholm, M., 1991, Cambrian to Silurian basin development and sedimentation, North Greenland, *in* Trettin, H.P., ed., Geology of the Innuitian Orogen and Arctic Platform of Canada and Greenland: Geological Survey of Canada, Geology of Canada, v. 3, p. 109–161, doi:10.1130/DNAG-GNA-E.109.
Hitzman, M.W., Proffett, J.M., Schmidt, J.M., and Smith, T.E., 1986, Geology and mineralization of the Ambler District, northwestern Alaska: Economic Geology and the Bulletin of the Society of Economic Geologists, v. 81, p. 1592–1618, doi:10.2113/gsecongeo.81.7.1592.
Hoskin, P.W.O., and Schaltegger, U., 2003, The composition of zircon and igneous and metamorphic petrogenesis: Reviews in Mineralogy and Geochemistry, v. 53, no. 1, p. 27–62, doi:10.2113/0530027.
Houseknecht, D.W., and Connors, C.D., 2016, Pre-Mississippian tectonic affinity across the Canada Basin–Arctic margins of Alaska and Canada: Geology, v. 44, p. 507–510.
Hubbard, R.J., Edrich, S.P., and Rattey, R.P., 1987, Geologic evolution and hydrocarbon habitat of the 'Arctic Alaska microplate': Marine and Petroleum Geology, v. 4, p. 2–34, doi:10.1016/0264-8172(87)90019-5.
Hurst, J.M., and Surlyk, F., 1984, Tectonic control of Silurian carbonate-shelf margin morphology and facies, North Greenland: American Association of Petroleum Geologists Bulletin, v. 68, p. 1–17.
Johansson, Å., Larionov, A.N., Gee, D.G., Ohta, Y., Teben'kov, A.M., and Sadelin, S., 2004, Grenvillian and Caledonian tectonomagmatic activity in northeasternmost Svalbard, *in* Gee, D.G., and Pease, V., eds., The Neoproterozoic Timanide Orogen of Eastern Baltica: Geological Society of London Memoir 30, p. 207–232.
Johansson, Å., Gee, D., Larionov, A., Ohta, Y., and Tebenkov, A., 2005, Grenvillian and Caledonian evolution of eastern Svalbard—A tale of two orogenies: Terra Nova, v. 17, p. 317–325, doi:10.1111/j.1365-3121.2005.00616.x.
Johnson, B.G., Strauss, J.V., Toro, J., Benowitz, J.A., Ward, W.P., and Hourigan, J.K., 2016, Detrital geochronology of the pre-Mississippian stratigraphy in the NE Brooks Range, Alaska: Insights to the tectonic evolution of northern Laurentia: Lithosphere, v. 8, no. 6, p. 649–667.
Jones, D.L., Silberling, N.J., Coney, P.J., and Plafker, G., 1987, Lithotectonic Terrane Map of Alaska: U.S. Geological Survey Miscellaneous Field Studies Map MF-1874A, scale 1:2,500,000.
Julian, F.E., 1989, Structure and Stratigraphy of Lower Paleozoic Rocks, Doonerak Window, Central Brooks Range, Alaska [Ph.D. thesis]: Houston, Texas, Rice University, 127 p.
Julian, F.E., and Oldow, J.S., 1998, Structure and lithology of the Lower Paleozoic Apoon assemblage, eastern Doonerak window, central Brooks Range, Alaska, *in* Oldow, J.S., and Ave Lallemant, H.G., eds., Architecture of the Central Brooks Range Fold and Thrust Belt, Arctic Alaska: Geological Society of America Special Paper 324, p. 65–80, doi:10.1130/0-8137-2324-8.65.
Kalsbeek, F., Thrane, K., Nutman, A.P., and Jepsen, H.F., 2000, Late Mesoproterozoic to early Neoproterozoic history of the East Greenland Caledonides: Evidence for Grenvillian orogenesis?: Journal of the Geological Society of London, v. 157, no. 6, p. 1215–1225, doi:10.1144/jgs.157.6.1215.
Kalsbeek, F., Jepsen, H.F., and Nutman, A.P., 2001, From source migmatites to plutons: Tracking the origin of ca. 435 Ma S-type granites in the East Greenland Caledonian orogen: Lithos, v. 57, no. 1, p. 1–21, doi:10.1016/S0024-4937(00)00071-2.
Kalsbeek, F., Higgins, A.K., Jepsen, H.F., Frei, R., and Nutman, A.P., 2008, Granites and granites in the East Greenland Caledonides, *in* Higgins, A.K., Gilotti, J.A., and Smith, M.P., eds., The Greenland Caledonides: Evolution of the Northeast Margin of Laurentia: Geological Society of America Memoir 202, p. 227–249, doi:10.1130/2008.1202(09).
Kelley, J.S., and Brosgé, W.P., 1995, Geologic framework of a transect of the central Brooks Range: Regional relations and an alternative to the Endicott Mountains allochthon: American Association of Petroleum Geologists Bulletin, v. 79, p. 1087–1115.
Kirkland, C.L., Daly, J.S., and Whitehouse, M.J., 2006, Granitic magmatism of Grenvillian and late Neoproterozoic age in Finnmark, Arctic Norway—Constraining pre-Scandian deformation in the Kalak Nappe Complex: Precambrian Research, v. 145, p. 24–52, doi:10.1016/j.precamres.2005.11.012.
Kirkland, C.L., Daly, J.S., and Whitehouse, M.J., 2008, Basement–cover relationships of the Kalak Nappe Complex, Arctic Norwegian Caledonides, and constraints on Neoproterozoic terrane assembly in the North Atlantic region: Precambrian Research, v. 160, no. 3–4, p. 245–276, doi:10.1016/j.precamres.2007.07.006.
Kirkland, C.L., Bingen, B., Whitehouse, M.J., Beyer, E., and Griffin, W.L., 2011, Neoproterozoic paleogeography in the North Atlantic region: Inferences from the Akkajaure and Seve Nappes of the Scandinavian Caledonides: Precambrian Research, v. 186, p. 127–146, doi:10.1016/j.precamres.2011.01.010.
Klaper, E.M., 1992, The Paleozoic tectonic evolution of the northern edge of North America: A structural study of northern Ellesmere Island, Canadian Arctic Archipelago: Tectonics, v. 11, p. 854–870, doi:10.1029/92TC00277.
Kos'ko, M.K., Cecile, M.P., Harrison, J.C., Banelin, V.G., Khandoshko, N.V., and Lopatin, B.G., 1993, Geology of Wrangel Island, between Chukchi and East Siberian Seas, Northeastern Russia: Geological Survey of Canada Bulletin 461, 101 p., doi:10.4095/193361.
Kośmińska, K., Majka, J., Mazur, S., Krumbholz, M., Klonowska, I., Manecki, M., Czerny, J., and Dwornik, M., 2014, Blueschist facies metamorphism in Nordenskiöld Land of west-central Svalbard: Terra Nova, v. 26, no. 5, p. 377–386, doi:10.1111/ter.12110.
Kristoffersen, M., Andersen, T., and Andresen, A., 2014, U-Pb age and Lu-Hf signatures of detrital zircon from Paleozoic sandstones in the Oslo Rift, Norway: Geological Magazine, v. 151, no. 5, p. 816–829, doi:10.1017/S0016756813000885.
Kuznetsov, N.B., Soboleva, A.A., Udoratina, O.V., Gertseva, O.V., and Andreichev, V.L., 2007, Pre-Ordovician tectonic evolution and volcano–plutonic associations of the Timanides and northern pre-Uralides, northeast part of the East European craton: Gondwana Research, v. 12, p. 305–323, doi:10.1016/j.gr.2006.10.021.
Kuznetsov, N.B., Natapov, L.M., Belousova, E.A., O'Reilly, S.Y., and Griffin, W.L., 2010, Geochronological, geochemical and isotopic study of detrital zircon suites from late Neoproterozoic clastic strata along the NE margin of the East European craton: Implications for plate tectonic models: Gondwana Research, v. 17, p. 583–601, doi:10.1016/j.gr.2009.08.005.
Labrousse, L., Elvevold, S., Lepvrier, C., and Agard, P., 2008, Structural analysis of high-pressure metamorphic rocks of Svalbard: Reconstructing the early stages of the Caledonian orogeny: Tectonics, v. 27, p. TC5003, doi:10.1029/2007TC002249.
Lane, L.S., 2007, Devonian–Carboniferous paleogeography and orogenesis, northern Yukon and adjacent Arctic Alaska: Canadian Journal of Earth Sciences, v. 44, p. 679–694, doi:10.1139/e06-131.
Lane, L.S., Gehrels, G.E., and Layer, P.W., 2015, Provenance and paleogeography of the Neruokpuk Formation, northwest Laurentia: An integrated synthesis: Geological Society of America Bulletin, v. 128, no. 1–2, p. 239–257, doi:10.1130/B31234.1.
Le Boudec, A.L., Ineson, J., Rosing, M., Døssing, L., Martineau, F., Lécuyer, C., and Albarède, F., 2014, Geochemistry of the Cambrian Sirius Passet Lagerstätte, northern Greenland: Geochemistry Geophysics Geosystems, v. 15, no. 4, p. 886–904, doi:10.1002/2013GC005068.
Lerand, M., 1973, Beaufort Sea, *in* McCrossam, R.G., ed., The Future Petroleum Provinces of Canada—Their Geology and Potential: Canadian Society of Petroleum Geology Memoir 1, p. 315–386.
Lindsley-Griffin, N., Griffin, J.R., and Farmer, J.D., 2008, Paleogeographic significance of Ediacaran cyclomedusoids within the Antelope Mountain Quartzite, Yreka terrane, eastern Klamath Mountains, California, *in* Blodgett, R.W., and Stanley, G.D., Jr., eds., The Terrane Puzzle: New Perspectives on Paleontology and Stratigraphy from the North American Cordillera: Geological Society of America Special Paper 442, p. 1–37, doi:10.1130/2008.442(01).
Lorenz, H., Gee, D.G., and Whitehouse, M.J., 2007, New geochronological data on Palaeozoic igneous activity and deformation in the Severnaya Zemlya archipelago, Russia, and implications for the Eurasian Arctic margin: Geological Magazine, v. 144, p. 105–125, doi:10.1017/S001675680600272X.
Lorenz, H., Gee, D.G., Larionov, A.N., and Majka, J., 2012, The Grenville–Sveconorwegian orogen in the High Arctic: Geological Magazine, v. 149, p. 875–891, doi:10.1017/S0016756811001130.
Lorenz, H., Gee, D.G., Korago, E., Kovaleva, G., McClelland, W.C., Gilotti, J.A., and Frei, D., 2013, Detrital zircon geochronology of Palaeozoic Novaya Zemlya—A key to understanding the basement of the Barents Shelf: Terra Nova, v. 25, no. 6, p. 496–503, doi:10.1111/ter.12064.
Ludwig, K.R., 2003, Isoplot 3.0—A Geochronological Toolkit for Microsoft Excel: Berkeley Geochronology Center Special Publication 4, 70 p.
Macdonald, F.A., McClelland, W.C., Schrag, D.P., and Macdonald, W.P., 2009, Neoproterozoic glaciation on a carbonate platform margin in Arctic Alaska and the origin of the North Slope subterrane: Geological Society of America Bulletin, v. 121, p. 448–473, doi:10.1130/B26401.1.
Majka, J., Mazur, S., Manecki, M., Czerny, J., and Holm, D., 2008, Late Neoproterozoic amphibolite facies metamorphism of a pre-Caledonian basement block in southwest Wedel Jarlsberg Land, Spitsbergen: New evidence from U-Th-Pb dating of monazite: Geological Magazine, v. 145, p. 822–830, doi:10.1017/S001675680800530X.
Majka, J., Be'eri-Shlevin, Y., Gee, D.G., Czerny, J., Frei, D., and Ladenberger, A., 2014, Torellian (c. 640 Ma) metamorphic overprint of Tonian (c. 950 Ma) basement in the Caledonides of southwestern Svalbard: Geological Magazine, v. 151, p. 732–748, doi:10.1017/S0016756813000794.
Majka, J., Kośmińska, K., Mazur, S., Czerny, J., Piepjohn, K., Dwornik, M., and Manecki, M., 2015, Two garnet growth events in polymetamorphic rocks in southwest Spitsbergen, Norway: Insight in the history of Neoproterozoic and early Paleozoic metamorphism in the High Arctic: Canadian Journal of Earth Sciences, v. 52, no. 12, p. 1–17, doi:10.1139/cjes-2015-0142.
Malone, S.J., McClelland, W.C., von Gosen, W., and Piepjohn, K., 2014, Proterozoic evolution of the North Atlantic–Arctic Caledonides: Insights from detrital zircon analysis of metasedimentary rocks from the Pearya terrane, Canadian High Arctic: The Journal of Geology, v. 122, p. 623–647, doi:10.1086/677902.
Mazur, S., Czerny, J., Majka, J., Manecki, M., Holm, D., Smyrak, A., and Wypych, A., 2009, A strike-slip terrane boundary in Wedel Jarlsberg Land, Svalbard, and its bearing on correlations of SW Spitsbergen with the Pearya terrane and Timanide belt: Journal of the Geological Society of London, v. 166, no. 3, p. 529, doi:10.1144/0016-76492008-106.
McArthur, K.L., Frost, C.D., Barnes, C.G., Prestvik, T., and Nordgulen, O., 2014, Tectonic reconstruction and sediment provenance of a far-travelled oceanic nappe,

Helgeland Nappe Complex, west-central Norway, *in* Corfu, F., Gasser, D., and Chew, D.W., eds., New Perspectives on the Caledonides of Scandinavia and Related Areas: Geological Society of London Special Publication 390, p. 583–602.

McClelland, W.C., Malone, S.J., von Gosen, W., Piepjohn, K., and Laufer, A., 2012, The timing of sinistral displacement of the Pearya terrane along the Canadian Arctic margin: Zeitschrift der Deutschen Gesellschaft für Geowissenschaften, v. 163, p. 251–259, doi:10.1127/1860-1804/2012/0163-0251.

McClelland, W.C., Colpron, M., Piepjohn, K., von Gosen, W., Ward, W., and Strauss, J.V., 2015a, Preliminary detrital zircon geochronology of the Neruokpuk Formation in the Barn Mountains, Yukon, *in* MacFarlane, K.E., Nordling, M.G., and Sack, P.J., eds., Yukon Exploration and Geology: Whitehorse, Yukon Geological Survey, p. 123–143.

McClelland, W.C., Strauss, J.V., Ward, W., Malone, S.J., Colpron, M., Piepjohn, K., von Gosen, W., Macdonald, F.A., Gehrels, G., and Gilotti, J.A., 2015b, Evidence for a Paleozoic strike-slip orogen on the North American Arctic margin: Geological Society of America Abstracts with Programs, v. 47, no. 7, p. 445.

McClelland, W.C., Gilotti, J.A., Ramarao, T., Stemmerik, L., and Dalhoff, F., 2016, Carboniferous basin in Holm Land records local exhumation of the North-East Greenland Caledonides: Implications for the detrital zircon signature of a collisional orogen: Geosphere, v. 12, p. 925–947, doi:10.1130/GES01284.1.

McDougall, I., and Harrison, T.M., 1999, Geochronology and Thermochronology by the ^{40}Ar/^{39}Ar Method (2nd ed.): New York, Oxford University Press, 288 p.

McKerrow, W.S., Mac Niocaill, C., and Dewey, J.F., 2000, The Caledonian orogeny redefined: Journal of the Geological Society of London, v. 157, p. 1149–1154, doi:10.1144/jgs.157.6.1149.

Mihalynuk, M.G., Smith, M.T., MacIntyre, D.G., and Deschenes, M., 1993, Tatshenshini Project, Part B: Stratigraphic and Magmatic Setting of Mineral Occurrences: British Columbia Ministry of Energy, Mines, and Petroleum Resources, Geological Fieldwork 1992, v. 1993-1, p. 189–228.

Miller, E.L., Toro, J., Gehrels, G., Amato, J.M., Prokopiev, A., Tuchkova, M.I., Akinin, V.V., Dumitru, T.A., Moore, T.E., and Cecile, M.P., 2006, New insights into Arctic paleogeography and tectonics from U-Pb detrital zircon geochronology [Sp.]: Tectonics, v. 25, p. TC3013, doi:10.1029/2005TC001830.

Miller, E.L., Gehrels, G., Pease, V., and Sokolov, S., 2010, Stratigraphy and U-Pb detrital zircon geochronology of Wrangel Island, Russia: Implications for Arctic paleogeography: American Association of Petroleum Geologists Bulletin, v. 94, no. 5, p. 665–692, doi:10.1306/10200909036.

Miller, E.L., Kuznetsov, N., Soboleva, A., Udoratina, O., Grove, M.J., and Gehrels, G., 2011, Baltica in the Cordillera?: Geology, v. 39, no. 8, p. 791–794, doi:10.1130/G31910.1.

Moore, T.E., 1987, Geochemical and tectonic setting of some volcanic rocks of the Franklinian assemblage, central and eastern Brooks Range, *in* Tailleur, I.L., and Weimer, P., eds., Alaskan North Slope Geology: Bakersfield, California, Society of Economic Paleontologists and Mineralogists, Pacific Section, and Alaska Geological Society, Publication 50, p. 691–710.

Moore, T.E., and Nilsen, T.H., 1984, Regional sedimentological variations in the Upper Devonian and Lower Mississippian(?) Kanayut Conglomerate, Brooks Range, Alaska: Sedimentary Geology, v. 38, p. 465–497, doi:10.1016/0037-0738(84)90090-3.

Moore, T.E., Wallace, W.K., Bird, K.J., Karl, S.M., Mull, C.G., and Dillon, J.T., 1994, Geology of northern Alaska, *in* Plafker, G., and Berg, H.C., eds., The Geology of Alaska: Boulder, Colorado, Geological Society of America, The Geology of North America, v. G-1, p. 49–140.

Moore, T.E., Wallace, W.K., Mull, C.G., Adams, K.E., Plafker, G., and Nokleberg, W.J., 1997, Crustal implications of bedrock geology along the Trans-Alaska Crustal Transect (TACT) in the Brooks Range, northern Alaska: Journal of Geophysical Research, v. 102, no. B9, p. 20,645–20,684, doi:10.1029/96JB03733.

Moore, T.E., Potter, C.J., and O'Sullivan, P.B., 2007, Detrital zircon U-Pb analysis of pre-Mississippian metasedimentary basement strata, North Slope, Alaska: Evidence of a Caledonian connection: Geological Society of America Abstracts with Programs, v. 39, no. 6, p. 488.

Moore, T.E., O'Sullivan, P.B., Potter, C.J., and Donelick, R.A., 2015, Provenance and detrital zircon geochronologic evolution of lower Brookian foreland basin deposits of the western Brooks Range, Alaska, and implications for early Brookian tectonism: Geosphere, v. 11, no. 1, p. 93–122, doi:10.1130/GES01043.1.

Morris, G.A., Kirkland, C.L., and Pease, V., 2015, Orogenic paleofluid flow recorded by discordant detrital zircons in the Caledonian foreland basin of northern Greenland: Lithosphere, v. 7, no. 2, p. 138–143, doi:10.1130/L420.1.

Mortensen, J.K., and Bell, R.T., 1991, U-Pb zircon and titanite geochronology of the Mount Sedgewick pluton, northern Yukon Territory, *in* Geological Survey of Canada Radiogenic Age and Isotopic Studies Report 4: Geological Survey of Canada Paper 90-2, p. 19–23.

Mull, C.G., 1982, The tectonic evolution and structural style of the Brooks Range, Alaska: An illustrated summary, *in* Powers, R.B., ed., Geological Studies of the Cordilleran Thrust Belt, Volume 1: Denver, Colorado, Rocky Mountain Association of Geologists, p. 1–45.

Mull, C.G., and Anderson, A.V., 1991, Franklinian Lithotectonic Domains, Northeastern Brooks Range, Alaska: Alaska Division of Geological and Geophysical Survey Public Data File 91-5, 41 p., 1 sheet.

Mull, C.G., Adams, K.E., and Dillon, J.T., 1987a, Stratigraphy and structure of the Doonerak fenster and Endicott Mountains allochthon, central Brooks Range, Alaska, *in* Tailleur, I., and Weimer, P., eds., Alaskan North Slope Geology: Bakersfield, California, Society of Economic Paleontologists and Mineralogists (SEPM), Pacific Section, and Alaska Geological Society, Publication 50, p. 663–679.

Mull, C.G., Roeder, D.H., Tailleur, I.L., Pessel, G.H., Grantz, A., and May, S.D., 1987b, Geologic Sections and Maps across the Brooks Range and Arctic Slope to Beaufort Sea, Alaska: U.S. Geological Survey Map and Chart Series MC-28S, scale 1:2,500,000, 1 sheet.

Myhre, P.I., Corfu, F., and Andresen, A., 2009, Caledonian anatexis of Grevillian basement and cover: A U/Pb study of Albert I Land, NW Svalbard: Norsk Geologisk Tidsskrift, v. 89, p. 173–191.

Natal'in, B.A., Amato, J.M., Toro, J., and Wright, J.E., 1999, Paleozoic rocks of northern Chukotka Peninsula, Russian Far East: Implications for the tectonics of the Arctic region: Tectonics, v. 18, p. 977–1003, doi:10.1029/1999TC900044.

Nilsen, T.H., 1981, Upper Devonian and Lower Mississippian redbeds, Brooks Range, Alaska, *in* Miall, A.D., ed., Sedimentation and Tectonics in Alluvial Basins: Geological Association of Canada Special Paper 23, p. 187–219.

Oldow, J.S., Avé Lallemant, H.G., Julian, F.E., and Seidensticker, C.M., 1984, The Doonerak window duplex: Regional implications: Geological Society of America Abstracts with Programs, v. 16, p. 326.

Oldow, J.S., Avé Lallemant, H.G., Julian, F.E., and Seidensticker, C.M., 1987a, Balanced Cross Sections through the Central Brooks Range and North Slope, Arctic Alaska: American Association of Petroleum Geologists Special Publication 19, 19 p., 8 plates.

Oldow, J.S., Avé Lallemant, H.G., Julian, F.E., and Seidensticker, C.M., 1987b, Ellesmerian(?) and Brookian deformation in the Franklin Mountains, northeastern Brooks Range, Alaska, and its bearing on the origin of the Canada Basin: Geology, v. 15, p. 37–41, doi:10.1130/0091-7613(1987)15<37:EABDIT>2.0.CO;2.

Oldow, J.S., Boler, K.W., Avé Lallemant, H.G., Gottschalk, R.R., Julian, F.E., Seidensticker, C.M., and Phelps, J.C., 1998, Stratigraphy and paleogeographic setting of the eastern Skajit allochthon, central Brooks Range, Arctic Alaska, *in* Oldow, J.S., and Ave Lallemant, H.G., eds., Architecture of the Central Brooks Range Fold and Thrust Belt, Arctic Alaska: Geological Society of America Special Paper 324, p. 109–125, doi:10.1130/0-8137-2324-8.109.

Oze, C., Cattell, H., and Grove, M., 2017, ^{40}Ar/^{39}Ar dating and thermal modeling of adularia to constrain the timing of hydrothermal activity in magmatic settings: Geology, v. 45, no. 1, p. 43–46, doi:10.1130/G38405.1.

Palmer, A.R., Dillon, J., and Dutro, J.T., Jr., 1984, Middle Cambrian trilobites with Siberian affinities from the central Brooks Range: Geological Society of America Abstracts with Programs, v. 16, p. 327.

Patchett, P.J., Roth, M.A., Canale, B.S., de Freitas, T.A., Harrison, J.C., Embry, A.F., and Ross, G.M., 1999, Nd isotopes, geochemistry, and constraints on sources of sediments in the Franklinian mobile belt, Arctic Canada: Geological Society of America Bulletin, v. 111, p. 578–589,doi:10.1130/0016-7606(1999)111<0578:NIGACO>2.3.CO;2.

Patrick, B.E., and McClelland, W.C., 1995, Late Proterozoic granitic magmatism on Seward Peninsula and a Barentian origin for Arctic Alaska–Chukotka: Geology, v. 23, p. 81–84, doi:10.1130/0091-7613(1995)023<0081:LPGMOS>2.3.CO;2.

Pease, V., 2011, Eurasian orogens and Arctic tectonics: An overview, *in* Spencer, A.M., Embry, A.F., Gautier, D.L., Stoupakova, A.V., and Sorensen, K., eds., Arctic Petroleum Geology: Geological Society of London Memoir 35, p. 311–324.

Pease, V., and Scott, R.A., 2009, Crustal affinities in the Arctic Uralides, northern Russia: Significance of detrital zircon ages from Neoproterozoic and Paleozoic sediments in Novaya Zemlya and Taimyr: Journal of the Geological Society of London, v. 166, p. 517–527, doi:10.1144/0016-76492008-093.

Pease, V., Daly, S.J., Elming, S.-A., Kumpulainen, R., Moczydlowska, M., Puchkov, V., Roberts, D., Saintot, A., and Stephenson, R., 2008, Baltica in the Cryogenian, 850–630 Ma: Precambrian Research, v. 160, p. 46–65, doi:10.1016/j.precamres.2007.04.015.

Pedersen, R.B., and Dunning, G.R., 1997, Evolution of arc crust and relations between contrasting sources: U-Pb (age), Nd and Sr isotope systematics of the ophiolitic terrane of SW Norway: Contributions to Mineralogy and Petrology, v. 128, p. 1–15, doi:10.1007/s004100050289.

Pedersen, R.B., and Hertogen, J., 1990, Magmatic evolution of the Karmoy ophiolite complex, SW Norway—Relationships between MORB–IAT–boninitic–calc-alkaline and alkaline magmatism: Contributions to Mineralogy and Petrology, v. 104, p. 277–293, doi:10.1007/BF00321485.

Pettersson, C.H., Tebenkov, A.M., Larionov, A.N., Andresen, A., and Pease, V., 2009, Timing of migmatization and granite genesis in the Northwestern terrane of Svalbard, Norway: Implications for regional correlations in the Arctic Caledonides: Journal of the Geological Society of London, v. 166, p. 147–158, doi:10.1144/0016-76492008-023.

Pettersson, C.H., Pease, V., and Frei, D., 2010, Detrital zircon U-Pb ages of Silurian–Devonian sediments from NW Svalbard: A fragment of Avalonia and Laurentia?: Journal of the Geological Society of London, v. 167, p. 1019–1032, doi:10.1144/0016-76492010-062.

Peucat, J.J., Ohta, Y., Gee, D.G., and Bernard-Griffiths, J., 1989, U-Pb, Sr and Nd evidence for Grenvillian and latest Proterozoic tectonothermal activity in the Spitsbergen Caledonides, Arctic Ocean: Lithos, v. 22, p. 275–285, doi:10.1016/0024-4937(89)90030-3.

Phelps, J.C., and Avé Lallement, H.G., 1998, Out-of-sequence thrusting and structural continuity of the Endicott Mountains allochthon around the eastern end of the Doonerak window, central Brooks Range, Alaska, *in* Oldow, J.S., and Avé Lallement, H.G., eds., Architecture of the Central Brooks Range Fold and Thrust Belt, Arctic Alaska: Geological Society of America Special Paper 324, p. 51–64, doi:10.1130/0-8137-2324-8.51.

Puchkov, V.N., 1997, Structure and geodynamics of the Uralian orogen, *in* Burg, J.-P., and Ford, M., eds., Orogeny through Time: Geological Society of London Special Publication 121, p. 201–236, doi:10.1144/GSL.SP.1997.121.01.09.

Raterman, N.S., McClelland, W.C., and Presnell, R.D., 2006, Geochronology and lithogeochemistry of volcanic rocks of the Ambler district, southern Brooks Range, Alaska: Geological Society of America Abstracts with Programs, v. 38, no. 5, p. 69.

Reed, B.L., 1968, Geology of the Lake Peters Area, Northeastern Brooks Range, Alaska: U.S. Geological Survey Bulletin 1236, 132 p.

Rehnström, E.F., 2010, Prolonged Paleozoic magmatism in the East Greenland Caledonides: Some constraints from U-Pb Ages and Hf isotopes: The Journal of Geology, v. 118, no. 5, p. 447–465, doi:10.1086/655010.

Repetski, J.E., Carter, C., Harris, A.G., and Dutro, J.T., Jr., 1987, Ordovician and Silurian fossils from the Doonerak anticlinorium, central Brooks Range, Alaska, *in* Hamilton, T.D., and Galloway, J.P., eds., Geologic Studies in Alaska by the U.S. Geological Survey during 1986: U.S. Geological Survey Circular 998, p. 40–42.

Roberts, D., 2003, The Scandinavian Caledonides: Event chronology, palaeogeographic settings and likely modern analogues: Tectonophysics, v. 365, p. 283–299, doi:10.1016/S0040-1951(03)00026-X.

Roberts, D., and Siedlecka, A., 2002, Timanian orogenic deformation along the northeastern margin of Baltica, northwest Russia, and northeast Norway, and Avalonian–Cadomian connections, *in* Gee, D.G., and Pease, V., eds., The Neoproterozoic Timanide Orogen of Eastern Baltica: Geological Society of London Memoir 352, p. 169–184, doi:10.1016/S0040-1951(02)00195-6.

Root, D., and Corfu, F., 2012, U-Pb geochronology of two discrete Ordovician high-pressure metamorphic events in the Seve Nappe Complex, Scandinavian Caledonides: Contributions to Mineralogy and Petrology, v. 163, p. 769–788, doi:10.1007/s00410-011-0698-0.

Rosa, D., Majka, J., Thrane, K., and Guarnieri, P., 2016, Evidence for Timanian-age basement rocks in North Greenland as documented through U-Pb zircon dating of igneous xenoliths from the Midtkap volcanic centers: Precambrian Research, v. 275, p. 394–405, doi:10.1016/j.precamres.2016.01.005.

Rubatto, D., 2002, Zircon trace element geochemistry: Partitioning with garnet and the link between U-Pb ages and metamorphism: Chemical Geology, v. 184, no. 1–2, p. 123–138, doi:10.1016/S0009-2541(01)00355-2.

Sable, E.G., 1977, Geology of the Western Romanzof Mountains, Brooks Range, Northeastern Alaska: U.S. Geological Survey Professional Paper 897, 84 p.

Sartini-Rideout, C., Gilotti, J.A., and McClelland, W.C., 2006, Geology and timing of dextral strike-slip shear zones in Danmarkshavn, North-East Greenland Caledonides: Geological Magazine, v. 143, p. 431–446, doi:10.1017/S0016756806001968.

Seidensticker, C.M., and Oldow, J.S., 1998, Structural development and kinematic history of ramp-footwall contraction in the Doonerak multiplex, central Brooks Range, Arctic Alaska, *in* Oldow, J.S., and Ave Lallemant, H.G., eds., Architecture of the Central Brooks Range Fold and Thrust Belt, Arctic Alaska: Geological Society of America Special Paper 324, p. 81–108.

Shephard, G.E., Muller, R.D., and Seton, M., 2013, The tectonic evolution of the Arctic since Pangea breakup: Integrating constraints from surface geology and geophysics with mantle structure: Earth-Science Reviews, v. 124, p. 148–183, doi:10.1016/j.earscirev.2013.05.012.

Silberling, N.J., Jones, D.L., Monger, J.W.H., and Coney, P.J., 1992, Lithotectonic Terrane Map of the North American Cordillera: U.S. Geological Survey Miscellaneous Investigations Series Map 2176, 2 sheets, 1:5,000,000.

Slagstad, T., Davidsen, B., and Daly, J.S., 2011, Age and composition of crystalline basement rocks on the Norwegian continental margin: Offshore extension and continuity of the Caledonian–Appalachian orogenic belt: Journal of the Geological Society of London, v. 168, p. 1167–1185, doi:10.1144/0016-76492010-136.

Slagstad, T., Pin, C., Roberts, D., Kirkland, C.L., Grenne, T., Dunning, G., Sauer, S., and Andersen, T., 2014, Tectonomagmatic evolution of the Early Ordovician suprasubduction-zone ophiolites of the Trondheim region, Mid-Norwegian Caledonides, *in* Corfu, F., Gasser, D., and Chew, D.W., eds., New Perspectives on the Caledonides of Scandinavia and Related Areas: Geological Society of London Special Publication 390, p. 541–561.

Slama, J., and Pedersen, R.B., 2015, Zircon provenance of SW Caledonian phyllites reveals a distant Timanian sediment source: Journal of the Geological Society of London, v. 172, p. 465–478, doi:10.1144/jgs2014-143.

Soja, C., and Antoshkina, A.I., 1997, Coeval development of Silurian stromatolite reefs in Alaska and the Ural Mountains: Implications for paleogeography of the Alexander terrane: Geology, v. 25, p. 539–542, doi:10.1130/0091-7613(1997)025<0539:CDOSSR>2.3.CO;2.

Soja, C., and Krutikov, L., 2008, Provenance, depositional setting, and tectonic implications of Silurian polymictic conglomerates in Alaska's Alexander terrane, *in* Blodgett, R.B., and Stanley, G.D., Jr., eds., The Terrane Puzzle: New Perspectives on Paleontology and Stratigraphy from the North American Cordillera: Geological Society of America Special Paper 442, p. 63–75, doi:10.1130/2008.442(04).

Sokolov, S.D., 2010, Tectonics of northeast Asia: An overview: Geotectonics, v. 44, no. 6, p. 493–509, doi:10.1134/S001685211006004X.

Strachan, R., Nutman, A., and Friederichsen, J., 1995, SHRIMP U-Pb geochronology and metamorphic history of the Smallefjord sequence, northeast Greenland Caledonides: Journal of the Geological Society of London, v. 152, p. 779–784, doi:10.1144/gsjgs.152.5.0779.

Strauss, J.V., Macdonald, F.A., Taylor, J.F., Repetski, J.E., and McClelland, W.C., 2013, Laurentian origin for the North Slope of Alaska: Implications for the tectonic evolution of the Arctic: Lithosphere, v. 5, no. 5, p. 477–482, doi:10.1130/L284.1.

Sturt, B.A., Pringle, I.R., and Ramsay, D.M., 1978, The Finnmarkian phase of the Caledonian orogeny: Journal of the Geological Society of London, v. 135, p. 597–610, doi:10.1144/gsjgs.135.6.0597.

Sun, S.S., and McDonough, W.F., 1989, Chemical and isotopic systematics of oceanic basalts: Implications for mantle composition and processes, *in* Saunders, A.D., and Norry, M.J., eds., Magmatism in Ocean Basins: Geological Society of London Special Publication 42, p. 313–345, doi:10.1144/GSL.SP.1989.042.01.19.

Surlyk, F., and Hurst, J.M., 1984, The evolution of the early Paleozoic deep-water basin of North Greenland: Geological Society of America Bulletin, v. 95, p. 131–154, doi:10.1130/0016-7606(1984)95<131:TEOTEP>2.0.CO;2.

Sweeney, J.F., 1982, Mid-Paleozoic travels of Arctic Alaska: Nature, v. 298, p. 647–649, doi:10.1038/298647a0.

Thorsteinsson, R., and Tozer, E.T., 1970, Geology of the Arctic Archipelago, *in* Douglas, R.J.W., ed., Geology and Economic Minerals of Canada (5th ed.): Geological Survey of Canada Economic Geology Report 1, p. 547–590.

Till, A.B., and Dumoulin, J.A., 2013, Detrital zircon results from Neoproterozoic metamorphic and Cambrian(?) sedimentary rocks, western Brooks Range, Alaska: Early signatures of the Arctic Alaska–Chukotka terrane: San Francisco, California, American Geophysical Union, Fall meeting, abstract T13B-2530.

Till, A.B., Dumoulin, J.A., Harris, A.G., Moore, T.E., Bleick, H., and Siwiec, B., 2008, Bedrock Geologic Map of the Southern Brooks Range, Alaska, and Accompanying Conodont Data: U.S. Geological Survey Open-File Report 2008-1149, 88 p., 2 sheets.

Till, A.B., Amato, J.M., Aleinikoff, J.N., and Bleick, H.A., 2014a, U-Pb detrital zircon geochronology as evidence for the origin of the Nome Complex, northern Alaska, and implications for regional and trans-Arctic correlations, *in* Dumoulin, J.A., and Till, A.B., eds., Reconstruction of a Late Proterozoic to Devonian Continental Margin Sequence, Northern Alaska: Its Paleogeographic Significance and Contained Base-Metal Sulfide Deposits: Geological Society of America Special Paper 506, p. 111–131, doi:10.1130/2014.2506(04).

Till, A.B., Dumoulin, J.A., Ayuso, R.A., Aleinikoff, J.N., Amato, J.M., Slack, J.F., and Shanks, W.C.P., III, 2014b, Reconstruction of an early Paleozoic continental margin based on the nature of protoliths in the Nome Complex, Seward Peninsula, Alaska, *in* Dumoulin, J.A., and Till, A.B., eds., Reconstruction of a Late Proterozoic to Devonian Continental Margin Sequence, Northern Alaska: Its Paleogeographic Significance and Contained Base-Metal Sulfide Deposits: Geological Society of America Special Paper 506, p. 1–28, doi:10.1130/2014.2506(01).

Tochilin, C.J., Gehrels, G.E., Nelson, J., and Mahoney, J.B., 2014, U-Pb and Hf isotope analysis of detrital zircons from the Banks Island assemblage (coastal British Columbia) and southern Alexander terrane (southeast Alaska): Lithosphere, v. 6, no. 3, p. 200–215, doi:10.1130/L338.1.

Trettin, H.P., 1987, Pearya: A composite terrane with Caledonian affinities in northern Ellesmere Island: Canadian Journal of Earth Sciences, v. 24, p. 224–245, doi:10.1139/e87-025.

Trettin, H.P., 1991, The Proterozoic to Late Silurian record of Pearya, *in* Trettin, H.P., ed., Geology of the Innuitian Orogen and Arctic Platform of Canada and Greenland: Boulder, Colorado, Geological Society of America, The Geology of North America, v. E, p. 241–259.

Trettin, H.P., 1992, New U-Pb and ^{40}Ar-^{39}Ar age determinations from northern Ellesmere Island and Axel Heiberg Islands and their tectonic significance, *in* Geological Survey of Canada Radiogenic Age and Isotopic Studies: Geological Survey of Canada Paper 92-2, p. 3–30.

Trettin, H.P., 1998, Pre-Carboniferous Geology of the Northern Part of the Arctic Islands: Geological Survey of Canada Bulletin 425, 248 p.

Trettin, H.P., Parrish, R., and Loveridge, W.D., 1987, U-Pb age determinations on Proterozoic to Devonian rocks from northern Ellesmere Island, Arctic Canada: Canadian Journal of Earth Sciences, v. 24, p. 246–256, doi:10.1139/e87-026.

Trettin, H.P., Mayr, U., Long, G.D.F., and Packard, J.J., 1991a, Cambrian to Early Devonian basin development, sedimentation, and volcanism, Arctic Islands, *in* Trettin, H.P., ed., Geology of the Innuitian Orogen and Arctic Platform of Canada and Greenland: Geological Survey of Canada, Geology of Canada, v. 3, p. 165–238, doi:10.4095/133959.

Trettin, H.P., Okulitch, A.V., Harrison, J.C., Brent, T.A., Fox, F.G., Packard, J.J., Smith, G.P., and Zolnai, A.I., 1991b, Silurian–early Carboniferous deformation phases and associated metamorphism and plutonism, Arctic Islands, *in* Trettin, H.P., ed., Geology of the Innuitian Orogen and Arctic Platform of Canada and Greenland: Geological Survey of Canada, Geology of Canada, v. 3, p. 293–341, doi:10.4095/133959.

Tucker, R., Robinson, P., Solli, A., Gee, D.G., Thorsnes, T., Krogh, T.E., Nordgulen, O., and Bickford, M.E., 2004, Thrusting and extension in the Scandinavian hinterland, Norway: New U-Pb ages and tectonostratigraphic evidence: American Journal of Science, v. 304, p. 477–532, doi:10.2475/ajs.304.6.477.

van Staal, C.R., and Barr, S.M., 2012, Lithospheric architecture and tectonic evolution of the Canadian Appalachians and associated Atlantic margin, *in* Percival, J.A., Cook, F.A., and Clowes, R.M., eds., Tectonic Styles in Canada: The Lithoprobe Perspective: Geological Association of Canada Special Paper 49, p. 1–55.

van Staal, C.R., Beranek, L., Israel, S., McClelland, W.C., Mihalynuk, M.G., Nelson, J., and Joyce, N., 2010, New data and ideas on the Paleozoic–Triassic evolution of the Insular superterrane of the North American Cordillera: Geological Society of America Abstracts with Programs, v. 42, no. 5, p. 574.

Vermeesch, P., 2013, Multi-sample comparison of detrital age distributions: Chemical Geology, v. 341, no. C, p. 140–146, doi:10.1016/j.chemgeo.2013.01.010.

Vervoort, J.D., and Blichert-Toft, J., 1999, Evolution of the depleted mantle: Hf isotope evidence from juvenile rocks through time: Geochimica et Cosmochimica Acta, v. 63, no. 3–4, p. 533–556, doi:10.1016/S0016-7037(98)00274-9.

Vervoort, J.D., and Patchett, P.J., 1996, Behavior of hafnium and neodymium isotopes in the crust: Constraints from Precambrian crustally-derived granites: Geochimica et Cosmochimica Acta, v. 60, no. 19, p. 3717–3733, doi:10.1016/0016-7037(96)00201-3.

Vervoort, J.D., Patchett, P.J., Blichert-Toft, J., and Albarede, F., 1999, Relationships between Lu-Hf and Sm-Nd isotopic systems in the global sedimentary system: Earth and Planetary Science Letters, v. 168, p. 79–99, doi:10.1016/S0012-821X(99)00047-3.

von Gosen, W., Piepjohn, K., McClelland, W.C., and Laufer, A., 2012, The Pearya shear zone in the Canadian High Arctic: Kinematics and significance: Zeitschrift der

Deutschen Gesellschaft für Geowissenschaften, v. 163, p. 233–249, doi:10.1127/1860-1804/2012/0163-0233.
Wallace, W.K., and Hanks, C.L., 1990, Structural provinces of the northeastern Brooks Range, Arctic National Wildlife Refuge, Alaska: American Association of Petroleum Geologists Bulletin, v. 74, no. 7, p. 1100–1118.
Wallin, E.T., and Metcalf, R.V., 1998, Supra-subduction zone ophiolite formed in an extensional forearc: Trinity terrane, Klamath Mountains, California: The Journal of Geology, v. 106, no. 5, p. 591–608, doi:10.1086/516044.
Watt, G.R., and Thrane, K., 2001, Early Neoproterozoic events in East Greenland: Precambrian Research, v. 110, no. 1–4, p. 165–184, doi:10.1016/S0301-9268(01)00186-3.
Watt, G.R., Kinny, P.D., and Friderichsen, J.D., 2000, U-Pb geochronology of Neoproterozoic and Caledonian tectonothermal events in the East Greenland Caledonides: Journal of the Geological Society of London, v. 157, p. 1031–1048, doi:10.1144/jgs.157.5.1031.
White, C., Gehrels, G.E., Pecha, M., Giesler, D., Yokelson, I., McClelland, W.C., and Butler, R.F., 2016, U-Pb and Hf isotope analysis of detrital zircons from Paleozoic strata of the southern Alexander terrane (southeast Alaska): Lithosphere, v. 8, no. 1, p. 83–96, doi:10.1130/L475.1.
Williams, H., Coleman-Sadd, S.P., and Swinden, H.S., 1988. Tectonic-stratigraphic divisions of central Newfoundland, *in* Current Research, Part B: Eastern and Atlantic Canada: Geological Survey of Canada Paper 88-1B, p. 91–98.
Wright, J.E., and Wyld, S.J., 2006, Gondwanan, Iapetan, Cordilleran interactions: A geodynamic model for the Paleozoic tectonic evolution of the North American Cordillera, *in* Haggert, J.W., Enkin, R.J., and Monder, J.W.H., eds., Paleogeography of the North American Cordillera: Evidence For and Against Large-Scale Displacements: Geological Association of Canada Special Paper 46, p. 377–408.
Yoshinobu, A.S., Barnes, C.G., Nordgulen, O., Prestvik, T., Fanning, M., and Pedersen, R.B., 2002, Ordovician magmatism, deformation, and exhumation in the Caledonides of central Norway: An orphan of the Taconic orogeny?: Geology, v. 30, p. 883–886, doi:10.1130/0091-7613(2002)030<0883:OMDAEI>2.0.CO;2.

Science Editor: Bradley S. Singer
Associate Editor: Cees R. van Staal

Manuscript Received 12 June 2016
Revised Manuscript Received 17 October 2016
Manuscript Accepted 10 December 2016

Printed in the USA